Investigation of Cell Movement and the Associated Cytoskeleton During Chick Gastrulation and Somitogenesis

By

Nicola Kennerley

A thesis submitted to the University of East Anglia for the degree of Doctor of Philosophy

The University of East Anglia, Norwich

School of Biological Sciences

May 2013

Abstract

Cell migration involves dynamic and spatially regulated changes to the cytoskeleton. During avian gastrulation, cells ingress through the primitive streak. Previous characterisation of microtubule organisation during this process revealed the distribution of cells with polarised and radial arrays across different regions of the embryo. Interestingly, many cells organised into groups arranged in rosette-like structures. As the primitive streak regresses and the neural folds gather at the centre of the embryo, bands of paraxial mesoderm that lie either side of the neural tube separate into somites. As new somites form caudally, the more rostral somites undergo a process of morphogenesis. Each somite divides into two regions: the dermomyotome and the sclerotome. Little is known about the cytoskeleton during this process.

Signalling by the Wnt family of secreted proteins influences the fate of cells during early embryonic patterning, cell movement, and cell polarity, processes in which the cytoskeleton is noticeably modified. The microtubule and actin crosslinking factor-1/actin crosslinking factor-7 (MACF1/ACF7) protein has been implicated in Wnt signalling and, additionally, its regulation has been shown to be important in cell migration.

This thesis concentrates on cellular dynamics and organisation (and the associated cytoskeleton) during chick gastrulation and somitogenesis. The aims of this project were to a) further characterise the cytoskeleton in cells that ingress into the avian primitive streak. b) Establish a published electroporation technique, which permits the targeting of different regions of the somite and subsequently observe cells (and their associated cytoskeleton) in real time. c) Determine the expression pattern for *MACF1/ACF7* in chick. d) To ascertain if there is a direct role for canonical Wnt signalling in somitic myofibre orientation/organisation.

Table of Contents

Abstract 2

Table of Contents 3-5

List of Figures 6-9

List of Tables 9

Acknowledgements 10

Chapter 1: Introduction 11

- 1.1. Cell Migration and the Cytoskeleton 11
- 1.2. Gastrulation 14
- 1.3. Somite Morphogenesis 18
- 1.4. Somite Morphogenesis and Signalling 22
- 1.5. Wnt Signalling 23
- 1.6. Spectraplakins 28

Overall Aims 31

Chapter 2: Materials and Methods 32

- 2.1. Frequently Used Solutions 32
- 2.2. Molecular Biology 33
- 2.3. Cell Culture 34
- 2.4. DF1, ARPE-19, and C2C12 Immunofluorescence Staining 35
- 2.5. Harvesting and Culturing Avian Embryos 36
- 2.6. Cryosectioning 37
- 2.7. Embryo Section Immunofluorescence Staining 38
- 2.8. Somite Wholemount Immunostaining 38
- 2.9. Somite Slice Cultures (Preparation for Microscopy) 39
- 2.10. Microinjection 40
- 2.11. Electroporation 41
- 2.12. Expressed Sequence Tag (EST; MACF1/ACF7) 41
- 2.13. Agarose Gel Electrophoresis 42
- 2.14. Preparation of DH5α *E.coli* competent cells 42
- 2.15. Heat Shock Transformation 42

- 2.16. Small Scale DNA Preparations (Mini Preps) 43
- 2.17. Diagnostic Restriction Digests 43
- 2.18. Sequencing 44
- 2.19. RNA Probe Synthesis 44
- 2.20. In Situ Hybridisation 45
- 2.21. Cell Transfection 47
- 2.22. Cell Protein Isolation and Quantification 47
- 2.23. Western Blot Protocol 48
- 2.24. Embryo Wholemount Immunostaining (MF20) 48
- 2.25. Preparation of Cells for Subsequent Microinjection into Embryos 49
- 2.26. Microscopy 49

Chapter 3: Cytoskeletal Arrangement in Primitive Streak Cells 51

- **Introduction 51**
  - 3.1. The Cytoskeleton 51
  - 3.2. Actin and Microtubule Structure and Functions 51
  - 3.3. Cell Migration 55
  - 3.4. Microtubule End Binding Molecules 56
  - 3.5. Microtubule Plus-End Tracking Proteins (+TIPs) 56
  - 3.6. Avian Gastrulation and the Cytoskeleton 59

- **Results 62**
  - 3.7. DF1 and ARPE-19 Immunofluorescence Staining 62

- **Discussion and Future Work 65**

Chapter 4: Cell Dynamics and the Associated Cytoskeleton During Somite Morphogenesis 70

- **Introduction 70**
  - 4.1. Myotome Morphogenesis 71
  - 4.2. NOTCH signalling and Myogenesis 77
  - 4.3. C2C12 Cells and Myogenesis 81

- **Results 82**
  - 4.4. C2C12 Immunofluorescence Staining 82
  - 4.5. Embryo Sections and Immunofluorescence Staining 82
  - 4.6. Wholemount Somite Immunofluorescence Staining 83
  - 4.7. Targeted Electroporation of the Dorsomedial Lip 86

- **Discussion and Future Work** **90**

Chapter 5: Microtubule-Actin Cross-linking Factor 1/ Actin Cross-linking Family 7 (MACF1/ ACF7) **97**

- **Introduction** **97**
  - 5.1. MACF1/ACF7 Structure and Isoforms 97
  - 5.2. MACF1/ACF7 Functions 100
  - 5.3. MACF1/ACF7 and its Role in Wnt Signalling 103

- **Results** **105**
  - 5.4. Characterisation of ChEST16M13 (MACF1/ACF7) 105
  - 5.5. MACF1/ACF7 Chick Expression Pattern 107
  - 5.6. MACF1/ACF7 Immunofluorescence Staining 110
  - 5.7. MACF1/ACF7 siRNA transfection in C2C12 cells 112

- **Discussion and Future Work** **113**

Chapter 6: Wnt Signalling in Somitogenesis and Myogenesis **121**

- **Introduction** **121**
  - 6.1. Somite Patterning and Wnt Signalling 121
  - 6.2. Wnt Signalling and Skeletal Muscle Development 123
  - 6.3. Wnt11 and Early Muscle Fibres 126
  - 6.4. Wnt Signalling and the Cytoskeleton 131
  - 6.5. GSK3β Regulates MACF1/ACF7 in Cell Migration 134

- **Results** **137**
  - 6.6. Wnt11 and Early Muscle Fibres 137
  - 6.7. Wnt3a and Early Muscle Fibres 139
  - 6.8. MACF1/ACF7 and Early Muscle Fibres 142

- **Discussion and Future Work** **147**

Chapter 7: Overall Summary **153**

References **155**

Abbreviations **174**

List of Figures

Chapter 1: Introduction

1.1. Model for the steps of cell migration. 12

1.2. General organisation of the three germ layers in a chick embryo and the morphogenetic movement of gastrulation EMT at stage HH Stage 3-4. 15

1.3. Epithelialisation and de-epithelialisation in chick embryo somites. 19

1.4. Transverse section through the trunk of a chick embryo during days 2-4 of development. 20

1.5. Somite organisation: the dermatome, myotome and sclerotome are established before the syndetome. 21

1.6. Proposed interactions in the patterning of the somite. 23

1.7. The canonical Wnt pathway. 25

1.8. Overview of Wnt signaling cascades. 27

Chapter 3: Cytoskeletal Arrangement in Primitive Streak Cells

3.1. Microtubule assembly. 54

3.2. Microtubule organisation in an HH Stage 3 embryo stained with α -tubulin in whole mount. 60

3.3. Actin staining confirms the formation of rosette structures in the primitive streak. 61

3.4. DF-1 and ARPE-19 cells fixed with methanol-MES and immunostained with various antibodies. 63-64

3.5. DF-1 cells fixed with PHEMO-fix and immunostained with various antibodies. 64-65

Chapter 4: Cell Dynamics and the Associated Cytoskeleton During Somite Morphogenesis

4.1. Two models of avian myotome formation. 73

4.2. The Four Borders of the Dermomyotome Generate Myocytes. 74

4.3. Morphogenetic cell events driving myocyte elongation**.** 76

4.4. Summary of the distinct steps involved in the oriented elongation of myocytes. 77

4.5. Schematic showing the expression of NOTCH signalling family members in the dorsomedial lip (DML), transition zone (TZ), and myotome. 78

4.6. Notch is active during early myogenesis. 78

4.7. Model proposed by Rios *et al* (2011), which "suggests an additional role of the NOTCH pathway during myogenesis. 80

4.8. C2C12 cells immunostained for microtubules at day 1 and day 4 of differentiation. 82

4.9. Microtubule immunofluorescence staining of a HH Stage 16 chick embryo cross section. 83

4.10. Confocal stack of an interlimb somite of a HH Stage 17 chick embryo immunostained for microtubules. 84

4.11. Confocal stack of an interlimb somite of a HH Stage 17 chick embryo immunostained for microtubules and DNA. 85

4.12. Dividing cell from a HH Stage 17 chick embryo interlimb somite. 86

4.13. Time-lapse confocal analysis showing GFP-tubulin expression in a HH Stage 20 chick interlimb somite injected and electroporated at HH Stage 16. 87

4.14. Time-lapse confocal analysis showing GFP-GPI expression in a HH Stage 20 chick interlimb somite injected and electroporated at HH Stage 16. 89

Chapter 5: Microtubule-Actin Cross-linking Factor 1/ Actin Cross-linking Family 7 (MACF1/ ACF7)

5.1. Schematic to show MACF1/ACF7 and its multiple domain structure. 98

5.2. Mammalian MACF1/ACF7 and BPAG1 isoforms. 99

5.3. A model to show the involvement of MACF1/ACF7 in the Wnt/β-catenin signaling pathway. 104

5.4. ChEST16M13 recognition sites on chick and human *MACF1/ACF7* transcripts. 106

5.5. The expression pattern of *MACF1/ACF7* in early chick embryos. 107

5.6. The expression pattern of *MACF1/ACF7* in a HH Stage 17 chick embryo. 108

5.7. The expression pattern of *MACF1/ACF7* in a HH Stage 20 embryo. 109

5.8. The expression pattern of *MACF1/ACF7* in a HH Stage 31 embryo. 110

5.9. MACF1/ACF7 and microtubule immunostaining in murine C2C12 cells. 111

5.10. MACF1/ACF7 and actin immunostaining in murine C2C12 cells. 111

5.11. MACF1/ACF7 knockdown in C2C12 cells. 112

Chapter 6: Wnt Signalling in Somitogenesis and Myogenesis

6.1. Wnt signaling and the embryonic origin of skeletal muscle of the trunk and limb. 124

6.2. The neural tube is necessary and sufficient for the oriented elongation of myocytes. 127

6.3. The sequential action of the Wnt/PCP and the Wnt/β-catenin pathways is essential for the formation of fully functional chick embryonic muscle fibres. 130

6.4. Wnt11 acts as an instructive cue during myocyte elongation. 131

6.5. GSK3β Is a Central Regulator of the Cytoskeleton during Cell Migration. 135

6.6. Myosin heavy chain expression in a HH Stage 20 Chick embryo. 137

6.7. *Wnt11* and myosin heavy chain expression in a HH Stage 20 Chick embryo following targeted fibroblast injection. 138

6.8. Effects of an exogenous source of Wnt11 on early myofibres. 139

6.9. *Wnt3a* and myosin heavy chain expression in a HH Stage 20 Chick embryo following targeted fibroblast injection. 140

6.10. Effects of an exogenous source of Wnt3a on early myofibres. 140

6.11. Exogenous Wnt3a in the myotome and lateral regions of the somite does not upregulate *Wnt11*. 141

6.12. Proposed additional pathway suggesting a role for MACF1/ACF7, downstream of GSK3β, in the organisation of chick embryonic muscle fibres. 142

6.13. Attempted MACF1/ACF7 knockdown in somites and its effects on myofibre organisation. 143

6.14. Simultaneous cell injection and electroporation is possible in early chick somites. 145

6.15. Preliminary experiments to test if Axin2 overexpression can perturb the myofibres response/orientation towards exogenous Wnt3a. 146

List of Tables

Chapter 2: Materials and Methods

2.1. Antibodies, both primary and secondary, used to immunostain chicken embryo fibroblasts. 36

2.2. Summary of constructs including enzymes used for linearisation and polymerases used for anti-sense probe transcription. 45

2.3. Pre-designed siRNAs against mouse MACF1/ACF7 supplied from Applied Biosystems, LifeTechnologies. 47

Chapter 3: Cytoskeletal Arrangement in Primitive Streak Cells

3.1. Attempted methods of embryo (HH stage 3-4) fixation using methanol-MES. 65

Chapter 6: Wnt Signalling in Somitogenesis and Myogenesis

6.1. Components of the canonical Wnt pathway and their associations with the cytoskeleton. 130

Acknowledgements

First and foremost I wish to thank my primary supervisor Professor Andrea Münsterberg. Thank you Andrea for this wonderful opportunity, and for all your invaluable expertise, support, guidance, and understanding over these last four years. I really appreciate it.

I would also like to thank Dr. Mette Mogensen, Dr. Gabriella Kelemen and Dr. Grant Wheeler for their additional support and guidance throughout my PhD.

A huge thanks to ALL past and present members of Lab 0.04, you guys are great ☺ Special thanks to Dr. Katarzyna Goljanek-Whysall, Dr. Timothy Grocott and Dr. James McColl for their continual help, advice, and encouragement. Also thanks to Dr. Deborah Goldspink and Dr. Ben Tyrrell for all their help and guidance, particularly during my first year.

I am also extremely grateful to Dr. Paul Thomas for all his help (and ideas!) with microscopy and imaging. Your help truly was instrumental!

I would like to thank the BBSRC for their financial support.

Finally, I would like to send my love and gratitude to ALL my family and friends. I sincerely appreciate every single one of you. You have all helped me tremendously during some of the toughest times I will ever experience. Thank you for all your support during the last few years. GemGem, I couldn't have done this without you.

Mum and NatNat, thinking of you each and every day. I hope 'I did you proud'. I love you both millions and billions, more than jelly tots and lolly pops. This one is for you!

Chapter 1: Introduction

1.1. Cell Migration and the Cytoskeleton

Cell migration is an integrated multistep process that contributes to tissue repair, angiogenesis, and the functioning of the immune system; it drives disease progression and is fundamental to the development of multicellular organisms (Affolter & Weijer, 2005; Bai *et al*, 2011; Dormann & Weijer, 2003; Ridley *et al*, 2003). Migration involves dynamic and spatially regulated changes to the cells cytoskeleton (composed primarily of actin, microtubules and intermediate filaments), cell-substrate adhesions and the extracellular matrix (ECM). It is typically initiated in response to extracellular cues. These cues, which can be diffusible factors (chemokines and growth factors for example), signals from neighbouring cells, and/or signals from the ECM, stimulate transmembrane receptors to initiate intracellular signalling (Ridley, 2001). An example of the many different intracellular molecules that have been implicated in cell migration includes the small guanosine-5'-triphosphatases (GTPases), in particular Rac1, RhoA and Cdc42 of the Rho-family, known principally for their pivotal role in regulating the actin cytoskeleton (Bai *et al*, 2011; Etienne-Manneville & Hall, 2002). Rho-family GTPases cycle between an inactive, GDP-bound, and an active GTP-bound conformation. In the GTP-bound form, they interact with downstream target proteins (effectors) to induce cellular responses. Effectors of Cdc42 include p21-activated kinase (PAK), Wiskott-Aldrich syndrome protein (WASP)/neuronal WASP, Ras GTPase-activating-like protein (IQGAP1), Par6 and myotonic-dystrophy kinase related Cdc42-binding kinase (MRCK). Rac1 effectors include p140Sra-1, IRSp53, PAK, and IQGAP1; the latter two are also effectors of Cdc42 as aforementioned. Examples of Rho effectors include Rho kinase (ROCK), the myosin-binding subunit of myosin phosphatase, protein kinase N (PKN), mDia, citron kinase, and rhoketin. The majority of these effectors perform their physiological functions during actin organisation. Accumulating evidence has shown that some of these effectors,

PAK, IQGAP1, Par6 and, mDia for example, are also involved in the regulation of microtubule dynamics and organisation during cell polarisation (Fukata *et al*, 2003; Ridley, 2001; Watanabe *et al*, 2005).

Ultimately, extracellular signals instigate the polarisation and extension of a protrusion in the direction of the cells movement (the so-called 'leading edge'). Different cell types generate different types of protrusive structures, including lamellipodia, filopodia and pseudopodia (differing primarily in the way the actin is organised). The protrusion attaches to the substratum on which the cell is migrating via the formation of adhesions, which serve as traction points. The cell body moves forward by way of contraction and attachments at the rear are released as the cell retracts. Thus, migration can be divided into four mechanistically separate steps: protrusion extension, formation of new adhesions, cell body contraction, and tail detachment (see figure 1.1; Alberts *et al*, 2002; Horwitz & Webb, 2003; Ridley, 2001; Ridley, 2011).

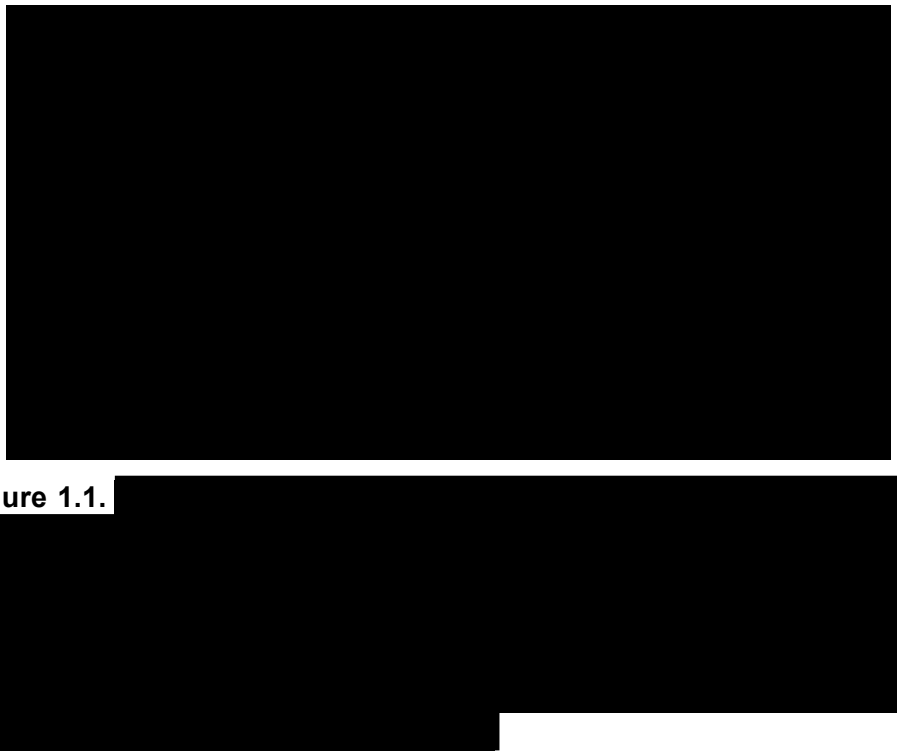

Figure 1.1.

Protrusive structures, like lamellipodia, extend owing to both the polymerisation of localised actin at the leading edge, and the loosening of the myosin thick filament network in the cell cortex (which allows expansion to occur). Rac1 and Cdc42 regulate actin polymerisation, while RhoA regulates the assembly of contractile actin and myosin, which leads to contraction at the rear of migrating cells (figure 1.1). Traction, which may involve microtubule function (see Small & Kaverina, 2003), is gained via attachment to the substrate; new contacts are made at the leading edge, while contacts are broken at the trailing edge (rear of the cell; Dormann & Weijer, 2003; Hollenbeck, 2001; Lauffenburger & Horwitz, 1996; Watanabe *et al*, 2005).

In addition to affecting the actin cytoskeleton and cell adhesion, recent evidence has shown that the Rho GTPases also affect microtubule function (for an extensive review see Watanabe *et al*, 2005). Microtubules are hollow tubes composed of thirteen protofilaments of α- and β-tubulin dimers organised in a head-to-tail fashion. They are essential for vesicle transport, cell division, cell polarisation, and cell migration (Etienne-Manneville, 2010). In most cells they are nucleated at their minus ends, which predominantly localise at the microtubule-organising centre (MTOC; also called the centrosome), and their plus-ends extend toward the cell periphery. In order to explore intracellular space their plus-ends alternate between two phases of growth and shrinkage in a manner known as dynamic instability (Mitchison and Kirschner, 1984). It is through this 'searching' process that the plus-ends are captured and stabilised at their target destinations, kinetochores on the mitotic spindle and the cell cortex, for example (Gunderson & Cook, 1999; Watanabe *et al*, 2005). Microtubule dynamics are highly regulated by multiple factors: tubulin post-translational modifications (acetylation or detyrosination for example) and microtubule-associated proteins (MAPs) such as plus-end tracking proteins. In migrating cells, selective stabilisation of the plus-ends of microtubules (i.e. at the cell cortex within the advancing lamellipodium) enables the MTOC to reorient towards the leading edge resulting in polarised microtubule arrays. Conversely, non-migrating cells have radial microtubule arrays that are anchored at a centrally located MTOC. Microtubule plus-end proteins (+TIPS), such as end-binding 1 (EB1), cytoplasmic linker associated

proteins (CLASPs), adenomatous polyposis coli (APC; a tumour suppressor), and microtubule and actin crosslinking factor-1/actin crosslinking factor-7 (MACF1/ACF7), and cortical receptors such as IQ motif containing GTPase activating protein 1 (IQGAP1) and Discs large 1 (Dlg1), also appear to be important for establishing cortical contact (Fukata *et al*, 2003; Watanabe *et al*, 2005; Wittmann & Waterman-Storer, 2001).

1.2. Gastrulation

At present, the majority of studies are still concerned with the investigation of the behaviour of individual cells. Many cell types migrate as solitary entities, lymphocytes, fibroblasts and neuronal cells for example. Yet, during angiogenesis, wound healing, and development, epithelial and endothelial cells often move as sheets or groups (Ridley, 2001; Rørth, 2007). Unsurprisingly, regulatory mechanisms and signalling pathways can differ considerably between individual- and collective-guidance modes (Rørth, 2007). A prime example of collective movement occurs during gastrulation. Gastrulation is the highly coordinated morphogenetic process in embryos by which the presumptive mesoderm and endoderm move inside the ectoderm to form a three-layered embryo. The ectoderm, which will later form the adult integument and nervous system, surrounds both the endoderm (innermost) and mesoderm, which themselves become the future lining of the gut and the middle layer of the adult body plan respectively (Keller, 2005). In frog (*Xenopus*) embryos, gastrulation is driven by radial intercalation of cells in the animal cap. This underlies the epiboly of the ectoderm and convergence and extension of the mesoderm (and overlying neuroectoderm), resulting in the elongation of the embryo (Keller *et al*, 2000). *Xenopus* gastrulation is, consequently, a result of the rearrangement of coherent cells that are embedded in epithelial sheets. In contrast, gastrulating mouse and chick embryos show large-scale epithelial-to-mesenchymal transitions (EMT; a morphogenetic process in which cells lose their epithelial characteristics and gain mesenchymal properties), whereby cells ingress from the epiblast to

form the mesoderm (see figure 1.2; Bellairs 1986, Nakaya & Sheng, 2009; Wallingford & Harland, 2007; Yang *et al*, 2002).

Figure 1.2.

The early avian embryo consists of two layers, the hypoblast and the epiblast. The hypoblast gives rise to extraembryonic structures only, while the epiblast produces extraembryonic structures and all the structures of the embryo proper (Wolpert *et al*, 2007). Structurally, the epiblast resembles a typical epithelial sheet. The apical end of each cell is in contact with other cells through E-cadherin (containing both adherens and tight junctions) and the basal side of each cell makes contact with a basal lamina (Andries *et al*, 1985; Chuai & Weijer, 2008). Interestingly, in 2008 Nakaya *et al* provided evidence that controlled basement membrane breakdown is the first step, and a crucial component of, gastrulation EMT. They propose that basal microtubule stability is vital to this process. Their model suggests that in lateral cells, neuroepithelial-transforming-protein 1 (Net1) activates basal RhoA, which locally stabilises microtubules through an unknown post-translational modification. While, in medial cells, at the onset of EMT, the disappearance of Net1 stops basal RhoA activity and as a consequence destabilises microtubules. It is this loss of microtubules that eventually drives

basement membrane disassembly (Levayer & Lecuit, 2008; Nakaya *et al*, 2008).

Unfortunately, little is known about how cells in the epiblast move. Several mechanisms have been implicated: the cells could move on a basal lamina substrate, they could move by pushing and pulling on each other, or the cells could use both mechanisms simultaneously. Epiblast cells produce a basal lamina, which is anchored in the surrounding Area Opaca. The cells could move by walking on this membrane using lamellipodia that extend in the direction of migration. It is possible that the cells exert traction on each other, involving filopodia formation. At their apical sides the cells stick together by way of well-developed adherens junctions. In addition to contributing to cell movement lamellipodia could potentially detect and interpret gradients of signalling molecules such as growth factors and Wnts associated with the ECM. Pushing and pulling, mediated via junctional contacts, would require extensive modulation of cell-cell adhesion. When guided by a signalling system, this mechanism, if active in a graded manner, could result in intercalation. In *Xenopus*, intercalation is controlled through the Wnt planar polarity pathway (first discovered in *Drosophila*). Wnt5 and Wnt11 signal through frizzled receptors (Frizzled 7 [Fzd7] in particular), which then via dishevelled activate small GTPases (Rac, Rho and CDC42), which as previously mentioned signal to downstream regulatory components of the actin-myosin cytoskeleton (Chuai *et al*, 2006; Chuai & Weijer, 2008; Cui *et al*, 2005; Keller *et al*, 2000; Keller, 2005).

In the chick, gastrulation begins with extensive rearrangements of cells in the epiblast resulting in the establishment of the primitive streak in the midline. During its formation the streak elongates in both anterior and posterior directions and prospective mesoderm cells begin to ingress (Chuai *et al*, 2006; Chuai & Weijer, 2008; Wagstaff *et al*, 2008; Wallingford & Harland, 2007). This formation and elongation gives rise to two of the three germ layers: the endoderm, which replaces the hypoblast, and the mesoderm. Cells remaining in the epiblast form the third germ layer, the ectoderm (Lopez-Sanchez *et al*, 2005). The anterior most part of the streak is known as Hensen's node, which acts as the organising centre for avian gastrulation

(Boettger *et al*, 2001; Mikawa *et al*, 2004). When the streak reaches half-maximal extension epiblast cells, within the streak, undergo EMT and move into the space between the epiblast and hypoblast to form axial and lateral mesoderm and the definitive endoderm (Lawson & Schoenwolf, 2001a; Yang *et al*, 2002).

Formation of the streak is initiated at Hamburger and Hamilton (HH) Stage 2 (Hamburger & Hamilton, 1951; Lawson & Schoenwolf, 2001a) and fate-mapping experiments show that it derives mainly from epiblast cells overlying Koller's sickle (Bachvarova *et al*, 1998; Lawson and Schoenwolf, 2001b). Early observations found directed cell movements into the forming streak; cells from the lateral posterior marginal zone move towards the posterior centre of the marginal zone where they merge, change direction and extend anteriorly in so-called polonaise movements. More recent evidence shows the existence of two counter-rotating streams in the epiblast that merge at the site of streak formation during streak initiation (Chuai *et al*, 2006; Cui *et al*, 2005; Graper, 1929). Interestingly, cells overlying Koller's sickle express many genes important in later development, fibroblast growth factor (FGF) signalling molecules and members of the Wnt family, for example (Chapman *et al*, 2004; Lawson & Schoenwolf, 2001a). The expression domain of these genes, during streak development, co-ordinately transforms from a sickle-shaped domain via an intermediate triangular shape into an elongated streak (stretching posterior-anteriorly) along the midline of the embryo (Chuai *et al*, 2006; Cui *et al*, 2005). Unfortunately, the cellular mechanisms responsible for streak formation and the signals that control them are far from understood. Numerous suggestions have been put forward; these include cell-cell intercalation (Lawson & Schoenwolf, 2001a; Lawson & Schoenwolf, 2001b; Voiculescu *et al*, 2007), oriented cell division (Wei & Mikawa, 2000), and chemotaxis (Mikawa *et al*, 2004). Chemotaxis would imply the secretion of an attractant by cells belonging to the epiblast or as proposed by Yang *et al* (2002) a combination of attractants and repellents. Their model suggests that cell movement is directed by repulsion from the streak by FGF8 and attraction toward the midline in response to FGF4. Both of these growth

factors previously established to be expressed in the primitive streak (Yang *et al*, 2002).

1.3. Somite Morphogenesis

One of the main tasks of gastrulation is to create a mesodermal layer between the endoderm and ectoderm. In avian embryos, the mesoderm arises from cells of Hensen's node and the primitive streak. It generates all the organs between the ectodermal wall and endodermal tissues. In a neurula-stage embryo, the trunk mesoderm can be divided into four areas: the axial (or chordamesoderm: which gives rise to the notochord, an organ that induces neural tube formation and establishes the anterior-posterior body axis), paraxial (or somitic), intermediate and lateral plate mesoderm. As the primitive streak regresses during gastrulation and the neural folds begin to gather at the centre of the embryo, the thick bands of paraxial mesoderm that lie between the intermediate mesoderm and the axial structures (referred to as the segmental plate in avian embryos and unsegmented mesoderm in other vertebrate embryos) separate into transient aggregates of cells, on either side of the neural tube, termed somites (Bellairs, 1963, 1979; Christ *et al* 1972, 1973; Christ and Ordahl, 1995; Gilbert, 2006; Packard, 1978). The total number of somites formed is characteristic of a species: 50 in chicks, 65 in mice, and some snakes form approximately 500 (Gilbert, 2006). As individual chick embryos can develop at slightly different rates (especially if they are incubated at slightly different temperatures), the number of somites present can provide a useful method for staging embryos between HH Stage 6 and 14. Stage 10 embryos have 10 somites and, generally, the embryo gains 3 somites during each additional stage (for example, Stage 11 and 12 embryos have 13 and 16 somites respectively). However, it is better to rely on other markers beyond 22 somites (HH Stage 14; Hamburger and Hamilton, 1951).

Somites, which give rise to all skeletal muscles in the vertebrate trunk, form in pairs in a rostral-caudal progression. Formation occurs periodically and regularly in time and space, depending on a 'clock and wave' mechanism

suggested by Cooke and Zeeman (1976): the Wnt and Notch pathways provide an oscillating signal (the 'clock') and a rostral-caudal gradient provides a moving 'wave' of FGF that sets somite boundaries (Dubrulle *et al*, 2001; Gilbert, 2006; Maroto and Pourquié, 2001; Palmeirim *et al*, 1997; Pourquié, 2003, 2004; Takahashi and Sato, 2008). Segmental organisation of the paraxial mesoderm occurs as somites pinch off from the anterior end of the paraxial mesoderm (or pre-somitic mesoderm, PSM) becoming newly formed separate structures. The mesenchymal cells making up the immature somite then undergo mesenchymal-epithelial transitions (MET) resulting in a spherical structure in which an internal mesenchyme is encapsulated by an epithelium (see figure 1.3; Duband *et al*, 1987; Gilbert, 2006; Nakaya *et al*, 2004; Yusuf and Brand-Saberi, 2006). Interestingly, using somitic MET as an *in vivo* model, Nakaya *et al* (2004) have shown that Cdc42 negatively acts on cell epithelialisation; activation of Cdc42 prevents MET, while its downregulation strongly promotes MET (Nakaya *et al*, 2004).

Figure 1.3.

The positional identity of paraxial mesoderm is determined by its location along the rostral-caudal axis before somitogenesis. If, for example, the

mesoderm region that gives rise to a thoracic somite is transplanted into the cervical region of a younger embryo, the host embryo will develop ribs in its neck (on the side of transplantation only; Kieny *et al*, 1972). In contrast, ectopically grafted or rotated tissue of newly formed somites will generate the same pattern of normal derivatives (Aoyama and Asamoto, 1988; Christ *et al*, 1992). When the somite matures, however, it will become committed to forming certain cell types. As new somites form caudally, the more rostral somites (in response to extrinsic signals from their surrounding structures, see figure 1.6) undergo maturation and differentiation in a dorsomedial and ventrolateral orientation. Each somite divides into two main regions: the dorsolateral epithelial dermomyotome (consisting of both the dermatome, which generates the dermis of the back, and the myotome, which forms the musculature of the back, ribs and limbs) and a ventral mesenchymal region called the sclerotome (which generates the vertebrae and rib cartilage; see figure 1.4; Brand-Saberi *et al*, 1996; Gilbert, 2006; Kahane *et al*, 1998).

Figure 1.4.

[redacted]

It is also worth noting that in 2003, Brent *et al* discovered a further region, the syndetome, which arises from cells within the sclerotome and generates the tendons (see figure 1.5).

Figure 1.5. [redacted]

The sclerotome is formed as the ventromedial epithelial cells of the somite undergo mitosis, lose their epithelial characteristics, and become mesenchymal again (EMT). The remaining epithelial portion of the somite, the dermomyotome, is formed as a consequence of dorsoventral patterning (see figure 1.4; Brand-Saberi *et al*, 1996; Gilbert, 2006; Ordahl and Le Douarin, 1992; Yusuf and Brand-Saberi, 2006). The dermomyotome is a transient structure that successively contributes cells to the dermis and the primary myotome (specifically the epaxial and hypaxial myotome).

1.4. Somite Morphogenesis and Signalling

Somite specification (maturation) is accomplished through a complex array of signals, which as previously mentioned, emanate from surrounding tissues (see figure 1.6). Ablation of dorsal tissues (ectoderm and dorsal neural tube), for example, results in defective dermomyotome development, while ablation of ventral tissues (notochord and floor plate) detrimentally affects sclerotome formation (Brand-Saberi *et al*, 1993; Brauner *et al*, 2010; Dietrich *et al*, 1997). The paracrine factors Sonic hedgehog (Shh) and Noggin, produced and secreted by the notochord (and Shh also by the floor plate of the neural tube), are necessary for induction (and maintenance) of the sclerotome (Brand-Saberi *et al*, 1993; Borycki *et al*, 1998; Christ *et al*, 1992; Dietrich *et al*, 1997; Dockter and Ordahl, 2000; Fan and Tessier-Lavigne, 1994). Sclerotome cells express Paired box protein (Pax1), a transcription factor that is required for their differentiation into cartilage and whose presence is required for vertebrae formation (Smith and Tuan, 1996). The dermatome differentiates in response to neurotrophin-3 (NT3) and Wnt1, both secreted by the neural tube. The myotome, in addition, is induced by distinct signals. The formation of the medial half is attributed to Wnt1 and Wnt3a signalling from the dorsal region of the neural tube and low levels of Shh from the ventral region. While the lateral half is influenced by a combination of Wnt proteins from the epidermis (ectodermal Wnt4, Wnt6, and Wnt7a) and bone morphogenetic protein-4 (BMP4) from the lateral plate mesoderm (see figure 1.6; Christ *et al*, 1992; Dietrich *et al*, 1998; Gilbert, 2006; Olivera-Martinez *et al*, 2001; Münsterberg *et al*, 1995a, 1995b; Pourquié *et al*, 1996; Stern *et al*, 1995; Yusuf and Brand-Saberi, 2006).

Figure 1.6. 

1.5. Wnt Signalling

The Wnt family of secreted lipoproteins (signalling proteins) participates in multiple developmental events during embryogenesis and in adult tissue homeostasis (Clevers, 2006; Logan and Nusse, 2004). The Wnt family, in mammals, comprises 19 members that share homologies in their sequence but often have fundamentally distinct signalling properties (Logan and Nusse, 2004). Wnt proteins are defined based on sequence homology to the original Wnt members: mouse Wnt1 (originally called Int-1; Nusse and Varmus, 1982) and *Drosophila melanogaster* Wingless (Wg; Sharma, 1973). Typically, Wnt proteins bind to Frizzled receptors (Fzd) that are located in the plasma membrane of the target cell. Fzd receptors are seven-'pass'-transmembrane proteins (which contain a large cysteine-rich domain that is implicated in Wnt binding) and they are known to interact with Dishevelled (Dvl; a cytoplasmic scaffold protein) and heterotrimeric G proteins, which are required for downstream signalling (reviewed by Clevers, 2006 and von Maltzahn *et al,*

2012). Wnt-receptor interactions can stimulate numerous intracellular responses. The most understood is the activation of β-catenin/TCF transcriptional complexes, known as canonical Wnt signalling (also referred to as classical Wnt signalling or Wnt/β-catenin signalling; review by von Maltzahn *et al,* 2012).

In the canonical signalling pathway, Wnt ligands such as Wnt1, Wnt3a, and Wnt8 bind to Fzd receptors, which in association with the Low-density lipoprotein receptor-related protein (LRP5/6) coreceptor initiate a signalling cascade that leads to the activation of Dvl, whose activation consequently results in the stabilisation of β-catenin (figure 1.7). The stability of β-catenin is regulated at various levels. In the absence of Wnt proteins, a so-called β-catenin destruction complex composed of the scaffold proteins Axin, adenomatous polyposis coli (APC), casein kinase-I (CKIα), and glycogen synthase kinase 3β (GSK3β) associates with β-catenin. β-catenin is, in turn, phosphorylated by CKIα and GSK3β. Hyperphosphorylated β-catenin is then subjected to ubiquitylation by the SKP1-cullin1-F-box ($SCF^{\beta\text{-}TRCP}$) E3 ligase complex, followed by degradation via the 26S proteasome (figure 1.7; review by Clevers, 2006). Conversely, when Wnts bind the cell surface receptors Fzd and LRP5/6, GSK3β-dependent β-catenin phosphorylation is suppressed via a mechanism that involves Dvl, and β-catenin is stabilised. Stabilised β-catenin enters the nucleus where it interacts with transcriptional regulators, including lymphoid enhancing factor-1 (LEF1) and T cell factors (TCFs) to activate gene transcription (reviews by Salinas, 2007; von Maltzahn *et al*, 2012; Wu and Pan, 2010).

Figure 1.7. 

Studies by Davidson *et al* (2005) and Zeng *et al* (2005) illustrated that dissociation of the destruction complex is also triggered by the recruitment of Axin to the plasma membrane, where Axin binds to the LRP5/6 receptors intracellular domain. Surprisingly, LRP5/6 receptor phosphorylation by CKIγ and GSK3β is required for Axin binding. Two different isoforms of CKI (α and γ) are therefore implicated in this pathway. These studies imply that while Wnt signalling in the cytoplasm inactivates GSK3β, active GSK3β is necessary at the plasma membrane to recruit Axin away from the destruction complex (Davidson, *et al*, 2005; Salinas, 2007[review]; Zeng *et al*, 2005). The sequence of these events is not completely understood. In 2006, Chen *et al*

demonstrated that Axin is recruited to the plasma membrane by microtubule and actin crosslinking factor-1/actin crosslinking factor-7 (MACF1/ACF7; see Chapter 5). MACF1/ACF7 is present in the destruction complex and is needed for the translocation of Axin to the membrane and binding to LRP5/6 (Chen *et al*, 2006).

Non-canonical Wnt signalling pathways are less understood, although they have been reported to contribute to developmental processes such as planar cell polarity (PCP) in *Drosophila* and convergent extension movements during gastrulation in *Xenopus*. In contrast to canonical Wnt signalling they do not require the transcriptional activity of β-catenin: they signal independently of β-catenin via Fzd receptors. Fzd-independent non-canonical Wnt signalling pathways have additionally been suggested. Non-canonical family members include Wnt4, Wnt5a and Wnt11 and non-canonical pathways include the PCP, the Wnt/Ca^{2+}, and the PI3K/AKT/mTOR cascades (figure 1.8; reviewed by von Maltzahn *et al*, 2012). First discovered in *Drosophila* the PCP pathway has been shown to be essential for epithelial and mesenchymal cell polarity in various organisms (Dale *et al*, 2009). Wnt/PCP signalling regulates changes in cytoskeletal organisation that are a requirement for cell polarisation and migration: controlling the hair cells in the inner ear for example (Montcouquiol et al, 2003). Fzd, Dvl, Prickle, and Vangl (Vang-like) are all core components of the Wnt/PCP pathway (Vladar *et al*, 2009). The interaction between these factors on Wnt signalling can lead to the activation of Rho and Rac, which leads to remodelling of the cytoskeleton and/or induction of Jun target genes (James *et al*, 2008).

Figure 1.8.

The Wnt/Ca^{2+} cascade has also been implicated in numerous functions, which include cell adhesion and cell movements during gastrulation. In this pathway, binding of Wnt to Fzd leads to the release of intracellular Ca^{2+}. This process is regulated by heterotrimeric G proteins, phospholipase C (PLC),

and calcium–calmodulin-dependent kinase II (CamKII), in addition to protein kinase C (PKC; Habas and Dawid, 2003; Kuhl, 2004). The increased intracellular Ca^{2+} concentration also stimulates calcineurin phosphatase, which results in activation of the transcription factor NFAT (nuclear factor of activated T cell; Hogan *et al*, 2003; reviewed by von Maltzahn *et al*, 2012).

Interestingly, GSK3β is one of the few signalling mediators that have a central part in a distinct range of signalling pathways, which include those activated by Wnts, hedgehog, growth factors, cytokines, and G protein-coupled ligands (reviewed by Wu and Pan, 2010). GSK3β was first linked with the canonical Wnt pathway due to the induction of a dorsal-ventral axis duplication phenotype by its dominant negative form in *Xenopus laevis* embryos (Dominguez *et al*, 1995; He *et al*, 1995; Pierce and Kimelman, 1995). β-catenin was successively identified as a GSK3β substrate: GSK3-mediated phosphorylation triggers the destabilisation of β-catenin (Peifer *et al*, 1994; Yost *et al*, 1996). This established a role for GSK3β in canonical Wnt signalling. Multifaceted roles for this kinase in Wnt signal transduction have since been demonstrated. However, the mechanisms for the regulation of GSK3β during Wnt signal transduction remain to be completely elucidated. Though it is evident that Wnt-mediated GSK3β does not utilise the phosphorylation events as in AKT signalling (AKT, itself activated by the PI3K pathway, inhibits GSK3β kinase activity via phosphorylation of Ser-9 (Buttrick and Wakefield, 2008).

1.6. Spectraplakins

The cytoskeleton, composed primarily of actin, microtubules and intermediate filaments, is highly dynamic. As aforementioned, it provides mechanical strength to the cell and regulates many other cellular events, including cell division, intracellular trafficking, and locomotion. The identification of proteins that can associate with the cytoskeleton is, therefore, of great importance. Spectraplakins are evolutionary conserved giant (>500kD), multifunctional cytoskeletal linker proteins that act as master coordinators between different

types of cytoskeletal filaments. They are able to bind to all three types of cytoskeletal filaments and, as their name implies, they contain domains found in two cytoskeletal families, the spectrins and plakins (Röper *et al*, 2002). The spectrin superfamily of linker proteins connects the actin-based cortical network to the plasma membrane (Hartwig, 1995), while plakins are a family of linker proteins that interact with all types of cytoskeletal elements connecting them to cellular junctions and the extracellular matrix (Leonova and Lomax, 2002). Spectraplakins display their most essential functions in muscle, neurons and skin epithelium, i.e. tissues that maintain complex yet dynamic cytoskeletal networks (Jefferson *et al*, 2004; Röper *et al*, 2002; Wu *et al*, 2008).

Spectraplakins evolved from the spectrin family of proteins, the most ancient of which is α-actinin. Defining features of α-actinin, and other spectrin superfamily members, include a calponin homology (CH) domain for calcium regulation, an EF-hand domain for direct calcium sensing/binding, and a series of spectrin repeats (Suozzi *et al*, 2012). Presently, the spectraplakin family consists of only two mammalian genes *MACF1/ACF7*, encoding microtubule-actin cross-linking factor 1/actin cross-linking factor 7, and *BPAG1/Dst*, encoding bullous pemphigoid antigen 1 (BPAG1)/dystonin. Additionally, the family comprises a single gene in zebrafish, *Magellan*, a single gene in *Drosophila melanogaster*, *short stop* (*shot*)/*Kakapo*, and a single *Caenorhabditis elegans* gene, *vab-10* (reviewed by Suozzi *et al*, 2012). The number of spectrin family genes in the genome is limited. Spectraplakins generate diversity via differential promoter usage and differential splicing. Different spectraplakins, therefore, contain combinations of various protein domains that bind to different filament types and filament-associated proteins. This awards the proteins with a diverse range of functions in cytoskeletal regulation. Spectraplakins, as a consequence, are very large proteins and remarkably, the activities of their protein domains are coordinated in spite of their separation along the length of the protein (Brown, 2008; Röper *et al*, 2002; Suozzi *et al*, 2012).

Spectraplakins have unique domain structures, including an actin-binding domain, spectrin repeats, EF-hand and GAR (glycine/arginine-rich) domain,

and a plakin domain. Most spectraplakin isoforms encompass a conserved sequence motif in their N-terminal domain (also found in the spectrins), which enables them to directly associate with actin. The F-actin binding domain comprises two CH domains, CH1 and CH2. CH1 alone can bind F-actin but affinity is increased with the addition of CH2 (Jefferson *et al*, 2004). Spectraplakins are classified as members of the spectrin superfamily owing to the existence of a large number of spectrin repeats. These repeats are believed to provide the proteins with flexibility and, in addition, act as spacer regions that separate the functional domains at the N and C termini. The EF-hand and GAR domain is situated within the C-terminal. Unlike EF-hand motifs, which are found in numerous members of the spectrin superfamily, the GAR domain is restricted to the spectraplakins and is not found in other spectrin family members (Röper *et al*, 2002). The GAR domain associates with and stabilises microtubules, suggesting that it evolved as a mechanism for spectraplakins to interact with microtubules and link microtubules to other cytoskeletal components (Leung *et al*, 1999; Sun *et al*, 2001; Suozzi *et al*, 2012). Furthermore, the GAR domain that is encoded by the *Drosophila melanogaster*, *short stop* (*shot*)/*Kakapo* gene can interact with end-binding 1 (EB1), a microtubule plus-end tracking protein (+TIP), which binds to the growing ends of cytoplasmic microtubules (Subramanian *et al*, 2003). The plakin domain, another signifying feature of the spectraplakins, is composed of six-nine spectrinlike repeats, suggesting that these domains are derived from spectrins. Typically, proteins containing plakin domains bind to membrane-associated juctional proteins (Jefferson *et al*, 2004).

Given that the following chapters cover different, albeit related, topics of research this introduction is somewhat brief and intended only to introduce the contents of this thesis. The beginning of each chapter, therefore, will encompass a more detailed introduction to its related subject.

Overall Aims

This thesis concentrates on cellular dynamics and organisation during chick gastrulation and somitogenesis, with a particular focus on the associated cytoskeleton. The aims of this project, therefore, were:

- To further characterise the cytoskeleton in cells that ingress into the avian primitive streak during gastrulation.

- To establish a previously published electroporation method (Scaal *et al*, 2004), which permits the targeting of different regions of the somite and, if possible, subsequently observe cells (and their associated cytoskeleton) migrating from the dorsomedial lip of the somite to the myotome in real time. Additionally, to immunostain somites with antibodies against cytoskeletal proteins to corroborate what might be seen in these electroporation experiments.

- To determine the expression pattern for the microtubule and actin crosslinking factor-1/actin crosslinking factor-7 (*MACF1/ACF7*) gene in the chick and explore its function during somitogenesis.

- To determine if there is a direct role for canonical Wnt signalling in somitic myofibre orientation/organisation and, if so, investigate if MACF1/ACF7 is involved.

Chapter 2: Materials and Methods

2.1. Frequently Used Solutions:

PBS (Phosphate Buffered Saline): 104mM NaCl, 2.5mM KCL, 6.5mM Na_2HPO_4, pH 7.4

PBST: PBS with the addition of 0.1% Tween-20

TBS (Tris Buffered Saline): 140mM NaCl, 2.5mM KCl, 25mM Tris, pH 8.0

TBST: TBS with the addition of 0.1% Tween-20

PFA: 4% Paraformaldehyde in PBS

SSC (20x): 3M NaCl, 0.3M Na3C6H5O7.2H2O (Na Citrate), pH 7.0 with citric acid

TAE: 40mM Tris, 1% Acetic acid, 1mM EDTA

MABT: 100mM Maleic acid, 150mM NaCl, 0.1% Tween-20, pH 7.5

NTM: 100mM NaCl, 100 mM Tris-HCL pH 9.5, 50mM $MgCl_2$

NTMT: NTM with the addition of 0.1% Tween-20

Simple Saline: 7.19M NaCl

PHEMO fix: 68mM PIPES, 25mM HEPES, 15mM EGTA, 3 mM $MgCl_2$, 3.7% PFA, 0.05% Glutaraldehyde, 0.5% TritonX-100

Methanol-MES: Methanol, 10% 0.5M MES (2-[*N*-morpholino]ethanesulfonic acid) buffer

2.2. Molecular Biology

Solutions and Reagents:

Antibodies for immunohistochemistry/immunocytochemistry and restriction enzymes were purchased from Roche (Roche Applied Science, UK) or Promega (Promega UK, Southampton UK). All other reagents were purchased from Sigma (Sigma-Aldrich Co. LLC.), Invitrogen (Life Technologies Corporation), or Fisher Scientific (Fisher Scientific UK Ltd) unless otherwise stated.

Bacterial Culture Media, Antibiotics and PFA preparation:

LB Medium: 1% Bacto-tryptone, 1.5% Yeast extract, 1% NaCl, pH 7.5

LB Agar: 1.5% Bacto-agar in LB medium

Ampicillin: Stock: 100mg/ml, Working concentration: 10mg/ml

Kanamycin: Stock: 100mg/ml, Working concentration: 5mg/ml

Preparation of 4% paraformaldehyde:

PBS containing one crystal of sodium hydroxide (NaOH) (Fisher Scientific) was first heated to 55°C. The addition of NaOH raises the pH of the PBS, so the PFA can dissolve quickly. PFA was subsequently added and dissolved with the aid of a magnetic stirring bead. When PFA was dissolved, the pH of the solution was corrected to pH7.4. PFA-PBS was stored at -20°C.

2.3. Cell Culture

Chick DF-1 fibroblast cells were cultured in Dulbecco's modified Eagle medium (DMEM) containing 1g/ml of glucose, 10% fetal bovine serum (FBS) (Gibco, Invitrogen) and 1% penicillin-streptomycin. The cells were passaged 1:5 every other day.

Mouse C2C12 myoblast cells were cultured in growth medium (GM): DMEM containing 4.5g/ml of glucose, 10% fetal bovine serum (FBS) (Gibco, Invitrogen) and 1% penicillin-streptomycin. The cells were passaged 1:5 after reaching ~ 70% confluence. C2C12 cells were differentiated via switching from growth medium to differentiation medium (DM): DMEM containing 2% horse serum when the cells were ~ 80% confluent. The myotubes started to appear after about 3 days, and by day 5 myotubes constituted most of the cell population.

Rat fibroblast cells expressing Wnt3a, Wnt11 and the control cell line LNCX2 were cultured in D-MEM tissue culture media with the addition of 10% inactivated foetal calf serum with G418 at 250µg/ml for selection.

All cells were cultured in a humidified cell culture incubator and maintained at 37°C and 5% CO_2.

Cell passaging was performed as follows: after removal of culture medium, cells were rinsed in sterile 1X phosphate buffered saline (PBS, prepared from tablets; Oxoid, Unipath Ltd., Basingstoke, UK). Next, cells were treated with enough (0.025%) trypsin-ethylendiamineteraacetic acid (EDTA) to cover the base of the flask for ~1 minute. The trypsin was then removed from the cells and flasks were returned to the incubator until the cells had become dissociated from the flask. Cells were then resuspended in an appropriate volume of fresh culture medium and passaged. Cells were counted using a haemocytometer to calculate required cell density for transfection/injection experiments.

2.4. DF1, ARPE-19, and C2C12 Immunofluorescence Staining

Chicken embryo fibroblasts (DF-1s), human retinal pigment epithelial (ARPE-19), and murine C2C12 myoblast cells were grown overnight, at 37°C, onto small gelatine coated glass cover slips. Cells, before becoming too confluent, were then rinsed in DEPC-PBS and fixed in either Methanol/10% MES, 4% PFA with 0.1% TritonX-100, or PHEMO-fix ready for immunofluorescence staining.

Cells fixed with methanol/10% MES or 4% PFA (with 0.1% TritonX-100) were removed from media and fixed at -20°C for 5 min or 20 min at RT respectively. Next, they were washed 3 times with 1% goat serum in PBS, incubated with 1% NP40 detergent for 3 min, washed again 3 times with 1% goat serum in PBS and then blocked with 10% goat serum in PBS for 30 min at room temperature (RT).

DF-1 cells fixed with PHEMO were removed from media, washed in PBS for 10 min at 37°C before fixing with PHEMO-fix solution (68mM PIPES, 25mM HEPES, 15mM EGTA, 3 mM $MgCl_2$, 3.7% PFA, 0.05% Glutaraldehyde, 0.5% TritonX-100). Cells were rinsed twice in PHEMO buffered solution (68 mM PIPES, 25 mM HEPES, 15 mM EGTA, 3 mM $MgCl_2$, 10% DMSO pH 6.9, with 10M KOH) for 10 min at 37°C. Subsequently, cells were washed twice with PBS for 5 min at room temperature (RT), incubated with 50 mM NH_4Cl/PBS for 10 min, washed three times with PBS (RT for 5 min), and then blocked with 10% goat serum in PBS for 30 min at RT.

For all cells, following fixation (either methanol/10% MES, 4% PFA with 0.1% TritonX-100 or PHEMO) and blocking, primary antibody, diluted in 1% goat serum in PBS, was applied for 1-2 h (see table 2.1). After washing 4 times for 15 min with 1% goat serum in PBS, secondary antibody (also diluted in 1% goat serum in PBS; see table 2.1) was applied and cells were incubated in a humidified chamber in the dark for 30 min. Following incubation, cells were washed 3 times for 10 min with 1% goat serum in PBS and cover slips (cells uppermost) were mounted onto slides. A drop of hydromount (with Dapco) was added and cells were covered with a large cover slip and stored at 4°C for up to 1 month.

Table 2.1. Antibodies, both primary and secondary, used to immunostain DF1-s, ARPE-19, and C2C12 cells (dilution factor and supplier also shown).

Primary Antibody and Dilution (in 1% goat serum in PBS)	Primary Antibody Supplier, Product Number, Clone Number (if known) and Host	Secondary Antibody*
α- tubulin (1:1000)	AbD Serotec, MCA77D680, clone YL1/2 (monoclonal), Rat	Anti-rat Alexa fluor 488 (green)
γ- tubulin (1:1000)	Abcam, ab11316, clone GLU-88, mouse	Anti-mouse Alexa fluor 488 (green)
APC (1:1000)	Abcam, ab58, clone Ali12-28, mouse	Anti-mouse Alexa fluor 488 (green)
EB1 (1:500)	BD biosciences, 610535, clone 5, mouse	Anti-mouse Alexa fluor 488 (green)
MACF1/ACF7 (1:1000)	Sigma, HPA013713, lot number A81498, rabbit	Anti-rabbit Alexa fluor 488 (green) or anti-rabbit Alexa fluor 568 (red)
α- tubulin (1:1000) & EB1 (1:500)	See above for α- tubulin and for EB1: abcam, ab50188, polyclonal, rabbit	Anti-rat Alexa fluor 488 (green) and anti-rabbit 568 (red) respectively
α- tubulin (1:1000) & γ-tubulin (1:1000)	See above α- tubulin and for γ-tubulin: sigma, T5192, polyclonal, rabbit	Anti-rat Alexa fluor 488 (green) and anti-rabbit 568 (red) respectively
-no primary-		Alexa fluor 488 phalloidin
-no primary-		DAPI (1:10,000)

*all secondary antibodies were diluted 1:1000 (antibody:1% goat serum in PBS)

2.5. Harvesting and Culturing Avian Embryos

White leghorn chicken eggs (Henry Stewart & Co. Ltd., UK) were stored at 16°C prior to incubation at 37°C. According to desired Hamburger-Hamilton (HH) stage (Hamburger and Hamilton, 1951), embryos were removed from eggs following appropriate incubation at 37°C. Embryos were either dissected directly (harvested) from the egg or cultured in Early Chick (EC) culture (Chapman *et al*, 2001). For EC culture, eggs were cracked/opened at their broad end and thick albumin was removed and discarded. Thin albumin was also removed but retained for media preparation (for EC culture). The yolk, with blastoderm positioned on top, was poured into a 10 cm Petri dish and any remaining albumin was carefully removed with tissue paper. Once the area of the vitelline membranes was cleared, a filter paper carrier (piece

of autoclaved filter paper with a central aperture) was gently placed onto the membranes framing the embryo accordingly. Using scissors, the membranes around the filter paper were cut and the filter paper (now holding the blastoderm) was lifted with forceps in an oblique direction. The filter paper was gently washed in autoclaved saline (to remove any yolk), an edge was dabbed onto tissue paper to absorb excess liquid, and the filter paper was placed with the blastoderm ventral side up onto an agar-albumin culture dish. Dish lids were replaced and cultures were put to 37°C, for appropriate time, in a storage container lined with moistened tissue. To prepare agar-albumin media, 0.3 g agar was added to 50 ml autoclaved saline (7.19 g NaCl /1 litre distilled water) and dissolved in the microwave. The solution was put to 50°C and once this temperature was reached 50 ml of thin albumin was added. Solution was mixed and kept at 50°C for a further minute. Carbenicillin, 10 µg/ml, was added and 1.5 ml aliquots were dispensed into 35 mm Petri dishes. Media was cooled and allowed to set at RT for 2 hours (Chapman *et al*, 2001).

Embryonic membranes were removed (in phosphate buffered saline [PBS]) from harvested (older) embryos, to avoid probe trapping when performing *in situ* experiments. Embryos were then fixed overnight in 4% paraformaldehyde (PFA)/PBS at 4°C. Following fixation, embryos were washed twice in PBST (PBS with 0.1% Tween-20) for 5 min at RT and then dehydrated in ascending concentrations of methanol/ PBS (25%, 50%, 75% and twice in 100%, 5 min each). Embryos were preserved and stored in 100% methanol at -20°C ready for future use.

Note: if subsequent microtubule immunostaining was required embryos were harvested and fixed as quickly as possible to avoid microtubule depolymerisation (see Somite Wholemount Immunostaining).

2.6. Cryosectioning

Previously fixed (and some already hybridised) embryos were washed twice in 1% PBS for 5 min at RT, then subjected to 30% sucrose/PBS solution for

3-4 h with gentle rotation. Next, embryos were embedded (following adjustment to appropriate position for plane of sectioning) in OCT (Miles, Inc.) overnight at -20°C. Embryos were sectioned at 15-20 µm using a Leica Cryostat at -20°C. Sections were transferred to Tespa treated slides and dried at RT. Sections were subsequently washed twice in 1% PBS (to remove OCT residue), rinsed in distilled water, (immunostained if necessary) then mounted in hydromount and covered with cover slides. Subsequent microscopy was performed using an upright microscope (Zeiss). Images were captured and analysed using AxioVision software.

2.7. Embryo Section Immunofluorescence Staining

Embryos were incubated in microtubule assembly buffer (BRB: 80 mM KPipes, pH 6.8; 5 mM EGTA; 1mM $MgCl_2$) containing 3.7% formaldehyde, 0.25% glutaraldehyde and 0.2% TritonX-100) for 2-4 h, followed by postfixation in absolute methanol at -20°C overnight. Embryos were then rehydrated in PBS and incubated for 6-10 h at RT in PBS containing 100mM $NABH_4$. Embryos were rised extensively in Tris-buffered saline (TBS: 155mM NaCl, 10mM Tris-Cl, pH 7.4, 0.1% NP-40), and then cryosectioned as described above.

Following sectioning, slides were washed 6 x 5min in PBS, washed in PBS/0.1% TritonX-100 for 10 min, and blocked in PBS, 5% BSA, 5% goat serum for 1 h. Next, primary antibody (α-tubulin) was applied (1:100) in block o/n at 4°C. Sections were washed 3 x 10 min in PBS, secondary antibody was applied (anti-rat Alexa fluor 488 1:500) for 1 h at RT, slides were washed again 3 x 10 min in PBS, and finally DAPI staining (1:10,000) and a 5 min PBS rinse. Sections were then mounted in hydromount with Dapco.

2.8. Somite Wholemount Immunostaining

To keep microtubule integrity intact, embryos were harvested individually (while remaining eggs were kept at 37°C) and put straight into fix (9ml methanol: 800µl formaldehyde) without removing membranes. Following

30min- 1h in fix, embryos were washed in PBS, 0.1%TritonX-100, and 1% goat serum. Next, using fine scalpels, somites were carefully excised from embryos and put into block PBS, 0.1%TritonX-100, and 10% goat serum for 2 h. Following block, somites were incubated o/n in primary antibody (α-tubulin, 1:100) at 4°C. Subsequently somites were washed for 2 h in PBS/1% goat serum and then incubated in secondary antibody (1:500) and, in some instances, propidium iodide (1:1000) for 2 h. More washing followed, PBS/1% goat serum for 1 h. Somites were then put in to 'slice culture' for microscopy (see below).

2.9. Somite Slice Cultures (Preparation for Microscopy)

Following electroporation and appropriate incubation at 37-39°C, embryos were harvested in Glutamax F12 media and injected somite(s) were dissected using fine scalpels. Agarose/media was simultaneously prepared. Low melting point agarose (0.2 g) was added to 17ml Glutamax F12 media and heated to 60°C (using a sterile thermometer to assess temperature) with continuous stirring. When 60°C was reached agarose/media was placed in 60°C water bath for 5 min to ensure agarose had completely dissolved. Once dissolved, solution was removed from water bath and allowed to cool to 40°C again with stirring. Foetal calf serum (3 ml), 500 μl penicillin:streptomycin and 200μl sodium pyruvate were then added when solution reached 40°C. The dissected tissue (somites) was positioned, dorsal side down, onto a Willco well (glass-bottomed dish) and warm agarose/media was gently dropped around and onto somite(s) until well was filled. The dish was then put on ice for 2 min to facilitate setting of agarose. Once set, sample was placed inside the microscope heat chamber (37°C) for 2-3 hrs to equilibrate ready for microscopy. If microscopy was not being performed within the next few hours Willco wells were placed into a sealed Petri dish, containing wet tissue, for up to 10hrs at 16°C.

Note: the same 'slice-culture' procedure was used for somites that were fixed and immunostained, however, PBS was used instead of F12 Glutamax media and no Foetal calf serum or sodium pyruvate was added.

2.10. Microinjection

Egg Preparation

Eggs were horizontally incubated at 37-39°C to the required embryonic stage. The upper side of the eggshell was reinforced with sellotape and 3-4 ml of albumen was withdrawn through the broad end of the egg using a syringe. Eggs were windowed; ink (diluted 1:10 with 1% PBS containing penicillin-streptomycin) was injected into the yolk underneath the embryo to increase its visibility. The vitellin membrane was removed at the site of manipulation.

Glass capillaries were drawn (1.0 mm O.D. x 0.78 mm I.D.; Harvard apparatus, UK) on a Vertical micropipette puller (P-30, Sutter Instrument Co., CA). To obtain an opening, the capillary tip was broken with tweezers (so it was fine as possible). The capillary was attached to a rubber tube with a mouth-piece (Sigma), and the DNA solution was aspired in the capillary and injected into the somite(s) by mouth. The capillary was inserted parallel to the neural tube through the tail bud, and carefully pushed into the somites I through IV (or V). DNA (~1μg/μl, mixed 1:1 with fast green) was injected into the somitocoele of somite IV (or V) by blowing, the capillary was retracted injecting each somite in turn (i.e. IV, III, II, I). DNA volume injected varied according to each experiment. Electroporation followed very soon after injection (no longer than 30 seconds).

Note 1: DNA constructs injected (and subsequently electroporated into developing somites) included pCAβ-GFP-tubulin, pCAGGs-GFP-GPI, and pCS2-Axin2 (kind gift from Prof. Andrea Streit, King's College, London).

Note 2: MACF1 transl. MO sequence: TCTCCTCGTCGGAGGACGACATGGC 3' Fluorescein (Supplied by Gene Tools, LLC). Control Morpholino was a generic control provided by Genetools, which they designed.

2.11. Electroporation

A total of 500 μl of 1% PBS containing penicillin-streptomycin was dropped onto the newly injected site and electrodes were positioned left and right of the embryo (flanking injected somites) at a distance slightly wider than the embryo itself. The anode was pressed carefully onto the surface of the extraembryonic membrane while the cathode was positioned slightly lower (into the yolk). Four square pulses of 65 V, 10-msec width were applied. As parameters, particularly voltage, can vary, they must be optimised for each experimental setup. To avoid coagulation of yolk/albumen, which can insulate electrodes, electrodes were gently washed in water/PBS between electroporations. The egg was then resealed with sellotape and re-incubated for required time (normally 12-16 h).

Electrodes were self-made both consisting of platinum wire. The wire on both electrodes was bent at a right angle to the tip (approximately 4mm in length) and insulated by nail polish on the underside of the tip. Insulation of the lower side prevented burning of the embryonic tissue. The electrodes were held in commercially available needle holders (Fine Science Tools for e.g.), which were insulated with thermoretractable plastic and connected to the pulse generator, which was equipped with a foot pedal to ease technique.

2.12. Expressed Sequence Tag (EST; MACF1/ACF7)

Clone (MACF1/ACF7: ChEST16M13), supplied by ARK-Genomics (http://www.ark-genomics.org), was provided as a stab in LB agar containing 50 µg/ml Ampicillin (Boardman *et al*, 2002). Stab was inoculated into a liquid culture of LB with 50 µg/ml Ampicillin and grown overnight at 37°C. To allow selection of individual clones, overnight culture was streaked onto LB agar containing 50 µg/ml Ampicillin and grown overnight at 37°C. Ten individual clones were selected and grown in LB, again containing 50 µg/ml Ampicillin, overnight at 37°C. Plasmid DNA was isolated (see small scale DNA preparations), diagnostic digests were performed and DNA was sent for

sequencing. Once verified, RNA riboprobe was synthesised and whole mount *in situ* hybridisation was performed.

2.13. Agarose Gel Electrophoresis

DNA and RNA samples, with the addition of the appropriate volume of 10x loading dye (4M Urea, 40% (w/v) sucrose, 120 mM Tris-HCl pH7.5, 30 mM EDTA, 0.25% (w/v) orange dye), were loaded onto agarose (Sigma) gels containing ethidium bromide (1 µg/ml). The gels were prepared and run in 1xTAE buffer. Electrophoresis was performed at 60 volts for 40 min. The concentration of agarose was 0.7%, except when expected fragments were small then agarose concentration was increased to 1%. DNA ladders, 100 bp and 1 kb, were used as a molecular weight markers.

2.14. Preparation of DH5α *Escherichia coli* competent cells

A 5 ml culture of bacterial strain, DH5α *E.coli*, in Luria Broth (LB) media was grown overnight at 37°C with constant shaking. The next day, 1 ml of bacterial culture was added to 200ml of LB in a sterile flask and grown again at 37°C with constant shaking till the optical density (OD) at 600 nm reached 0.3 – 0.4 (approximately 2 to 3 hours). Once desired OD was reached, the culture was divided into 4 x 50 ml falcon tubes and incubated on ice for 15 minutes. The cells were kept on ice from this step onwards. Following incubation, the cells were centrifuged at 4°C at 2000 rpm for 10 min. The supernatant was discarded and the pellet was resuspended in 16 ml TBI. The cells were further incubated on ice for 15 minutes and then centrifuged at 2000 rpm at 4°C for 10 min. The supernatant was discarded and the pellet was resuspended in 4 ml TBI. 200 µl aliquots were stored at -80°C.

2.15. Heat Shock Transformation

Plasmid DNA (~0.5-1µg/µl) was added to 100-200 µl competent DH5α *Escherichia coli* cells, mixed, put on ice for 15 min, subjected to 37°C for

exactly 5 min, and then returned to the ice for 2 min. Liquid broth (LB), 500 µl, was added, cells were gently inverted and incubated at 37°C for 1 h (inverting every 15 min). Cells were centrifuged for 2 min at 6500 rpm and 500-600 µl supernatant was removed and discarded. Pellet was resuspended in remaining 100 µl supernatant, plated onto LB agar plates with appropriate antibiotic in a sterile environment and then incubated overnight at 37°C.

2.16. Small Scale DNA Preparations (Mini Preps)

Desired *E. coli* (transformed with plasmid) were grown overnight on a shaker in 5 ml LB (supplemented with appropriate antibiotic) at 37°C. Cells from 1.5 ml overnight culture were collected by centrifugation (2 min at 14000 rpm) and resuspended in 100 µl of QIAgen solution I (50mM Tris/HCl pH 8; 10mM EDTA pH 8). Two hundred µl QIAgen solution II (200 mM NaOH, 1% SDS) was added and cells were inverted 4-6 times. QIAgen solution III (3M potassium acetate pH5.5), 200 µl, was subsequently added, cells were mixed immediately and collected by centrifugation (10 min at 14000 rpm). To precipitate DNA, supernatant was transferred to a fresh tube containing both 1 ml 100% ethanol and 50 µl 3M pH 5.2 sodium acetate. Following 1 h incubation at -20°C DNA was collected via centrifugation (10 min at 14000 rpm), supernatant was discarded and DNA pellet was washed in 1 ml 70% ethanol. To remove ethanol, pellet was centrifuged for a final time (1 min at 14000 rpm), ethanol was discarded, pellet was air dried for 10 min and then resuspended in 50 µl Sigma water.

2.17. Diagnostic Restriction Digests

Digests were carried out in 20 µl reactions. DNA volume depended on concentration following elution. Appropriate restriction enzymes (1 µl of each) and buffer (1/10 of the final volume) were added and final digest volume was attained via the addition of sterile water. Reaction was mixed and incubated

at 37°C for 2-3 h. Loading dye (10X), 2 µl, was added, and reaction was assessed using agarose gel electrophoresis.

2.18. Sequencing

Constructs, 15 µl mini prep with 15 µl Sigma water, were sent for sequencing (The Sequencing Service, University of Dundee, Dundee, Scotland, DD1 5EH) to facilitate verification of the correct gene (gene fragment). Returned sequences were subjected to BLAST searches (available at http://www.ncbi.nlm.nih.gov/BLAST/) and, in addition, EST sequence was matched to EST library (available at www.chick.manchester.ac.uk).

2.19. RNA Probe Synthesis

The plasmid containing the EST (gene fragment) was linearised by restriction digest, using an appropriate downstream restriction enzyme (see table 2.2). The digest, consisting of approximately 5 µg DNA, 5 µl 10X buffer, 1 µl restriction enzyme, and made up to a final volume of 50 µl with Sigma water, was incubated at 37°C for 2-3 h and analysed via gel electrophoresis. Phenol/chloroform extraction was then performed to purify linearised DNA. Sigma water was added to DNA to increase volume to 100 µl. Phenol/chloroform (100 µl) was added; DNA was thoroughly vortexed and centrifuged at 14000 rpm for 5 min. The upper aqueous layer was transferred to an Eppendorf containing an equal volume of chloroform with isoamyl alcohol. This was again vortexed and centrifuged for 5 min at 14000 rpm. Upper aqueous phase was transferred to a new Eppendorf. One tenth volume of 3M sodium acetate (pH 5.2) and 3 volumes of 100% ethanol were added and 1 h incubation at -20°C followed to allow precipitation of DNA. Following incubation, DNA was collected by centrifugation at 14000 rpm for 30 min, supernatant was removed, and pellet was washed in 500 µl 70% ethanol and centrifuged again to allow complete removal of ethanol. Pellet was air dried for 10 min and resuspended in 30 - 50 µl Sigma water. DNA concentration was assessed via gel electrophoresis and synthesised into

probe according to the following conditions: 4 µl transcription buffer, 1 µl DIG mix (labelled UTPs), 2 µl Dithio threitol (DTT), approximately 1 µg linearised and purified DNA template, 1 µl RNase inhibitor and 1 µl of appropriate RNA polymerase (T3, T7 or SP6 depending on orientation in plasmid- see table 2.2), and made up to 20 µl with Sigma water. Following brief centrifugation mixture was incubated for 2-3 h at 37°C, analysed via gel electrophoresis and diluted with 30 µl RNase free H_2O. Unincorporated UTPs were removed by G50 column centrifugation, according to manufacturer's protocol. Finally, transcription efficiency and probe quality was assessed by gel electrophoresis and 5 µl of probe was added to hybridisation buffer (see *In Situ* Hybridisation) for long-term storage at -20°C.

Table 2.2. Summary of constructs including enzymes used for linearisation and polymerases used for anti-sense probe transcription.

Construct	Plasmid	Restriction enzymes to linearise plasmid	Primer used for sequencing	Polymerase used to transcribe anti-sense probe	Construct source
Wnt3a	pGem	BamHI	-	SP6	ISH probe supplied by D. Sweetman, UEA, Norwich
Wnt11	pGem	-	-	-	ISH probe supplied by M. Abu-Elmagd, UEA, Norwich
MACF1/ACF7 chEST16M13	pBluescript II KS+	SacI	T7	T3	EST (Boardman *et al*, 2002)

- \- unknown

2.20. In Situ Hybridisation

For hybridisation, (stored) embryos were rehydrated in descending concentrations of methanol/PBS (75%, 50%, 25%, 5 min each) and then washed twice in PBST for 5 min at RT. Most embryos did not require proteinase K treatment owing to their HH stage. However, embryos between Stage HH25 – HH31 were treated with 10-20 µg Proteinase K for 25-40 min, depending on the Stage. These particular embryos were then fixed in 4%

PFA with 0.1% glutaldehyde for 20 minutes and rinsed in PBT with rocking. Following washing, all embryos (including those not treated and those treated with Proteinase K) were put in 1:1 PBST/hybridisation buffer (50% formamide, 1.3X SSC [pH 5], 0.5% CHAPS, 0.2% Tween-20, 5mM EDTA [pH 8], 100 µg/ ml heparin, 50 µg/ ml yeast tRNA, made up to required volume with DEPC-H_2O) and allowed to settle. Embryos were transferred to hybridisation buffer and again allowed to settle. Hybridisation buffer was changed again and embryos were incubated at 65°C for 1 h. Hybridisation buffer was replaced for a final time with pre-warmed hybridisation buffer containing desired RNA probe (1µg RNA probe/ 1 ml hybridisation buffer- see 2.19. RNA probe synthesis) and embryos were incubated overnight at 65°C. Probe was removed (and stored for future use) and embryos were washed twice in hybridisation buffer for 10 min at 65°C, four times in wash buffer (50% formamide, 1X SSC, 0.1% Tween-20, made up to required volume with DEPC-H_2O) for 30 min at 65°C, once in 1:1 wash buffer/ MABT (100mM maleic acid, 150mM NaCl [pH 7.5]) for 10 min at 65°C and twice in MABT for 10 min at RT. To prevent non-specific antibody binding embryos were then incubated in MABT/ 2% BBR (blocking reagent) for 1 h at RT and MABT/ 2% BBR & 20% goat serum for 2.5 h at RT. Subsequently, embryos were incubated overnight in MABT/ 2% BBR/ 20% goat serum & anti-DIG-AP antibody (1:2000) at 4°C with rocking.

Antibody solution was discarded but to ensure complete elimination of excess antibody embryos were washed five times in MABT for 1 h at RT with rocking and then in MABT overnight at 4°C with rocking. Embryos were then washed twice in NTMT buffer (0.1M Tris[HCl] pH 9.5, 50mM $MgCl_2$, 0.1M NaCl, 1% Tween-20, made up to required volume with distilled H_2O) for 10 min at RT. Finally, for colour development embryos were incubated in the dark in NTMT buffer containing 7µl/ ml BCIP (50 mg/ ml in dimethyle formamide [DMF]) and 9µl/ ml NBT (75mg/ ml in 70% DMF) until desired colour was reached. Colour reaction was stopped via 2 PBST washes for 5 min at RT and embryos were stored in 4% PFA/ PBS ready for analysis and sectioning. If background colour was present after colour development embryos were washed overnight in 5X TBST (for 500 ml 10X: 40 g NaCl, 1 g

KCl, 125 ml 1M Tris[HCl] pH 7.5, 50 ml Tween-20, made up to 500 ml with distilled H_2O) and either fixed or further developed. Embryos were imaged with an upright microscope (Leica MZ 16F).

2.21. Cell Transfection

Cells were split into 75 ml flasks. Lipofectamine 2000, 10 µl, was added to DMEM and incubated at room temperature. siRNA (50nmol) was added to 500 µl DMEM and then added to Lipofectamine 2000 solution. Following incubation at room temperature for 20 minutes, cells were washed twice with 1 ml DMEM, which was then replaced with 10 ml DMEM per flask. Transfection mix was added to the cells, drop by drop, and they were incubated for 5 hours. Next, the DMEM with the transfection mix was replaced with 10 ml DMEM containing 10% FBS and penicillin-streptomycin solution.

Table 2.3. Pre-designed siRNAs against mouse MACF1/ACF7 supplied from Applied Biosystems, LifeTechnologies.

siRNA	ID ♯	Sense	Antisense
MACF1/ACF7 siRNA1	s232033	GCAGAUUGCAAACAAGAUAtt	UAUCUUGUUUGCAAUCUGCag
MACF1/ACF7 siRNA2	s232031	GGAUAGUAUGCAUAAGGGAtt	UCCCUUAUGCAUACUAUCCag

2.22. Cell Protein Isolation and Quantification

C2C12 cells were washed twice in PBS and harvested with a scraper. Next, the cells were centrifuged for 5 min at 1000 rpm; the resulting pellet was resuspended in 1ml PBS, and then centrifuged again for 5 min at 1000 rpm. The pellet was resuspended in the equal volume of NP-40 lysis buffer*,

vortexed, left on ice for 30 minutes, and then centrifuged for 30 minutes at 4500 rpm. The supernatant containing protein was transferred into a fresh Eppendorf tube. Protein quantification was performed using a spectrophotometer and BioRad Assay Bradford Reagent.

* NP-40 lysis buffer: 150 mM NaCl, 1% NP-40 (IGEPAL), 50 mM Tris-HCl pH 8.0, Sigma water (up to 100ml), 1 tablet of Protease Inhibitor Coctail Complete (Roche) was also added to 1 ml of the lysis buffer.

2.23. Western Blot Protocol

20 µg of cell lysate was added to loading buffer and denatured at 85°C for 5 minutes. Next, samples were loaded on 8% polyacrylamide gels and run at 100V for ~ 2 hours. Following electrophoresis, samples were blotted onto nitrocellulose using a semidry blotter (Biorad). Membrane was blocked in 10% normal goat serum (GS) for 1 hour at room temperature. Primary antibody diluted 1:500 in 10% GS was applied for one hour at room temperature, the excess was washed off and secondary antibodies coupled to HRP (Jackson Laboratories) were applied (1:1000) for one hour at room temperature. Primary antibody used: MACF1/ACF7. Protein expression was detected via chemiluminescence, the membrane was incubated with 250 mM ECL (Sigma) and 90 mM β-coumaric acid (Sigma) in Tris-HCl pH 8.5 and imaged on a Fujifilm LAS 3000 imager (Fuji Photo Film Co., Ltd).

2.24. Embryo Wholemount Immunostaining (MF20)

Embryos were harvested as previously described and during an ISH or mock ISH experiment, MF20 immunostaining was performed. That is, at the end of day 2 of an ISH experiment (i.e. when embryos are incubated overnight in MABT/ 2% BBR/ 20% goat serum & anti-DIG-AP antibody) MF20 antibody (1:50) or MF20 supernatant (1:8) was added. ISH proceeded and then consequent to fixing (i.e. when the ISH was finished) embryos were put into secondary antibody overnight in PBST.

2.25. Preparation of Cells for Subsequent Microinjection into Embryos

Mouse Wnt3a-expressing (supplied by Dr. Jan Kitajewski, Columbia University, New York, 10032; Münsterberg, *et al*, 1995b) and mouse Wnt11-expressing (supplied by Dr. Chen-Ming Fan, Carnegie Institution of Washington, Baltimore, MD 21218) rat fibroblasts were isolated with trypsin and allowed to recover for 1 h at RT in 20% FBS-containing medium. They were centrifuged and resuspended in a solution comprising of 10% sucrose, 10% CM-DiI (Molecular Probes) and 10% ethanol. Following 15 min incubation at 37°C, the cells were resuspended in a large volume (approximately 10ml) of PBS and then pelleted. Cells were then resuspended in as little as 10µl PBS and then injected into somites or between two somites using a pressure injector (Microinjector, Eppendorf FemtoJet). In each experiment empty vector-containing parent cells (LNCX2 lentiviral backbone) were also injected.

Note: When fibroblasts were injected simultaneous to electroporation, injection of DNA construct was as described above (i.e. with a mouth pipette), followed by electroporation and finally by cell injection with the pressure injector.

2.26. Microscopy

Widefield inverted microscopy was performed using a Zeiss Axiovert 200M with AxioCam MRm CCD camera. Using AxioVision software.

- Green channel: Excitation = 469 ± 17.5 nm; Emission = 525 ± 19.5 nm
- Red channel: Excitation = 559 ± 17 nm; Emission = 630 ± 34.5 nm

Inverted confocal two-photon (multi-photon) microscopy* was performed using a LaVision Biotec TriM Scope II with Coherent Vision II Ti:Sapphire pulsed laser. Using LaVision's ImSpector software.

- GFP somite time-lapse experiments: Excitation = 840nm; Emission = 525 ± 25 nm
- Somite Z stack with propidium iodide: Excitation = 870nm; Emission = 525 ± 25 nm and 620 ± 30 nm

*** All multi-photon microscopy was performed by Dr. Paul Thomas.**

Chapter 3: Cytoskeletal Arrangement in Primitive Streak Cells

Introduction

3.1. The Cytoskeleton

The cytoskeleton, which extends throughout the cell, is a complex network of protein filaments. It is composed of three distinct elements: actin, microtubules and intermediate filaments. Intermediate filaments are thought to be the most rigid component of the cell and are responsible for maintaining the cells overall shape. The actin cytoskeleton is known to provide protrusive and contractile forces, whereas microtubules form polarised networks that allow protein and organelle movement throughout the cell (Etienne-Manneville, 2004). The cytoskeleton is highly dynamic and undergoes continuous reorganisation. This reorganisation allows the cell to change shape, to divide, and to participate in directed migration. To achieve such complex cellular functions cytoskeletal elements must be co-ordinately regulated. Co-ordination is accomplished via signalling pathways that, as previously stated (see 1.1. Cell Migration and the Cytoskeleton), involve common regulators such as the Rho GTPases (Etienne-Manneville & Hall, 2002; Etienne-Manneville, 2004). Accruing evidence demonstrates that the cytoskeletal elements themselves can also directly affect these signalling pathways (see Watanabe *et al*, 2005) and furthermore these elements can regulate each other. Thus their functions are in fact overlapping, with actin involved in membrane trafficking and microtubules playing a role in the control of protrusive and contractile forces (Etienne-Manneville, 2004).

3.2. Actin and Microtubule Structure and Functions

Actin is the most abundant protein in many eukaryotic cells (Pollard and

Borisy, 2003). It is a globular multi-functional protein that can exist as either a free monomer, so-called G-actin, or as part of a microfilament named F-actin (Alberts *et al*, 2002). Actin filaments comprise of double helical polymers of globular subunits (G-actin monomers) all arranged head-to-tail. They are intrinsically polarised with fast-growing 'barbed' ends and slow-growing 'pointed' ends. This polarity is fundamental to the mechanism of actin assembly (Pollard and Borisy, 2003) and is used to drive cell membrane protrusion (Ridley *et al*, 2003). The organisation of actin filaments, however, depends on the type of membrane protrusion: in filopodia filaments are organised into long parallel bundles, while in lamellipodia they form a branching network (Ridley *et al*, 2003).

Filopodia protrusion occurs by a filament 'treadmilling' mechanism, wherein actin filaments within a bundle elongate at their 'barbed' ends and liberate actin monomers from their 'pointed' ends. In lamellipodia, however, the Arp2/3 complex mediates actin polymerisation. It is a seven-subunit assembly and two of its subunits, the Actin-Related Proteins ARP2 and ARP3, serve as nucleation sites for new actin filaments (Gournier *et al*, 2001). The complex binds to the sides or the tip of a pre-existing filament and induces the formation of a new filament, which braches from the pre-existing filament (Pollard and Borisy, 2003; Ridley *et al*, 2003). Intrinsically inactive, the Arp2/3 complex relies on nucleation promoting factors for activation. Activation is localised by Wiskott-Aldrich syndrome protein (WASP) family members (WASPs and WAVES/SCAR), which are well-known cellular nucleation promoting factors (Higgs and Pollard, 2001; Pollitt and Insall, 2009). These WASP/WAVE activators are themselves the main targets of Rac and Cdc42, Rho GTPases that are required for the protrusion of lamellipodia (and filopodia; see 1.1. Cell Migration and the Cytoskeleton). In protrusions, numerous actin-binding proteins regulate the rate and organisation of actin polymerisation by altering the pool of available monomers and free ends. Profilin, for example, prevents self-nucleation by binding to actin monomers and also acts to selectively target monomers to 'barbed' ends. Capping proteins terminate filament elongation thus restricting polymerisation to new filaments close to the plasma membrane. Additionally,

proteins of the actin-depolymerising factor (ADF)/cofilin family sever filaments and promote actin dissociation from the ‘pointed’ end. The disassembly of older filaments is required to generate actin monomers for polymerisation at the front end (dos Remedios *et al*, 2003; Ridley *et al*, 2003).

Microtubules are highly dynamic structures that are ubiquitously present in all eukaryotic cells. In dividing cells they are the core components of the mitotic spindle. In interphase and terminally differentiated cells they form a scaffold crucial for the maintenance of cell morphology, distribution, intracellular transport, cell polarisation and motility. Microtubules are stiff, cylindrical hollow tubes composed of thirteen protofilaments of α- and β-tubulin heterodimers organised in a head-to-tail fashion. The polarised arrangement of the tubulin dimers gives the microtubule a molecular polarity with a fast growing ‘plus’ (β-tubulin) end and a slow growing ‘minus’ (α-tubulin) end (Etienne-Manneville, 2010; Jaworski *et al*, 2008; Watanabe *et al*, 2005). Microtubule polymerisation occurs by head-to-tail addition of α-β tubulin heterodimers. Each heterodimer includes an α-tubulin that is constitutively associated to a stable guanosine-5’-triphosphate (GTP) and a β-tubulin that cycles between a GTP-bound form and a guanosine diphosphate (GDP)-bound form (Etienne-Manneville, 2010; Mitchison and Kirschner, 1984). The hydrolysis of GTP to GDP at this site has an important effect on microtubule dynamics (see figure 3.1). Binding of GTP to β-tubulin and then integration to the protofilament straightens the dimer, which facilitates extension (Wang and Nogales, 2005). The tubulin dimer further straightens subsequent to association with the microtubule wall (Rice *et al*, 2008). Thus, growing microtubule plus-ends are formed of GTP-bound dimers included in straight protofilaments that organise as a sheet before making a hollow tube (Gardner *et al*, 2008). Hydrolysis of the GTP occurs after polymerisation (and usually when the dimer is incorporated within the microtubule). Protofilaments are more prone to depolymerisation when dimers are bound by GDP as they exhibit increased curvature. The protofilaments, in the absence of GTP-bound tubulin at the end of the microtubule, curve outwards and depolymerise rapidly (Etienne-Manneville, 2010). Delayed hydrolysis of the GTP, when the microtubule is growing rapidly, results in the existence of

a ‘GTP-cap’. It is believed that the GTP-cap stabilises the open sheet formation of the growing plus-ends and prevents microtubule shrinkage and catastrophe (Chretien *et al*, 1999).

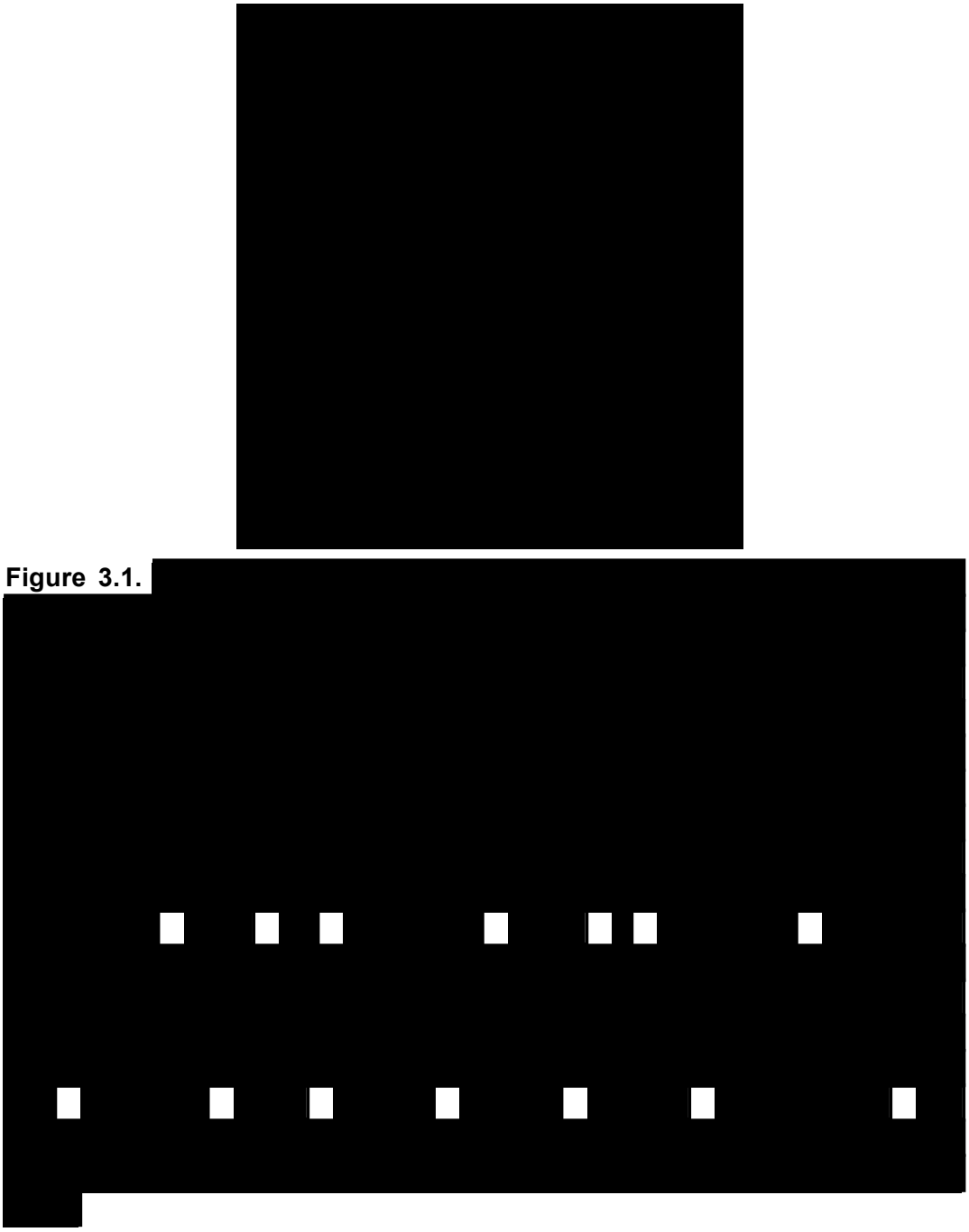

Figure 3.1.

In interphase animal cells, the microtubule network usually extends as a radial array from the microtubule-organising centre (MTOC), where microtubule minus-ends are predominantly anchored and plus-ends extend

toward the cell periphery. To facilitate frequent exploration of the cytoplasm microtubule plus-ends display dynamic instability. This is an essential process that encompasses a succession of slow polymerisation and rapid depolymerisation phases that are separated by transitions. The transition between polymerisation and shortening of the microtubule is known as a catastrophe, while the transition between depolymerisation and growth is termed a rescue. Dynamic instability enables microtubules to search and find various architectural elements of the cell. It is through this process that microtubule plus-ends are captured and stabilised at target destinations (Etienne-Manneville, 2010; Gunderson & Cook, 1999; Howard and Hyman, 2003; Mitchison and Kirschner, 1984; Watanabe *et al*, 2005). Transiently stabilised microtubules may function as markers for cell polarity or act to stabilise a cellular protrusion or extension (Siegrist and Doe, 2007). Serving as preferential tracks for intracellular transport, stabilised microtubules may also allow localised delivery within the cell (Jaworski *et al*, 2008). Microtubules that are locally captured may transmit a force between the cell cortex and the MTOC, which in turn might facilitate cell polarisation (Levy and Holzbaur, 2007).

Microtubule search and capture is fundamental for generating an asymmetrical microtubule array and maintaining cell shape (Kirschner and Mitchison, 1986; Mimori-Kiyosue and Tsukita, 2003). Non-migrating cells, as previously stated, have radial microtubule arrays that are anchored at a centrally located MTOC. Migrating cells, however, exhibit selective stabilisation of the plus-ends of microtubules (i.e. at the cell cortex within the advancing lamellipodium). This enables the MTOC to reorient towards the leading edge, which results in a polarised microtubule array that facilitates cell migration.

3.3. Cell Migration

(See 1.1. Cell Migration and the Cytoskeleton)

3.4. Microtubule End Binding Molecules

The polarised organisation, dynamics, and functions of microtubules are likely to reflect a differential distribution of microtubule-associated proteins (MAPs), predominantly microtubule end binding molecules (Eteinne-Manneville, 2004). Microtubule end binding proteins can be divided into microtubule plus-end tracking proteins (+TIPs) and microtubule destabilising factors, Kin I kinesins for example (Akhmanova and Hoogenraad, 2005). Kinesins, a large superfamily of microtubule motor proteins, use energy from adenosine-5'-triphosphate (ATP) hydrolysis to produce force. Kin I kinesins function as microtubule depolymerases that disassemble microtubules in an ATP-dependent fashion. They have the ability to target (and consequently depolymerise) microtubule ends. Interestingly Kin N and Kin C kinesins, however, have a higher affinity for the microtubule lattice and translocate toward the plus-ends and minus-ends of microtubules, respectively (Ovechkina and Wordeman, 2003).

3.5. Microtubule Plus-End Tracking Proteins (+TIPs)

In short, +TIPs are evolutionarily conserved proteins that mediate the interaction between microtubules and numerous subcellular structures (actin, organelles, and the cell cortex for example) and can help to locally concentrate regulatory molecules (Eteinne-Manneville, 2010). They encompass structurally unrelated proteins including microtubule motors, motor-cargo adaptors and non-motor MAPs. When compared to other MAPs, their distinguishing feature is their specific accumulation at the plus-ends of growing microtubules: in mammalian cells +TIPs form transient comet-like accumulations at the growing, but not depolymerising plus-ends of microtubules (Akhmanova and Hoogenraad, 2005; Lansbergen and Akhmanova, 2006a). This dynamic localisation was originally discovered via the live observation of the behaviour of the cytoplasmic linker protein-170 - green fluorescent protein (CLIP-170 - GFP) fusions, which appeared as comet-like structures coinciding with the tips of polymerising microtubules

(Perez *et al*, 1999). Most +TIPs can bind directly to microtubules, but the mechanism of their dynamic plus-end localisation remains to be fully elucidated. Numerous microtubule plus-end binding factors, yeast CLIP-170 homologues for example, are delivered to the tip of the microtubule by kinesin motors (Busch *et al*, 2004; Carvalho *et al*, 2004). Yet the mammalian CLIP-170 (Folker *et al*, 2005; Komarova *et al*, 2005; Perez *et al*, 1999), and many of the known +TIPs, seems to be stationary regarding the microtubule lattice: data collected using fluorescent speckle microscopy indicates that +TIPs attach to the freshly polymerised microtubule end and then detach gradually from the older part of the microtubule. This suggests that +TIPs either co-polymerise with tubulin (and consequently incorporate at the growing microtubule plus-ends), or that they have an increased affinity for the plus-end owing to its distinct biochemical and/or structural state (Dixit *et al*, 2009; Lansbergen and Akhmanova, 2006a). Through binding to the microtubule ends, +TIPs can alter the microtubules structure and accessibility for interaction with other proteins. Many +TIPs function to stabilise microtubules: dynamically (via reduction of the number of catastophes or promotion of repeated rescues), or by being captured in a paused state (Akhmanova and Hoogenraad, 2005). Proteins of the CLIP-170 family can act as anti-catastrophe (Brunner and Nurse, 2000) or rescue factors (Komarova *et al*, 2002) and, therefore, are implicated in microtubule stabilisation (Carvalho *et al*, 2004). Furthermore, CLIP-170 and its homologues are capable of promoting microtubule capture at cortical sites via direct interaction with dynein-dynactin (Goodson *et al*, 2003; Lansbergen *et al*, 2004).

CLIP-170 was the first +TIP identified (Perez *et al*, 1999; Pierre, *et al*, 1992). More than twenty structurally unrelated +TIP proteins have since been recognised, some of which have been shown to interact with one another and may even form higher order plus-end complexes (Akhmanova and Hoogenraad, 2005; Akhmanova and Steinmetz, 2010). End-binding (EB) proteins represent the key components of +TIP networks as, unlike most +TIPs, they can track microtubule plus-ends in an autonomous manner independently of any binding partners (Bieling *et al*, 2007; Dixit *et al*, 2009).

Furthermore, EB proteins directly interact with the majority of all other known +TIPs and, by doing so, target them to growing microtubule plus-ends (see Akhmanova and Steinmetz, 2010). In cells, EB proteins typically promote microtubule dynamics and growth, and suppress catastrophes (Komarova *et al*, 2009). There are three mammalian EB proteins: EB1, EB2, and EB3. To date, most functional analyses have focused on EB1. EB1 directly stimulates microtubule nucleation and growth by assisting the integration of tubulin dimers and promotes microtubule sheet closure through strengthening the lateral interactions between straight adjacent protofilaments (Vitre *et al*, 2008). In mouse fibroblasts, depletion of EB1 promotes microtubule pausing and decreases the time microtubules spend in growth (Kita *et al*, 2006). EB1, additionally, acts as a loading factor of other +TIPs (Dixit *et al*, 2009; Etienne-Manneville, 2010). Less is known about EB2 and EB3, although analysis in differentiating muscle cells has illustrated a specific function of EB3 (Straube and Merdes, 2007, see Chapter 4 Discussion).

Synonymous to CLIP-170 other +TIPs (cytoplasmic linker associated proteins [CLASPs], adenomatous polyposis coli [APC], and microtubule and actin crosslinking factor-1/actin crosslinking factor-7 [MACF1/ACF7]) participate in cortical capture and microtubule stabilisation, possibly via interactions with the actin cytoskeleton or the plasma membrane (Akhmanova and Hoogenraad, 2005). For example, CLASP1/2, APC (maybe in a complex with EB1 and mDia), MACF1/ACF7 and CLIP-170 (in a complex with IQGAP [a Rac1/Cdc42 effector]) were shown to stabilise microtubules at the leading edges of motile cells (Akhmanova *et al*, 2001; Fukata *et al*, 2002; Kodama *et al*, 2003; Wen *et al*, 2004). Both CLASP/Orbit/MAST and APC stabilise microtubules in axonal growth cones (Lee *et al*, 2004; Zhou *et al*, 2004) and in mitotic spindles (Dikovskaya *et al*, 2004; Inoue *et al*, 2004). CLASPs attach microtubule plus-ends to the cell cortex through a complex with LL5ß (Lansbergen *et al*, 2006b). Other +TIPs can interact with actin fibres: either directly, spectraplakins like MACF1/ACF7 for example (Applewhite *et al*, 2010; Kodama *et al*, 2003), or with the requirement of intermediary factors (Fukata *et al*, 2002). Finally, Short stop (the *Drosophila* homologue of MACF1/ACF7) and Orbit/MAST regulate the interactions

between microtubules and the fusome (a specialised membranous structure) during oogenesis (Mathe *et al*, 2003; Röper and Brown, 2004).

To highlight the importance of +TIPs, further examples of their functions include (but are not limited to), a role in coordinating microtubule attachment and dynamics at kinetochores (CLIP-170, CLASPs, dynein and Dam1 for example; see Maiato *et al*, 2004), they contribute to loading cargo for minus-end directed microtubule transport (dynactin, CLIP-170; Lomakin *et al*, 2009) and many accumulate at MTOCs where they may play a role in microtubule nucleation and anchoring (see Bettencourt-Dias and Glover, 2007 [Akhmanova and Steinmetz, 2010]).

In conclusion, accruing evidence demonstrates that +TIPs play important roles in several aspects of cell functioning. They can regulate microtubule dynamic instability either by promoting microtubule growth, stabilisation and pausing, or by inducing switches from depolymerisation to rescues or the reverse. They provide an interface for the interaction of microtubules with the cell cortex or the actin cytoskeleton, and are vital for intracellular transport and cellular structure positioning. Lastly and significantly, owing to their localisation, +TIPs can be used as tools for visualising microtubule dynamics in cells and tissues (Jaworski *et al*, 2008).

3.6. Avian Gastrulation and the Cytoskeleton

Recently, distinct patterns of cellular organisation have been demonstrated in different regions of the early chick embryo (Wagstaff *et al*, 2008). Following the establishment of a fixation and staining protocol that allowed the examination of microtubule arrays in primitive streak stage chick embryos (early to late Hamburger-Hamilton Stage 3; Hamburger & Hamilton, 1951), Wagstaff *et al* (2008) investigated cytoskeletal organisation in gastrulating embryos. Microtubule organisation, in cells along the length and width of the primitive streak and cells in the neighbouring epiblast, was characterised via confocal microscopy (figure 3.2A). At the tip of the streak cells were densely packed with disorganised microtubule networks. Many lacked central focus

and displayed non-radial arrays, which suggests most of the microtubules were not anchored at the MTOC (figure 3.2B and C). Posterior to the tip, various microtubule organisations were observed. Typical of migrating cells, the majority of cells in this region demonstrated polarised microtubule arrays, with microtubules organised in bundles that stretched along the full length of the cell (figure 3.2D, F, and G). Interspersed within the polarised cells, a few cells illustrated radial arrays with microtubules presumed to be anchored at a centrally located MTOC and their plus-ends projecting towards the cell periphery (figure 3.2E). Intriguingly, many of the cells demonstrating polarised microtubule networks were organised into groups of six or more cells. These groups of cells were arranged in a rosette-like structure, resulting in a regular pattern of cellular organisation within the central streak (figure 3.2D).

Figure 3.2.

In the examined HH Stage 3-4 embryos (n=15) approximately 20 rosettes appeared along the length of the streak. Most rosettes resided in the central region with a few in the anterior and occasionally 1 or 2 in the posterior regions. The majority of cells in the posterior region exhibited radial arrays (figure 3.2H). Some rosettes were also found in the outer edge of the streak in the boundary between streak and epiblast. Cells in the epiblast demonstrated a uniform organisation throughout, resulting in a regular appearance in this region. Like the posterior streak, most cells in the epiblast had radial microtubule networks (figure 3.2I and J). Three-dimensional reconstructions of the microtubule arrays within the rosettes showed that the tips of some cells were protruding from the plane of the rosette towards the hypoblast (see Wagstaff *et al*, 2008). Visualisation of the actin cytoskeleton (via rhodamin-conjugated phalloidin) within the primitive streak cells confirmed the organisation of six or more polarised cells into rosettes (figure 3.3A). In addition, it revealed a distinct accumulation of actin, converging at the centre of the rosettes, which is assumed to be the leading edge of the cells (figure 3.3A and B). Further 3D reconstruction showed that the actin containing tips protruded towards the hypoblast (figure 3.3C; Wagstaff *et al*, 2008).

Figure 3.3.

Aims

- To fix gastrulating chick embryos and investigate the localisation of cytoskeletal components and their interacting proteins (+TIPs for example) in cells within the avian epiblast and primitive streak.
- To examine the formation and resolution of previously described rosette structures (within the primitive streak) to determine their significance for directional movements. For example, does the organisation of cells into higher order structures facilitate their ingression during gastrulation?

Results

3.7 DF1 and ARPE-19 Immunofluorescence Staining

In order to characterise cytoskeletal proteins in gastrulating chicken embryos, the cross-reactivity of antibodies first had to be tested. DF-1 (chicken embryo fibroblasts) and ARPE-19 (human retinal pigment epithelial 'control' cells; kind gift from B. Tyrrell, UEA, Norwich) cells were fixed with methanol-MES and immunostained with various mouse, rat and rabbit antibodies (α-tubulin, γ-tubulin, APC, and EB1; see table 2.1). Figure 3.4 demonstrates both the cross-reactivity of all of these antibodies with chicken, and methanol-MES as an adequate fixative for each antibody. As expected, in both DF-1 and retinal epithelial cells, α-tubulin illustrates microtubule expression (figure 3.4A, A2, E and, E2), γ-tubulin illustrates the expression of centrosomes (or MTOCs; figure 3.4B and B2), APC appears throughout the cytoplasm and also at the junctions between ARPE-19 cells (figure 3.4C and C2), and EB1 is predominantly on the plus tips of microtubules (although some antibody has bound along the lengths of the microtubules; figure 3.4D, D2, E, and E2).

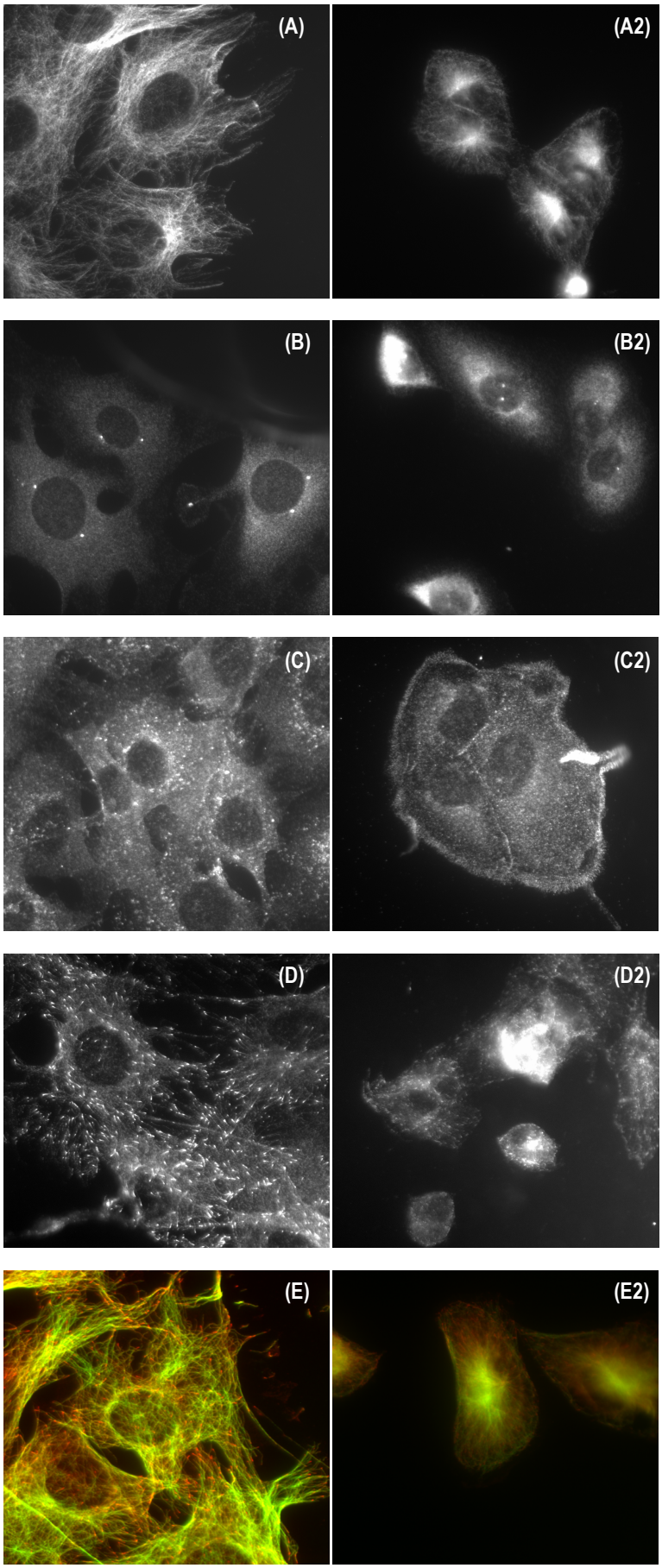
(A)
(A2)
(B)
(B2)
(C)
(C2)
(D)
(D2)
(E)
(E2)

Figure 3.4. DF-1 (chicken fibroblast) and ARPE-19 (retinal epithelial) cells fixed with methanol-MES and immunostained with various antibodies, including **A:** α-tubulin, **B:** γ-tubulin, **C:** APC, **D:** EB1, and **E:** α-tubulin (green) and EB1 (red). DF-1 cells are depicted in the left-hand column (**A**, **B**, **C**, **D**, and **E**), while corresponding ARPE-19 cells are depicted in the right-hand column (**A2**, **B2**, **C2**, **D2** and **E2**). For further experimental detail including specific antibodies and their usage please see materials and methods.

Next, to test the efficiency of PHEMO-fix with these cytoskeletal antibodies, DF-1 cells were fixed with PHEMO and immunostained with the same mouse, rat and rabbit antibodies (α-tubulin, γ-tubulin, APC, EB1, and, additionally, MACF1/ACF7; see table 2.1). Figure 3.5 demonstrates the cross-reactivity of the α-tubulin antibody with chick (figure 3.5A) and possibly the MACF1/ACF7 antibody (figure 3.5F). However when compared to fixation with methanol-MES it is apparent that PHEMO-fix interferes with the function of γ-tubulin, APC, and EB1 antibodies (compare figures 3.4 and 3.5).

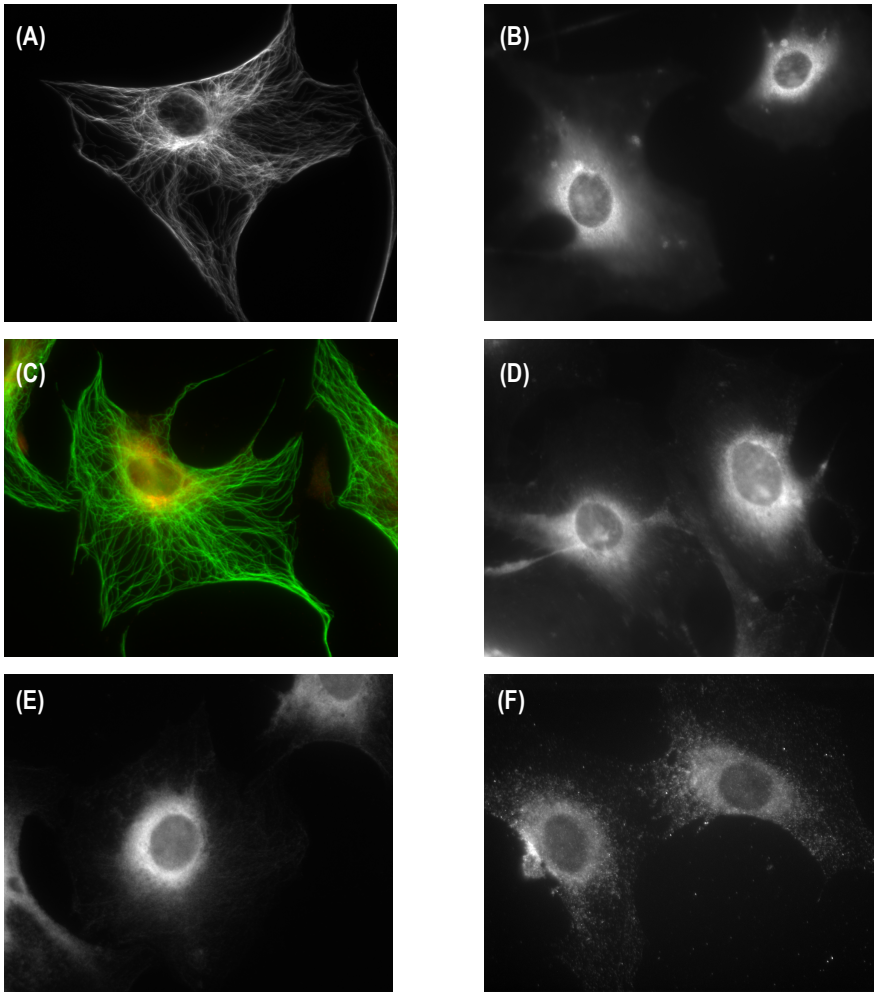

Figure 3.5. DF-1 (chicken fibroblast) cells fixed with PHEMO-fix and immunostained with various antibodies, including **A:** α-tubulin, **B:** γ-tubulin, **C:** α-tubulin (green) and γ-tubulin (red), **D:** APC, **E:** EB1, and **F:** MACF1/ACF7. For further experimental detail including specific antibodies and their usage please see materials and methods.

Since PHEMO-fix was shown to interfere with the function of several cytoskeletal antibodies (figure 3.5) it was anticipated that gastrulating chick embryos could be fixed with methanol-MES (or methanol alone) to allow investigation of the localisation of various cytoskeletal components. Several methods were attempted, including (combinations of) different concentrations of methanol-MES (or methanol only), varying incubation periods in fixative, and different temperatures while in fix. Unfortunately methanol and methanol-MES appeared to be too harsh a fixative for these embryo stages and embryo integrity was compromised using all of the below conditions (see table 3.1).

Table 3.1. Attempted methods of embryo (HH stage 3-4) fixation using methanol or methanol-MES.

Various methanol and methanol-MES concentrations	Attempted incubation times while in fixative (min)	Attempted temperatures during fixation (°C)
Absolute Methanol/10%Mes	6, 8, 10, 60, 240	-20, 4, 37
80% Methanol/10%Mes	6, 8, 10, 60, 240	-20, 4, 37
100% Methanol	6, 8, 10, 60, 240	-20, 4, 37
80% Methanol/PBST	6, 8, 10, 60, 240	-20, 4, 37

Discussion and Future Work

In 2001, using both transmission electron microscopy and scanning electron microscopy (TEM and SEM respectively), Lawson and Schoenwolf (2001a)

noted the organisation of cells (in all three germ layers) during the early stages of avian gastrulation. Studies aforementioned illustrated the microtubule organisation of cells in the epiblast and primitive streak during this morphogenesis (Wagstaff *et al*, 2008). Cells in the epiblast displayed mostly radial microtubule-arrays, while most cells in the streak had polarised microtubule networks consistent with cells undergoing directional migration. Additionally, cells in the streak organised into rosette-structures, which have been proposed to facilitate the co-ordinated movement and ingression of groups of cells through the streak (Wagstaff *et al*, 2008). At present, the functional significance of multicellular rosettes is not clear. It is interesting to note, however, that similar structures have been reported to form during migration in the lateral line primordium of zebrafish (Lecaudey *et al*, 2008) and during germband extension in *Drosophila* (Blankenship *et* al, 2006). Hair cell organ progenitors (proneuromasts) of the zebrafish lateral line primordium have been shown to form repeatedly as multicellular rosette structures that appear behind the leading edge of the migrating epithelial tissue (Lecaudey *et al*, 2008). Similarly, through live imaging studies, Blankenship *et al* (2006) reveal that intercalating cells in the *Drosophila* germband locally organise to generate multicellular rosette structures. Based on three lines of evidence, they suggest rosettes are associated with the fundamental cell behaviours that drive axis elongation. First, rosettes were shown to form and resolve in a directional fashion, which in agreement with structural changes at the tissue level, results in the convergence and extension of a cellular array. Second, the majority of germband cells were seen to participate in multicellular rosettes, and third, the frequency and directionality of rosettes was selectively disrupted in anterior-posterior-patterning mutants that were defective for axis elongation (*bicoid nanos torso-like* mutants for example). Blankenship *et al* (2006) further illustrate that, in intercalating cells, cytoskeletal and junctional proteins are polarised with respect to the axes of the embryo and are dynamically remodelled during rosette formation and resolution.

While different cellular movements are used during the ingression of avian primitive streak cells following EMT, during *Drosophila* germband extension,

and during migration in the zebrafish lateral line primordium, rosette formation appears important in all three processes. It is, therefore, not unreasonable to speculate that the formation of such higher order cellular structures co-ordinates cell behaviours during tissue reorganisation and morphogenesis. Further characterisation of multicellular rosettes in the avian primitive streak, particularly the cytoskeletal components of the cells belonging to them, is necessary to determine any significance for directional movements.

To further characterise the rosettes described in gastrulating chick embryos, it was anticipated that through the immunostaining of PHEMO-fixed embryos (as described by Wagstaff *et al*, 2008) it would be possible to investigate the localisation of additional cytoskeletal components and their interacting proteins (+TIPs for example). However, though it was possible to reproduce the results (data not shown) with regard to the microtubule cytoskeleton (shown previously by Wagstaff *et al*, 2008), the use of PHEMO-fix proved problematic (see below). It is also worth noting that embryo quality had a really important part to play in this approach. Poor quality (less robust) embryos that were harvested, for example in the winter months, rarely made it through this protocol intact.

The cross-reactivity of various mouse, rat and rabbit antibodies (specifically α-tubulin, γ-tubulin, APC, and EB1) has been demonstrated in chicken fibroblast cells (DF-1s) fixed with methanol-MES (figure 3.4). As expected, in both DF-1 and ARPE-19 cells, α-tubulin illustrated microtubule expression (figure 3.4A, A2, E and, E2), γ-tubulin demonstrated the expression of centrosomes (or MTOCs; figure 3.4B and B2), APC appeared throughout the cytoplasm and also at the junctions between ARPE-19 cells (figure 3.4C and C2), and EB1 was predominantly on the plus tips of microtubules (although some antibody had bound along the lengths of the microtubules; figure 3.4D, D2, E, and E2). Unfortunately however, the function of these antibodies (excluding α-tubulin) was impaired when cells were fixed with PHEMO-fix solution (figure 3.5).

As numerous antibodies were demonstrated to cross-react with methanol-MES fixed DF1-s, it was predicted that gastrulating chick embryos (HH Stage 3-4) could also be fixed with methanol-MES (and not PHEMO owing to it's destructive properties towards the majority of tested antibodies) to enable the investigation of the localisation of additional cytoskeletal components. Regrettably, despite numerous efforts this was not the case. Several methods were attempted, including (combinations of) different concentrations of methanol-MES (or methanol alone), varying incubation periods in fixative, and different temperatures while in fix (table 3.1). It became apparent that both methanol and methanol-MES are too harsh on such fragile embryos. It was, therefore, concluded that HH Stage 3-4 chick embryos and methanol or methanol-MES are not a good combination. Again, embryo quality had an important part to play in this assay.

Clearly, this assay requires further development. It is anticipated that the discovery of a methanol-based fixative that does not destroy HH3-4 Stage chick embryos would allow for further investigation of the cytoskeleton in multicellular rosettes. Additionally, in order to characterise rosettes more completely the localisation of microtubule interacting proteins, proteins involved in cell polarisation (RhoGTPases and APC for example), and Wnt pathway components (as Wnt signalling has been implicated in vertebrate gastrulation movements), would be of particular interest. Furthermore, following the establishment of protein localisation, interference with protein function using RNA interference (RNAi) experiments would reveal any affects on cell organisation. Other functional inhibition studies, such as the application of nocodazole (which interferes with the polymerisation of microtubules), could also be used to determine the role of polarised microtubule arrays in rosette formation and ingression movements.

Alternatively, the combination of electroporation of a GFP reporter construct in chick primitive streak cells and live time-lapse confocal microscopy, may prove an adequate assay to directly observe any changes in cell shape during the formation of rosettes. Additionally, electroporation of GFP fusions to cytoskeletal components (i.e. GFP-tubulin) or cytoskeletal interacting components (i.e. GFP-EB1) may enable visualisation of the cytoskeleton

during this process. A transgenic chick embryo where microtubules or cell membranes are labelled may also prove useful.

In conclusion, owing to the difficulties encountered, it was not possible to characterise the rosettes (or cytoskeletal components of the cells belonging to them) previously seen in gastrulating chick embryos. Thus, following numerous attempts and various methods, the decision was made to pursue the characterisation of the cytoskeleton (*in vivo*) within the somites of older, more robust embryos.

Chapter 4: Cell Dynamics and the Associated Cytoskeleton During Somite Morphogenesis

Introduction

During avian gastrulation as the primitive streak regresses and the neural folds begin to gather at the centre of the embryo, the thick bands of paraxial mesoderm that lie between the intermediate mesoderm and the axial structures separate into transient aggregates of cells, on either side of the neural tube, termed somites (Bellairs, 1963, 1979; Christ *et al* 1972, 1973; Christ and Ordahl, 1995; Gilbert, 2006; Packard, 1978). Somites, which give rise to all skeletal muscles in the vertebrate trunk, form in pairs in a rostral-caudal progression. As new somites form caudally, the more rostral somites (in response to extrinsic signals from their surrounding structures) mature and commit to forming certain cell types. During maturation and differentiation each somite divides into distinct regions: the dermomyotome, the sclerotome and the syndetome. The sclerotome generates the vertebrae and rib cartilage and the syndetome, which arises within the sclerotome, generates the tendons. The dermomyotome, however, consists of both dermatome and myotome. The dermatome generates the dermis of the back while the myotome produces the musculature of the back, ribs and limbs (Brand-Saberi *et al*, 1996; Brent *et al*, 2003; Gilbert, 2006; Kahane *et al*, 1998).

A newly formed somite comprises an outer epithelial layer that surrounds a central cavity named the somitocoele. Within a few hours of formation the ventral portion of the somite disaggregates into ventral mesenchyme (the sclerotome), while the medial wall and dorsal portion of the somite (the dermomyotome) remain epithelial. The medial wall subsequently folds under the dermomyotome initiating formation of primitive skeletal muscle (the

myotome). The dorsomedial lip (DML), the medial border of the dermomyotome, remains epithelial for a significant period of time during which it generates muscle cells that contribute to myotome growth. Notably, during early embryonic muscle development DML progenitor cells can adopt two fates: to self-renew and remain in the epithelial border of the dermomyotome or to translocate in the myotome and terminally differentiate (Gros *et al*, 2004; Ordahl *et al*, 2001; Rios *et al*, 2011). Limb and girdle muscles derive from progenitors in the lateral dermomyotome, which migrate into the limb mesenchyme prior to undertaking myogenic differentiation. During later embryogenesis muscle masses separate into deep back (epaxial) and abdominal and appendicular (hypaxial) muscles. The dermomyotome is composed of proliferative polarised epithelial cells that express dermomyotome-specific genes (such as *Pax3* and *Pax7*). However, the early myotome comprises postmitotic myocytes, observed as mononucleated elongated cells aligned parallel to the embryonic axes, which express muscle-specific genes (Myogenic Transcription Factor, *Myf5* for example). Evidently, myotome formation is a highly coordinated process that combines cell migration from the dermomyotome into the myotome, changes in cell shape together with an arrest of the cell cycle, and the activation of muscle-specific genes (Gros *et al*, 2004).

4.1. Myotome Morphogenesis

Myotome morphogenesis has been comprehensively studied (Cinnamon *et al*, 1999, 2001; Denetclaw *et al*, 1997, 2001; Denetclaw and Ordahl, 2000; Kahane and Kalcheim, 1998; Kahane *et al*, 1998a, 2001, 2002; Ordahl *et al*, 2001; Venters and Ordahl, 2002). During the late 1990's, it was well established that the myotome precursor cells translocate from the dermomyotome to form the underlying myotome (Kahane *et al*, 1998b). Yet how these precursors were generated and stimulated to migrate remained contentious for a number of years. Despite the use of similar techniques and the same animal model (the chick embryo) two distinct models were proposed.

The first model, from Ordahl and colleagues, proposed that the myotome is generated by two permanent stem cell systems: one located at the border of the dermomyotome nearest to the neural tube, the dorsomedial lip (DML, Denetclaw *et al*, 1997), and the other at the ventrolateral lip (VLL, Denetclaw and Ordahl, 2000). DML and VLL cells, which are the main source of the epaxial and hypaxial muscles respectively, translocate directly underneath the dermomyotome to form the subjacent myotome layer. Once in the myotome they directly elongate to reach the rostral and caudal borders of the dermomyotome. Myotome expansion proceeds medio-laterally with older myofibres being displaced as newer fibres arise at the DML and VLL and translocate into the myotome (see figure 4.1; Brent and Tabin, 2002; Denetclaw *et al*, 2001; Gros *et al*, 2004; Hollway and Currie, 2003). This mode of myotome growth, named incremental growth, implies that progenitors within the stem cell population gradually become further apart from their progeny in the myotome, which results in a non-coherent organisation of the myotome (Denetclaw *et al*, 2001).

The second model, from Kalcheim and colleagues, stated that the myotome arises from the dermomyotome through distinct waves of cell migration. In agreement with Ordahl and colleagues, the first wave originates from cells in the dorsomedial region of the epithelial somite. But instead of translocating directly into the myotome, these proposed postmitotic pioneer cells (myoblasts) bend underneath the dermomyotome and migrate rostrally before integrating into the incipient myotome (once at the rostral border they elongate toward the caudal border forming the first myofibres; Kahane *et al*, 1998a; Kahane and Kalcheim, 1998). Subsequent growth occurs when a second wave of myoblasts emanate from all four edges of the dermomyotome, but translocate directly into the myotome only from the rostral and caudal borders, where they intercalate with the pre-existing myofibres. Any DML or VLL contribution to the myotome was thought to be preceded by migration (as mesenchymal cells) to the rostral and caudal dermomyotome egdes before entering the myotome. This second wave of migration causes expansion of the myotome (containing both old and young fibres throughout) in both the rostrocaudal and dorsoventral directions and

also increases the myotome thickness in the transverse plane (see figure 4.1; Brent and Tabin, 2002; Cinnamon *et al*, 1999, 2001; Gros *et al*, 2004; Hollway and Currie, 2003; Kahane *et al*, 1998a, 2002). This mode of myotome growth was termed intercalating growth as cells from the second wave of migration were observed to elongate among older pioneer myofibres. Via this process, the relative position of the dermomyotome progenitors is maintained with their progeny in the myotome and defined, therefore, as coherent myotomal growth (Kahane *et al*, 2002).

Figure 4.1.

In 2004, the controversy between the two models was resolved. Through the combination of electroporation of a GFP reporter construct in chick somites (Scaal *et al*, 2004) and time-lapse confocal microscopy, Gros *et al*, (2004) demonstrated that all four borders of the dermomyotome give rise to myocytes. Two sequential phases in myotome formation were identified: the first phase illustrates incremental myotome growth and results from a contribution of myocytes derived solely from the medial border of the dermomyotome (through the DML). Once in the myotome, these cells (with no prior migration) elongate to reach the rostral and caudal borders. In a second phase, myocytes from all four dermomyotome borders (caudal, rostral and ventrolateral) enter the myotome, combining incremental growth at the DML and VLL and coherent growth at the rostral and caudal borders (see figure 4.2). Further analyses of the distribution of myocytes from the four borders confirmed that DML-derived myocytes colonise only the epaxial myotome, whereas the VLL exclusively produces hypaxial myotome (Gros *et al*, 2004; Gros *et al*, 2005).

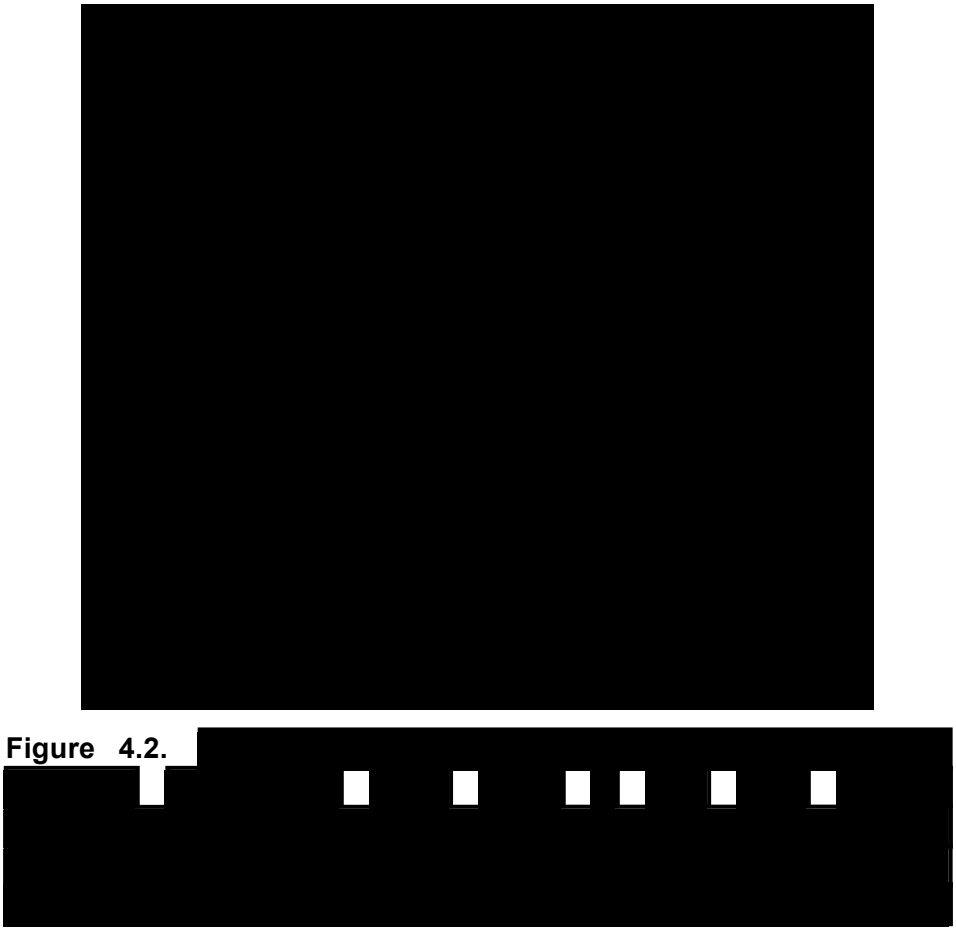

Figure 4.2.

The central portion of the dermomyotome also has a major role in myotome morphogenesis. Once the myoblasts from the lateral borders of the dermomyotome have formed the ‘primary myotome’, the centralmost region of the dermomyotome gives rise to a further population of muscle cells. Following their delamination from the dermomyotome, these muscle cells undergo EMT and join the primary myotome cells to produce a ‘secondary myotome’. In contrast to the marginal myoblast cells, these undifferentiated central cells rapidly proliferate. Some will eventually differentiate to form muscle but others sustain their undifferentiated state, surround the mature muscle cells and become the satellite cells responsible for postnatal growth and muscle repair (Ben-Yair and Kalcheim, 2005; Gilbert, 2006; Gros *et al*, 2005; Manceau *et al*, 2008; Relaix, *et al*, 2005).

As aforementioned, myotome formation in amniotes is initiated at the DML (Gros *et al*, 2004), directly opposite to the neural tube (figure 4.3a’, a’’). Cells from the DML enter a transition zone (figure 4.3b, c), via a morphogenetic process that is not fully understood, where they instigate the expression of muscle-specific markers and shut off the expression of dermomyotome-specific genes (figure 4.3d).

Figure 4.3.

Using time-lapse confocal microscopy (combined with electroporation of a GFP reporter construct) to analyse a live chick specimen, Gros *et al* (2009) have summarised that, within the transition zone, cells first lose their typical bottle-shaped morphology (present in the DML) and then initiate protrusive activity that is characterised by filopodia formation. The filopodia extend in all directions and are later replaced by lamellipodia, which form at the anterior and posterior ends of the cells. Extensive cell elongation along the antero-posterior embryonic axis results in the formation of full-sized myocytes (figure 4.4).

Figure 4.4.

4.2. NOTCH signalling and Myogenesis

The NOTCH pathway has previously been shown to influence myogenesis. Interaction of the NOTCH receptor with one of its ligands, Delta or Serrate/Jagged, triggers NOTCH signalling (Mumm and Kopan, 2000). The NOTCH receptor, succeeding ligand binding, undergoes a proteolytic cleavage, which releases the NOTCH intracellular domain (NICD) to the cytoplasm. Translocation of the NICD to the nucleus results in its association with members of the CSL (CBF1/RBP-Jκ, Suppressor of hairless [Su(H)], LAG-1) family, which modulates the transcriptional activity of these proteins. The NCID-CSL complex activates the expression of downstream targets including members of the Hairy/Enhancer-of-Split (HES) family of basic Helix-Loop-Helix (bHLH) transcription factors. Forced expression of either NOTCH ligands or activated NOTCH receptor has been shown to inhibit muscle differentiation (Kopan *at al*, 1994; Kuroda *et al*, 1999; Nofziger *et al*, 1999; Shawber *et al*, 1996; Wilson-Rawls *et al*, 1999).

While the translocation of DML cells into the myotome is not fully characterised, Rios *et al* (2011) have recently shown that muscle progenitors in the somites require the transient activation of NOTCH signalling to undergo terminal differentiation. During the first phase of myogenesis NOTCH family members are expressed in the DML, the transition zone, and

the myotome (figure 4.5). *HES1*/cHairy2 and lunatic fringe (*LFNG*), the NOTCH target genes, are expressed in a salt and pepper pattern in the DML (Hirsinger *et al*, 2001; Rios *et al*, 2011).

Figure 4.5.

Using live video microscopy, Rios *et al* (2011) followed the morphogenetic movements of NOTCH-activating cells (cells electroporated with a NOTCH reporter construct, consisting of the mouse *Hes1* promoter region upstream of a destabilised GFP, which responds to NOTCH activation and inhibition). Epithelial cells in the DML that activated the NOTCH reporter rapidly translocated to the transition zone (figure 4.6).

Figure 4.6.

Furthermore, inhibition of NOTCH activity in somites, using both small interfering RNAs (siRNAs) and a truncated dominant negative form of mastermind (DN MAML1; a NOTCH transcriptional co-activator), showed a drastic reduction of myogenic differentiation (characterised by a reduction of Myf5-positive cells), with almost all cells in which NOTCH signalling was inhibited remaining epithelial in the dermomyotome. Interestingly, sustained activation of NOTCH signalling (gained via electroporation of NICD in newly formed somites) reverses the myogenic program, also resulting in a downregulation of Myf5 and MyoD expression. Rios and colleagues (2011) illustrated, with a doxycyclin-inducible system that drives NICD expression, that the majority of electroporated cells with maintained NCID expression (i.e. in the continuous presence of doxycyclin) translocated to the transition zone but did not maintain Myf5 expression. Yet a transient activation of NOTCH signalling, achieved via the removal of doxycyclin (whereby NICD was expressed 6 h later, but was undetectable after overnight incubation), resulted in the translocation of most electroporated cells to the transition zone and the myotome with virtually all cells expressing Myf5. Additionally, electroporated cells that were located in the myotome had elongated into myocytes, implying that they had initiated terminal differentiation (Rios *et al*, 2011). Moreover, neural crest cells, which express the NOTCH ligand Delta1 (DLL1) in a mosaic pattern, migrate in close proximity to the DML. Gain and loss of Delta1 function in neural crest cells was shown to modify NOTCH signalling resulting in delayed or premature myogenesis (Rios *et al*, 2011). Gain-of-function (via overexpression of DLL1 in neural crest) resulted in a robust activation of chick *HES1* mRNA expression and of the NOTCH reporter activity in somites, while loss-of-function (via electroporation of a dominant-negative form of DLL1, and siRNAs against chick *DLL1*) resulted in a significant reduction in Myf5 staining. A model proposed by Rios *et al* (2011) indicates that the neural crest regulates early muscle formation via a mechanism that relies on the migration of neural crest cells, which are expressing DLL1, to initiate the transient activation of NOTCH signalling in selected muscle progenitors (see figure 4.7 for proposed ‘kiss and run’ model).

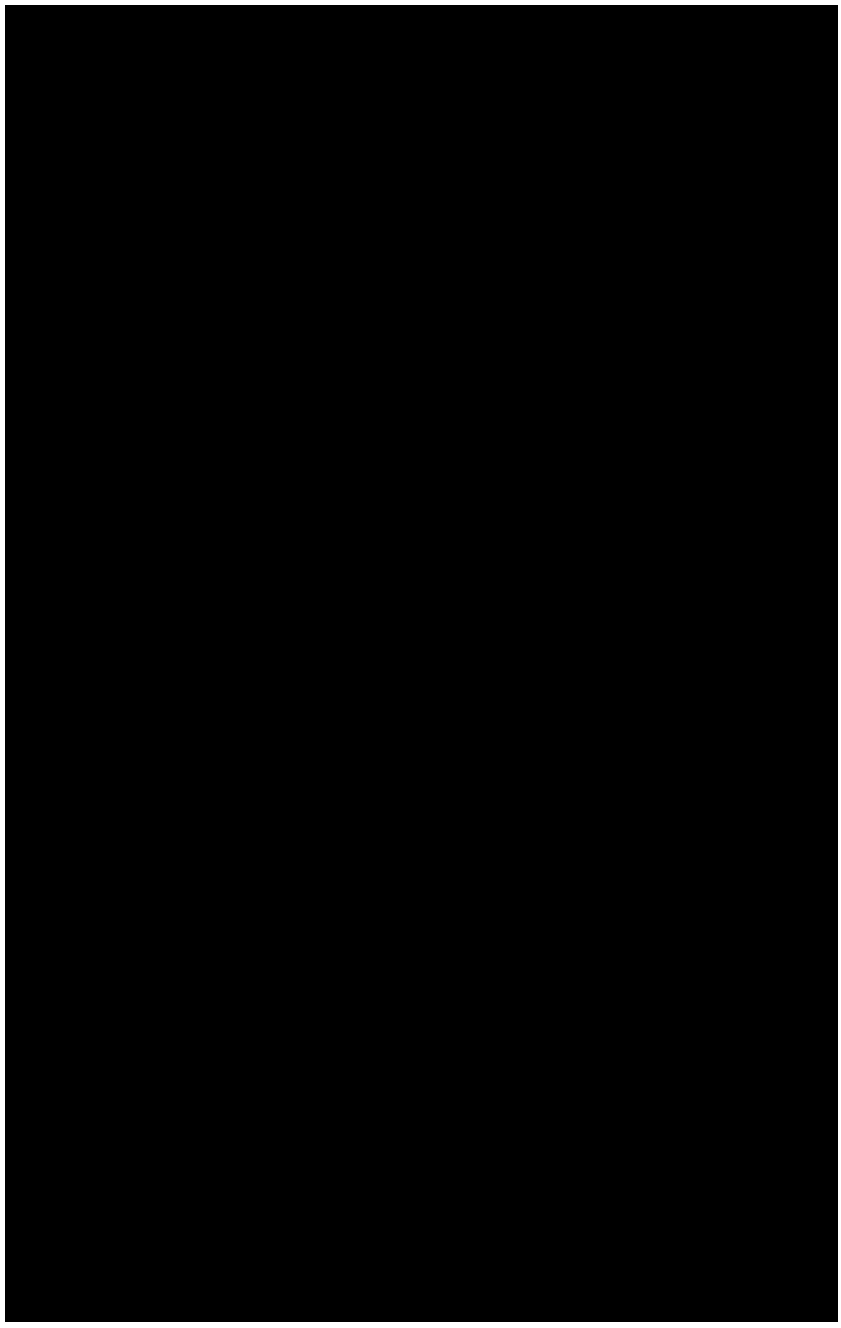

Figure 4.7.

4.3. C2C12 Cells and Myogenesis

Embryonic myogenesis is a multistep process, which is regulated by the myogenic regulatory factors (MRFs): Myf5, MyoD, myogenin and MRF4. It begins with the commitment of an embryonic precursor to the myogenic lineage, followed by the proliferation of these committed myoblasts, the differentiation of myoblasts into postmitotic myocytes, and finally fusion of myocytes to form a multinucleated myotube. This process is accompanied by extensive cytoskeletal reorganisation. The C2C12 mesenchymal cell line is a widely used *in vitro* model for myogenesis. C2C12 cells originate from the laboratory of Helen Blau (Blau *et* al, 1983) and are a subclone of C2 myoblasts (Burattini *et al*, 2004). Yaffe and Saxel (1977) originally derived C2 cells from mouse thigh muscle. C2C12 cells mimic skeletal muscle differentiation *in vitro*: when serum is withdrawn from culture medium the myoblasts spontaneously differentiate into contractile myotubes within five days. When cultured in high serum conditions C2C12 myoblasts remain undifferentiated and express *Myf5* and *MyoD* but not *myogenin* and *Mrf4*. Myf5 and MyoD actively determine the committed state of C2C12 cells but their ability to induce myogenic differentiation is blocked in high serum conditions. Depletion of growth factors and/or the downregulation of growth factor receptors initiate myogenic differentiation, which is marked by increased expression of *myogenin* and other muscle differentiation markers like myosin heavy chain.

Aims

- To perform microtubule immunostaining of avian somites, which may reveal similar rosette structures to that previously described in the avian primitive streak. Further characterisation of which may determine any significance for cell movement.
- To electroporate a GFP marker, in combination with time-lapse microscopy, to visualise the translocation of cells from the dorsomedial lip (DML) of the somite to the myotome in real time. Also

electroporation of tubulin-GFP may allow observation of the microtubule cytoskeleton during this process.

Results

4.4. C2C12 Immunofluorescence Staining

Prior to instigating the immunostaining of microtubules in avian somites, C2C12 mouse myoblast cells (an *in vitro* model of myogenesis) were fixed with methanol-MES and immunostained with α-tubulin antibody. Figure 4.8 demonstrates both the cross-reactivity of this rat antibody with mouse myoblasts and methanol-MES as an adequate fixative. As expected, α-tubulin illustrates microtubule expression in cells at day 1 (figure 4.8a) and day 4 (figure 4.8b) of differentiation.

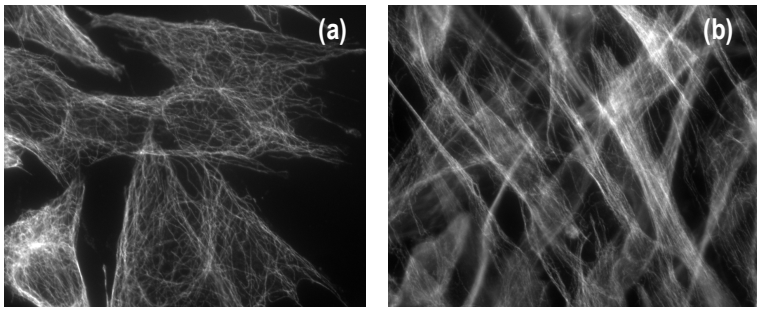

Figure 4.8. C2C12 cells immunostained for microtubules (using α- tubulin antibody) at day 1 (**a**) and day 4 (**b**) of differentiation. For further experimental detail please see materials and methods.

4.5 Embryo Sections and Immunofluorescence Staining

To enable visualisation of the microtubule cytoskeleton within cells of the avian somite, HH Stage 16 chick embryos were fixed with microtubule assembly buffer (BRB; containing formaldehyde and glutaraldehyde). Following fixation, trunks of embryos were cryosectioned (section thickness 15μm). Sections were subsequently immunostained with α-tubulin antibody and DAPI (see figure 4.9 for an example).

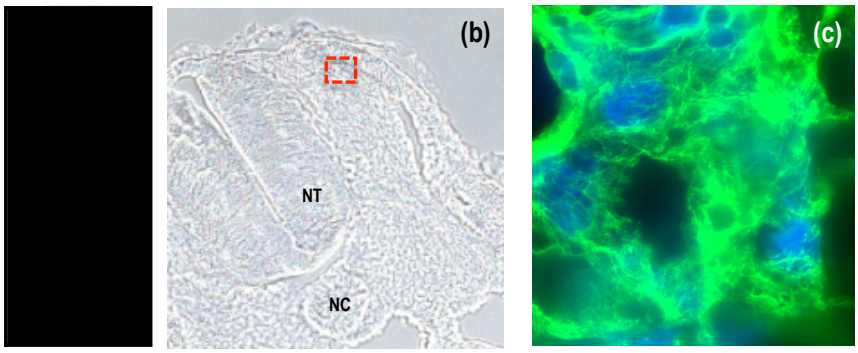

Figure 4.9. Microtubule immunofluorescence staining of a HH Stage 16 chick embryo cross section. The embryo was fixed with BRB (containing formaldehyde and glutaraldehyde) and the trunk was cryosectioned. Sections were then immunostained with α-tubulin antibody and DAPI. At high magnification there appears to be stained microtubules and nuclei in the somite (c). The dashed square in (b) highlights the magnified area in (c). The position of the section (b, c) with regard to the embryo is marked on (a). [redacted]

The α-tubulin antibody appears to be staining for something that resembles microtubules (as anticipated) however this is not very clear in the tissue section (figure 4.9c).

4.6. Wholemount Somite Immunofluorescence Staining

Owing to problems encountered with both the microtubule assembly buffer and the cryosectioning the decision was made to try immunostaining (isolated) somites in wholemount. HH Stage 17 chick embryos were fixed in a solution containing both methanol and formaldehyde (recommended by Dr. Deborah Goldspink, UEA, Norwich) and interlimb somites were excised. Excised somites were immunostained for either microtubules (using α-tubulin antibody) or microtubules and DNA (using α-tubulin antibody and propidium iodide). Following immunostaining, somites were imaged with an inverted confocal two-photon microscope. Figure 4.10 illustrates a Z-stack (a series of confocal slices) through one of the interlimb somites stained for microtubules only, while figure 4.11 demonstrates a Z-stack through an interlimb somite stained for microtubules and DNA.

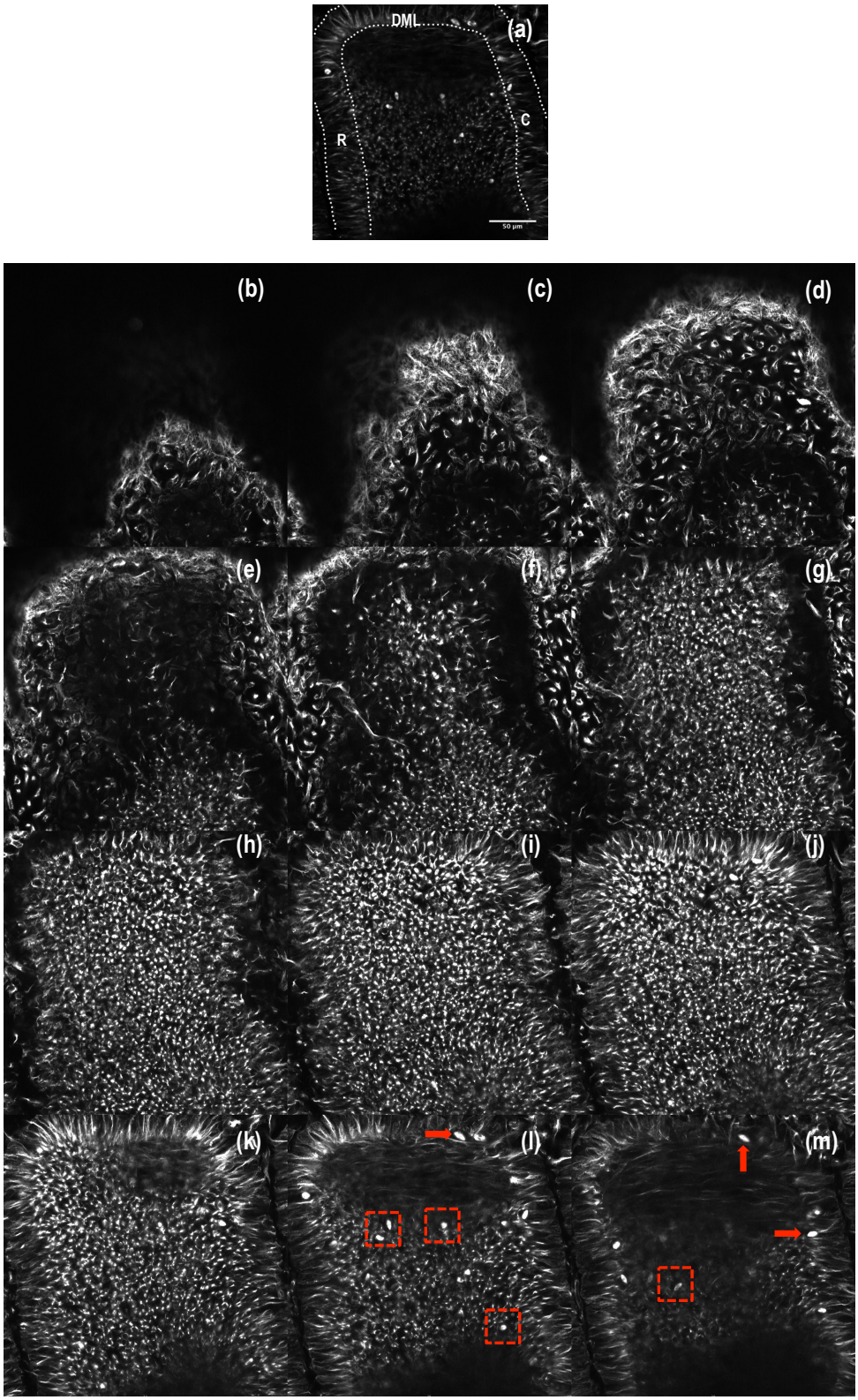

Figure 4.10. Confocal stack of an interlimb somite of a HH Stage 17 chick embryo immunostained for microtubules. Z-stack is shown from dorsal (**b**) to ventral (**m**). Image illustrated in **b** is 10 µm into the somite from its most dorsal side and every image thereafter is a further 6 µm deeper into the tissue i.e. image in **c** is 16 µm deep; image in **d** is 22 µm deep and so on. The image shown in **a** is purely to familiarise the reader with the structure of the somite in images **b**-**m**. The dashed red boxes highlight examples of dividing cells in the dermomyotome while red arrows highlight examples of dividing cells in the lips of the somite. *__DML__: dorsomedial lip, **R:** rostral lip, **C**: caudal lip. Scale bar (a) is 50µm.

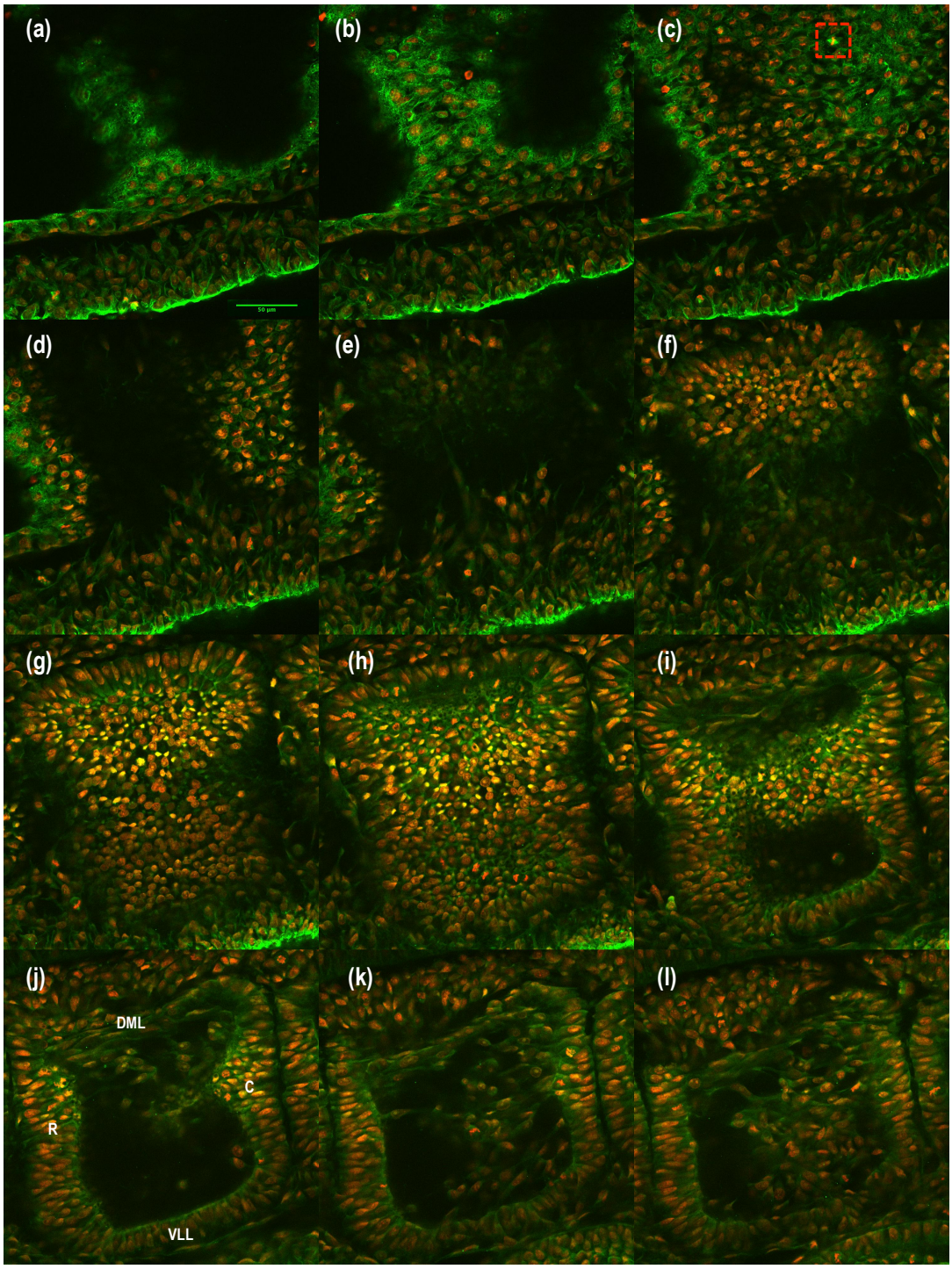

Figure 4.11. Confocal stack of an interlimb somite of a HH Stage 17 chick embryo immunostained for microtubules and DNA. Z-stack is shown from dorsal (**a**) to ventral (**l**). Image illustrated in **a** is 9 µm into the somite from its most dorsal side and every image thereafter is a further 9 µm deeper into the tissue i.e. image in **b** is 18 µm deep; image in **c** is 27 µm deep and so on. Microtubules are in green and DNA is in red. The dashed red box highlights a dividing cell. Labels on the image shown in **j** are purely to familiarise the reader with the structure of the somite. *__DML__: dorsomedial lip, **VLL**: ventrolateral lip, **R:** rostral lip, **C**: caudal lip. Scale bar (a) is 50µm.

The α-tubulin antibody illustrates microtubule expression within the Z-stacks (somites; figure 4.10 and figure 4.11). Dividing cells have been detected, particularly in the lips of the somite (see red arrows in figures 4.10l and 4.10m for examples) and what is believed to be the dermomyotome (see dashed red boxes in figure 4.10l for examples). Intriguingly, the dividing cells appear to be dividing in the plane of the epithelial dermomyotomal sheet and not in an apico-basal fashion. Figure 4.12 is a close up of the dividing cell highlighted in figure 4.11c (dashed red box). This corroborates the specificity of the α-tubulin antibody for microtubules (which in this instance are spindle microtubules) and propidium iodide for DNA staining.

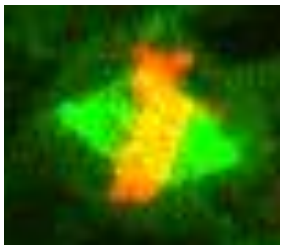

Figure 4.12. Dividing cell from a HH Stage 17 chick embryo interlimb somite. Microtubules are shown in green and DNA is shown in red. This image is a close up of a cell highlighted in figure 4.11c.

4.7. Targeted Electroporation of the Dorsomedial Lip

To enable visualisation of the microtubule cytoskeleton within cells that have been reported to translocate from the dorsomedial lip (DML) of the somite to the myotome in real time, epithelial somites I-V of HH Stage 16 chick embryos were injected with GFP-tubulin and electroporated. Following electroporation (with electrodes positioned to target the DML), embryos were re-incubated for 13-16 hours. Electroporated somites, now interlimb (embryos now at HH Stage 19-20), were then isolated and prepared for imaging (see materials and methods for more details about slice cultures). Live somites were imaged for a minimum of 3 hours (and in some instances up to 10 hours) with an inverted confocal two-photon microscope (see figure 4.13 for an example).

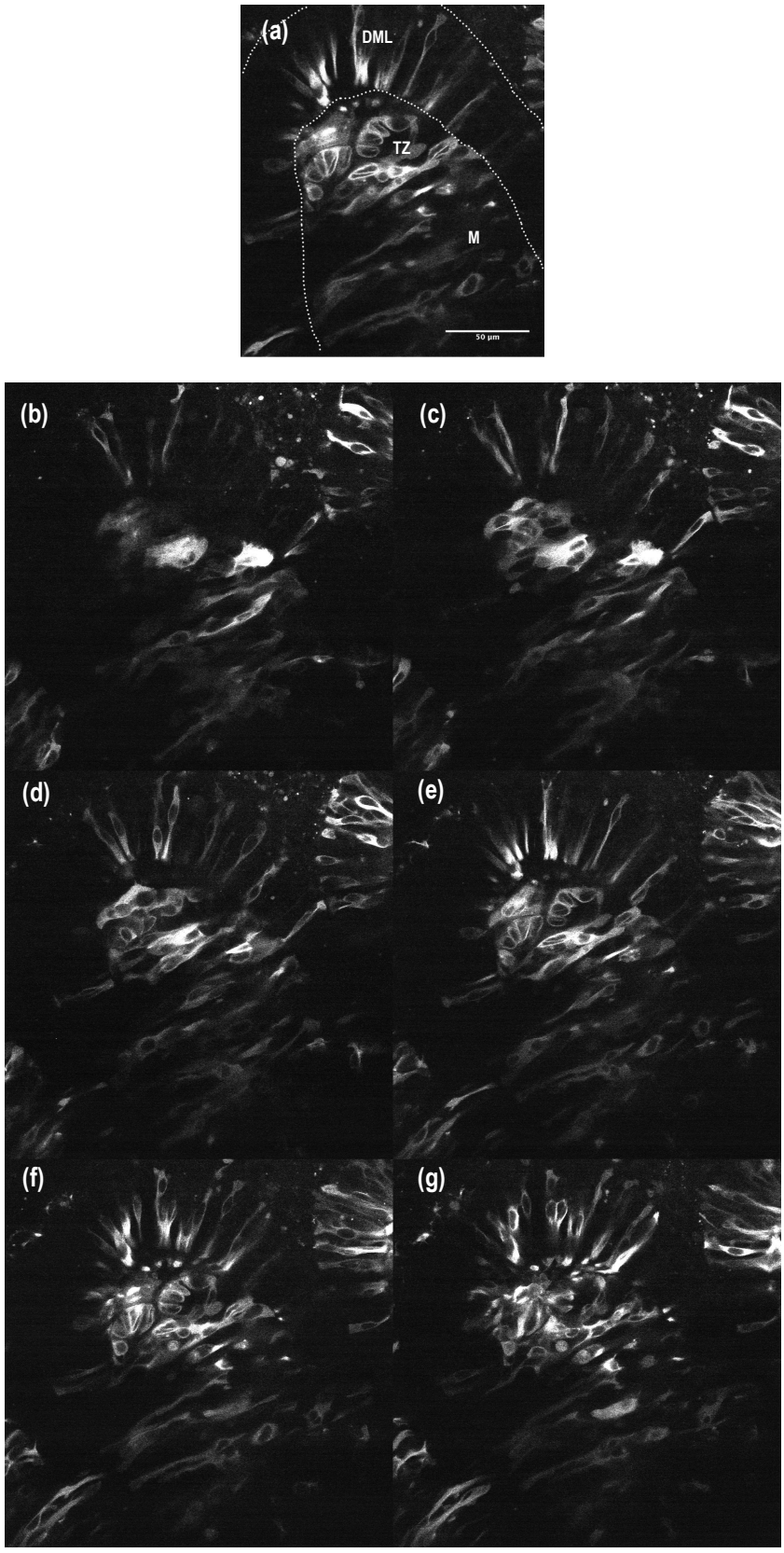

Figure 4.13. Time-lapse confocal analysis showing GFP-tubulin expression in a HH Stage 20 chick interlimb somite injected and electroporated at HH Stage 16. **b** indicates the start of the time-lapse and each subsequent image is 50 min after the previous image (i.e. **c** is 50 min after the start, **d** is 100min after the start and

so on). The image shown in **a** is purely to familiarise/orient the reader with the structure of the somite in images **b**-**g**. All images are across one plane (i.e. the same slice within the Z-stack) and are, therefore, the same depth within the tissue. *__DML__: dorsomedial lip, **TZ**: transition zone, **M:** myotome. Scale bar (a) is 50μm.

The injection and electroporation of GFP-tubulin into the developing somite has permitted the observation of cells in the epithelial DML, the mesenchymal transition zone, and the myotome (figure 4.13). Various changes to the cells are evident during the course of the 4 h 10 min time-lapse experiment; however, it is not possible to easily detect the microtubule cytoskeleton (as was anticipated with the overexpression of GFP-tubulin; figure 4.13). It is difficult to determine the exact depth of the slice within the somite (i.e. the depth from the dorsal side) as the Z-stack only visualises the electroporated cells. The Z-stacks for the immunostained somites described above, however, represent the whole somite as all of the excised tissue was stained.

Epithelial somites I-V of HH Stage 16 chick embryos were also injected with a membrane bound GFP (GFP-GPI) and electroporated. Following targeted electroporation to the DML, embryos were re-incubated for 13-16 hours. Electroporated somites (now interlimb, as embryos at HH Stage 19-20) were subsequently excised and prepared for imaging. Live somites were imaged for a minimum of 2 hours (and in some instances up to 12 hours) with an inverted confocal two-photon microscope (see figure 4.14 for an example). Like GFP-tubulin, the injection and electroporation of GFP-GPI into the developing somite has allowed the observation of cells in the DML, the transition zone, and the myotome (figure 4.14). The electroporated cells highlighted throughout the 2 h 45 min time-lapse (figure 4.14) appear to be very dynamic, particularly in the dorsomedial lip. The DML cells display high levels of activity, characterised by the formation of filopodia, which appear to extend from the anterior end of the cells (see red arrows in figure 4.14). Again it is difficult to ascertain the exact depth of the slice within the somite as the Z-stack only visualises the electroporated cells.

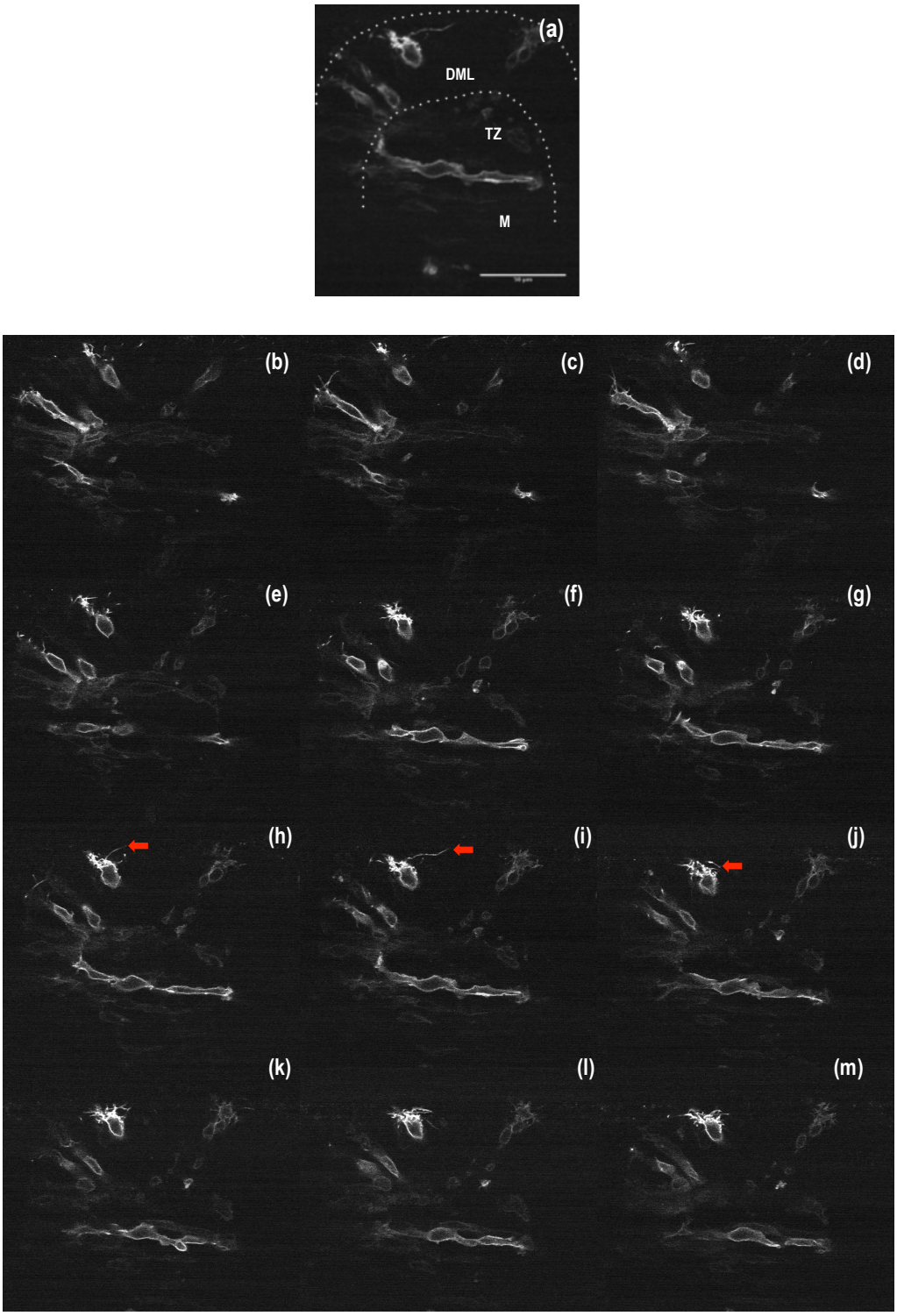

Figure 4.14. Time-lapse confocal analysis showing GFP-GPI expression in a HH Stage 20 chick interlimb somite injected and electroporated at HH Stage 16. **b** indicates the start of the timelapse and each subsequent image is 15 min after the previous image (i.e. **c** is 15 min after the start, **d** is 30min after the start and so on). The image shown in **a** is purely to familiarise/orient the reader with the structure of the somite in images **b**-**g**. All images are across one plane (i.e. the same slice within the Z-stack) and are, therefore, the same depth within the tissue. Red arrows

highlight a filopodia extension *__DML__: dorsomedial lip, __TZ__: transition zone, __M:__ myotome. Scale bar (a) is 50μm.

Discussion and Future Work

The cross-reactivity of rat α-tubulin antibody with mouse C2C12 myoblasts has been demonstrated (figure 4.8). As anticipated, α-tubulin immunostaining has illustrated the expression of the microtubule cytoskeleton. At day 4 of differentiation microtubules appear to be predominantly oriented in the longitudinal axes of the cells (figure 4.8b), whereas they are much less organised at day 1 of differentiation (figure 4.8a). This is in agreement with Tassin *et al* (1985) who illustrated that the microtubule cytoskeleton (and the organelles associated with it) is reorganised as myoblasts differentiate, elongate, and fuse into myotubes. They demonstrated that, during skeletal muscle cell differentiation, the classic network of microtubules nucleated at the centrosome changes into an array of mostly parallel longitudinal microtubules that are no longer focused on centrosomes (Tassin *et al*, 1985).

Microtubule stabilizing and destabilizing agents have been shown to compromise myotube differentiation; therefore, microtubule dynamics are believed to be essential for myotube formation (Guo *et al*, 1986; Pizon *et al*, 2005; Saitoh *et al*, 1988). Musa *et al* (2003) have shown that myotube development includes alternate phases of cell fusion and elongation. Furthermore they illustrate that EB1 (a +TIP protein; see 3.5. Microtubule Plus-End Tracking Proteins [+TIPs]) can be detected throughout the entire myotube. It is more intense, however, at the ends of the cell suggesting a role for microtubule dynamics in cell elongation (Musa *et al*, 2003). Straube and Merdes (2007) have shown that EB3, an EB1 homolog, is specifically upregulated during myogenic differentiation and is vital for myoblast elongation and fusion. Vector-based RNAi studies in cultured myoblasts showed that EB3 regulates microtubule dynamics and cortical microtubule capture (i.e. knockdown of EB3 prevented myoblast elongation and fusion into myotubes), which may be required for cell fusion and for the stabilisation

of polarised membrane protrusions. Furthermore, EB1 depletion in undifferentiated myoblasts was shown to have no negative effect on microtubule organization or on the centrosomal focusing of microtubule minus ends. Despite high homology between EB3 and EB1, overexpression of EB1 did not rescue the effect of EB3 depletion on myoblast differentiation. Straube and Merdes (2007), following detailed mapping studies, demonstrated that this could be attributed to a few amino acid substitutions between EB1 and EB3 located in the N-terminal calponin homology domain, which suggests the existence of muscle-specific partners recognising the N-terminus of EB3 (Jaworski *et al*, 2008; Straube and Merdes, 2007). Prior to their investigation, this EB protein domain had only been implicated in microtubule binding (Hayashi and Ikura, 2003), and all known interactions with multiple EB binding partners had been shown to rely on the EB C-terminus (Jaworski *et al*, 2008; Lansbergen and Akhmanova, 2006). However, in 2009 Zhang *et al* demonstrated that EB1 is required for the microtubule stabilisation that takes place in myoblasts at the onset of differentiation. They generated C2 (mouse muscle) cell lines that permanently expressed EB1-targeted shRNAs (short/small hairpin RNAs) and illustrated that, before any differentiation-related changes can take place, EB1 is specifically knocked down by more than 90%. Zhang *et al* revealed that differentiation (assessed via myogenin expression), elongation, and fusion were all prevented. Microtubule stabilization and the accumulation of cadherin and β-catenin on the plasma membrane (two events that normally precede differentiation) were also inhibited. Interestingly, the re-expression of EB1 (as EB1-GFP) was shown to restore all aspects of normal differentiation, while EB3-GFP re-expression only restored elongation and not fusion (Zhang *et al*, 2009). Zhang *et al* (2009) suggest that this divergence in the relative importance of EB1 compared with EB3 might be somewhat reconciled by considering experimental differences: the isolation of their permanently knocked down cells compared with the transient transfections performed by Straube and Merdes (2007) for example.

Following fixation with microtubule assembly buffer (BRB; containing formaldehyde and glutaraldehyde), the trunks of HH Stage 16 chick embryos

were cryosectioned and subsequently immunostained with α-tubulin antibody (figure 4.9). Unfortunately, sections were not great quality. This could be due to the fixing conditions or the cryosectioning itself. Nonetheless, α-tubulin staining appears to be detecting microtubules (as expected), however it is difficult to characterise the microtubule cytoskeleton (i.e. look for rosette structures) within the somites of the sectioned tissue. Compared to the microtubule staining shown in C2C12 myoblasts (figure 4.8 above) and the staining previously shown by Wagstaff *et al* (2008) in early HH Stage 3-4 chick embryos it is clear that this approach needs optimising. It ought to be noted that, like with the younger HH Stage 3-4 embryos (see previous chapter), several alternative methods to fix HH Stage 16 embryos were attempted: which included (combinations of) different concentrations of methanol-MES, varying incubation periods in fixative, and different temperatures while in fix. Again, like before, methanol-MES did not appear to be a suitable fix for (HH Stage 16) chick embryos (with some embryos shrinking and others disintegrating, particularly during sectioning [despite appearing 'normal' in wholemount]). It was anticipated that fixing in methanol-MES would be possible so that the range of cytoskeletal antibodies shown to cross-react with chick DF-1s (again see chapter 3) could subsequently be utilised. Attempts were also made to PHEMO-fix HH Stage 16 embryos (using the method described by Wagstaff *et al*, 2008). While this fix seemed less harsh on the embryos, in that they endured fixation and sectioning, successive attempts at staining microtubules (α-tubulin immunostaining) were unsuccessful; even following attempts with (combinations of) different antibody concentrations, various detergent concentrations during fixing, and different incubation periods in primary and secondary antibodies (i.e. adjusted from the method described by Wagstaff *et al*, 2008). In conclusion, fixation with microtubule assembly buffer (BRB; containing formaldehyde and glutaraldehyde), of all the fixation methods attempted, gave the best results (i.e. something resembling microtubules appears to be stained; figure 4.9). However, as aforesaid, this fixation method still needs improving and any interference with the function of antibodies, other than α-tubulin, remains to be tested.

Due to the problems encountered with cryosectioning the decision was made to try immunostaining (isolated) somites in wholemount. After numerous attempts with various fixes, a solution containing both methanol and formaldehyde was found to give the best results for successive microtubule immunostaining (with α-tubulin antibody). Figure 4.10 illustrates a series of confocal slices (a Z-stack) through an interlimb somite of a HH Stage 17 chick embryo stained for microtubules only, while figure 4.11 demonstrates a Z-stack through an interlimb somite, also from a HH Stage 17 embryo, stained for microtubules and DNA. Microtubule expression is apparent within both Z-stacks (somites; figure 4.10 and figure 4.11). However, the stain appears to have only penetrated some of the tissue. In figure 4.10, α-tubulin antibody is seen in what is believed to be the ectoderm and dermomyotome (figure 4.10a-l), however the fluorescence fades significantly when myotomal depth is reached (i.e. it is difficult to observe staining in myofibres; figure 4.10m). Similarly, in figure 4.11, α-tubulin antibody is seen in what is believed to be the ectoderm and possibly the (most dorsal part of the) dermomyotome (figure 4.11a-c) but, again, it is difficult to see any stain for microtubules deeper within the tissue: it looks as if there is some autofluorescence emitting from the tissue (figure 4.11f-l). Also in figure 4.11(j-l) it appears as if there is a 'hole' in the somite where the myotome should be. This could be due to the high level of methanol in the fixative. This method was somewhat successful, in that it is possible to detect microtubules within certain regions of the somite, unfortunately however, it is very difficult to distinguish rosette structures like those that were seen in the primitive streak of gastrulating HH3-4 embryos (see 3.6 Avian Gastrulation and the Cytoskeleton). Dividing cells were detected however (figures 4.10-4.12), particularly in the lips of the somite (figure 4.10l and figure 4.10m) and the presumed dermomyotome (figure 4.10m), which validates the specificity of the α-tubulin antibody for microtubules (in this instance spindle microtubules). Interestingly, cells that are dividing appear to be dividing in the plane of the presumed epithelial dermomyotomal sheet (i.e. not apico-basal division).

The dermomyotome is a highly proliferative tissue (Gros *et al*, 2005; Kohler *et al*, 2005). It is a heterogeneous pool of progenitor cells, which have

varying proliferative capacities and cell division patterns (Ordahl *et al*, 2001; Venters and Ordahl, 2005). Dermomyotomal cells provide precursors for the dermis of the back, the muscle of the back and limbs, and endothelia (Scaal and Christ, 2004). Two types of cell divisions have been defined in the dermomyotome: planar and apico-basal divisions (which are described in relation to the plane of the epithelial dermomyotomal sheet). Planar cell divisions produce daughter cells that lie adjacent to each other on the basement membrane of the dermomyotome, whereas apico-basal divisions push the daughter cells either dorsally to form dermis, or ventrally into the myotome (Venters and Ordahl, 2005; Yusuf and Brand-Saberi, 2006). Intriguingly, using electroporations as a marking technique, Ben-Yair and Kalcheim (2005) have shown that a single cell in the central dermomyotome can give rise to both dermogenic and myogenic progenitors that later translocate under the ectoderm or into the myotome ventrally, respectively. In addition, they noted that this fate segregation is associated with a sharp change in the plane of cell division from the young epithelium (wherein symmetrical divisions occur parallel to the mediolateral plane of the dermomyotome [shown in figure 4.10]), to the dissociating dermomyotome (wherein cell divisions become mostly perpendicular). The dermomyotomal progenitor cell populations, therefore, undertake a series of planar cell divisions that result in an increase in the number of the stem cell pool and later restore to asymmetrical cell divisions through altering the plane of division (Ben-Yair and Kalcheim, 2005; Yusuf and Brand-Saberi, 2006). Change in cell division has been shown to correlate with the rise of more differentiated cell types (Cayouette and Raff, 2003). Morrison and Kimble (2006) have reported that, in stem cells, asymmetrical cell divisions are a means of preservation of the stem pool: a stem cell divides mitotically to yield one daughter cell that retains the stem cell characteristics, whereas the other daughter cell is a more differentiated cell committed to a specific lineage.

A previously published electroporation technique (Scaal *et al*, 2004), which permits the targeting of different regions of the avian somite, was established within the laboratory. It was anticipated that targeted electroporation (i.e. electroporation of the medial portion of the somite to transfect the medial lip

of the dermomyotome) of reporter constructs into developing somites would enable the visualisation, in real time, of cells which have been reported to translocate from the dorsomedial lip to the transition zone and subsequently to the myotome (Gros *et al*, 2009; Rios *et al*, 2011; Scaal *et al*, 2004). In addition, it was speculated, that the electroporation of tubulin-GFP would allow observation of the microtubule cytoskeleton during this morphogenesis. Electroporation was successful (i.e. the dermomyotome and dorsomedial lip were effectively electroporated with numerous constructs, which included GFP-tubulin and GFP-GPI, figures 4.13 and 4.14 respectively), as was time-lapse microscopy (somites were imaged between 3 and 12 hours and tissue appeared to survive throughout as previously reported by Gros *et al*, 2004). However, the successive analysis proved to be much more difficult than expected. It was presumed that if sequential Z-stacks of the same somite were taken over time (i.e. every 15 min) then it would be possible to track cell movement in 3D. Unfortunately, due to unforeseen limitations in the software that was available at the time of analysis, it was not possible to view Z-stacks in 3D over time. Thus, the time-lapse images shown here (figures 4.13 and 4.14) are only across one slice in the Z-stack, that is to say they are all at the same depth in the tissue. So, although it may appear that cells are migrating (and in some cases they probably are) from one region of the somite to another it cannot be conclusively decided from this data: for example, cells in the DML that appear to have 'moved' toward the transition zone (figure 4.13) may in fact just have 'dipped' below or above the focal plane. Having said that, it does appear that a myofibre is forming in figure 4.14b-f, but this would have to be verified using software that enables 3D analysis over time. Because of these limitations it was not possible to confidently visualise cells moving from the DML to the myotome.

It is worth mentioning that individual Z-stacks were analysed in 3D by eye (i.e. a Z-stack at the start of a time-lapse, and then one 30 min later and so on), but it was extremely difficult to track cells this way (3D stacks not shown). Software that can create 3D movies over time would allow a much more comprehensive and concrete analysis and is strongly recommended. Nonetheless, despite the limitations of our analyses, it is possible to see, as

might be expected, that cells in the dorsomedial lip, the transition zone, and the myotome are all active at this stage of development. Even in a very short time-lapse experiment it is clear that the cells in the dorsomedial lip are highly active (figure 4.14). Filopodia, similar to those previously described in cells in the transition zone (Gros *et al*, 2009), appear to be forming and extending from the anterior ends of the cells.

Evidently, it is not possible to distinguish the microtubule cytoskeleton following GFP-tubulin electroporation into developing somites (figure 4.13). This might be because too much non-polymerised tubulin is being expressed, which might be masking any polymerised tubulin. Immunostaining with α-tubulin antibody, as aforementioned, highlighted microtubules in the presumed ectoderm and dermomyotome (figures 4.10 and 4.11), but this was also unsuccessful with regard to enabling observation of the microtubule cytoskeleton in the myotome (embryonic myofibres).

On a final note, the somite immunostaining looks promising but does require further improvements. To help with the penetration issue abovementioned, perhaps the somites could be incubated in antibody/antibodies for longer, or a higher concentration of detergent could be used, or even very small incisions could be made within the tissue. Also, different percentages of methanol or formaldehyde could be attempted to try and prevent damage to the tissue. Once optimised, it may be possible to try interference experiments. For example, treat isolated somites with nocodazole, fix them at different recovery times, and then stain for microtubules to see any overall affects or delays in somite development. It would be also interesting to stain for other cytoskeletal components or their interacting proteins (following assessment in cells to ensure that this fixative does not interfere with the chosen antibodies). It might also be worth trying to fix HH Stage 3-4 embryos this way or with the BRB (containing formaldehyde and glutaraldehyde) fixative as this may allow for improved immunostaining of the cytoskeleton (see Chapter 3 Discussion).

Chapter 5: Microtubule-Actin Cross-linking Factor 1/ Actin Cross-linking Family 7 (MACF1/ ACF7)

Introduction

Microtubule-actin cross-linking factor 1/actin cross-linking factor 7 (MACF1/ACF7) is a multi-domain cytoskeletal protein that belongs to the spectraplakin family of proteins, which also includes bullous pemphigoid antigen 1 (BPAG1; see 1.6. Spectraplakins). It has an important role in the association with actin filaments and microtubules, and participates in protein transportation, signal transduction, and embryonic development (Chen *et al*, 2006; Leung *et al*, 2002; Jefferson *et al*, 2004). Spectraplakins are enormous (>500kD), multifunctional cytoskeletal linker proteins that act as master coordinators between different types of cytoskeletal filaments. They are able to bind to all three types of cytoskeletal filaments (actin, microtubules, and intermediate filaments) and, as their name implies, they contain domains found in two cytoskeletal families, the spectrins and plakins (Röper *et al*, 2002). Spectraplakins' genes are characterised by multiple tissue-specific promoters, large numbers of coding exons, and differentially spliced transcripts. This results in a diversity of different isoforms (that contain combinations of various protein domains) each with the ability to interact with different cytoskeletal and/or membrane components (Röper *et al*, 2002; Suozzi *et al*, 2012).

5.1. MACF1/ACF7 Structure and Isoforms

Structurally, full length MACF1/ACF7 is a large, 608kD, protein that can be divided into 3 domains: an N-terminal domain that comprises both a calponin type actin-binding domain (ABD) and a globular plakin domain; followed by a

rod domain that contains dystrophin-like spectrin repeats; and a C-terminal domain that can directly bind microtubules (figure 5.1; Sun *et al*, 2001). The N-terminal domain, which shares 63-88% amino acid sequence homology to BPAG1, contains an M1 domain that has been shown to interact with microtubules (Karakesisoglou *et al*, 2000). The C-terminal domain can be divided into three regions: (1) two calmodulin-like EF-hand calcium-binding motifs; (2) a glycine/arginine-rich (GAR) domain that is homologous to regions of the Gas2 (growth arrest-specific protein 2) and GAR22 (gas2-related protein on chromosome 22) proteins; and (3) at the extremity of the C-terminal, a serine and proline-rich region containing several glycine-serine-arginine (GSR) repeats (GSR-containing domain; figure 5.1; Sun *et al*, 2001). Leung *et al* (1999) have illustrated that this entire C-terminal domain can interact with microtubules *in vitro* and *in vivo*.

Figure 5.1.

As in all spectraplakins, the transcripts of MACF1/ACF7 and BPAG1 are alternatively spliced resulting in varying isoforms with different functional domains (figure 5.2; Leung *et al*, 1999; Suozzi *et al*, 2012). MACF1a/ACF7 and BPAG1a have similar domain organisation with an actin-binding domain, a plakin domain, a rod domain with spectrin repeats, and a C-terminus comprising an EF-hand motif and a GAR domain (Karakesisoglou *et al*, 2000; Leung *et al*, 1999; Sun *et al*, 2001). However, MACF1b/ACF7 and BPAG1b, alternatively spliced isoforms, contain variable numbers of plakin repeats between the plakin domain and spectrin repeats. MACF1b/ACF7 has a more

complicated plakin repeat domain (PRD) region than BPAG1b, in that it contains three full and two partial PRDs (Sonnenberg and Liem, 2007; Suozzi *et al*, 2012). MACF1b/ACF7 has been shown to interact with and maintain the structure of the Golgi apparatus (Lin *et al*, 2005).

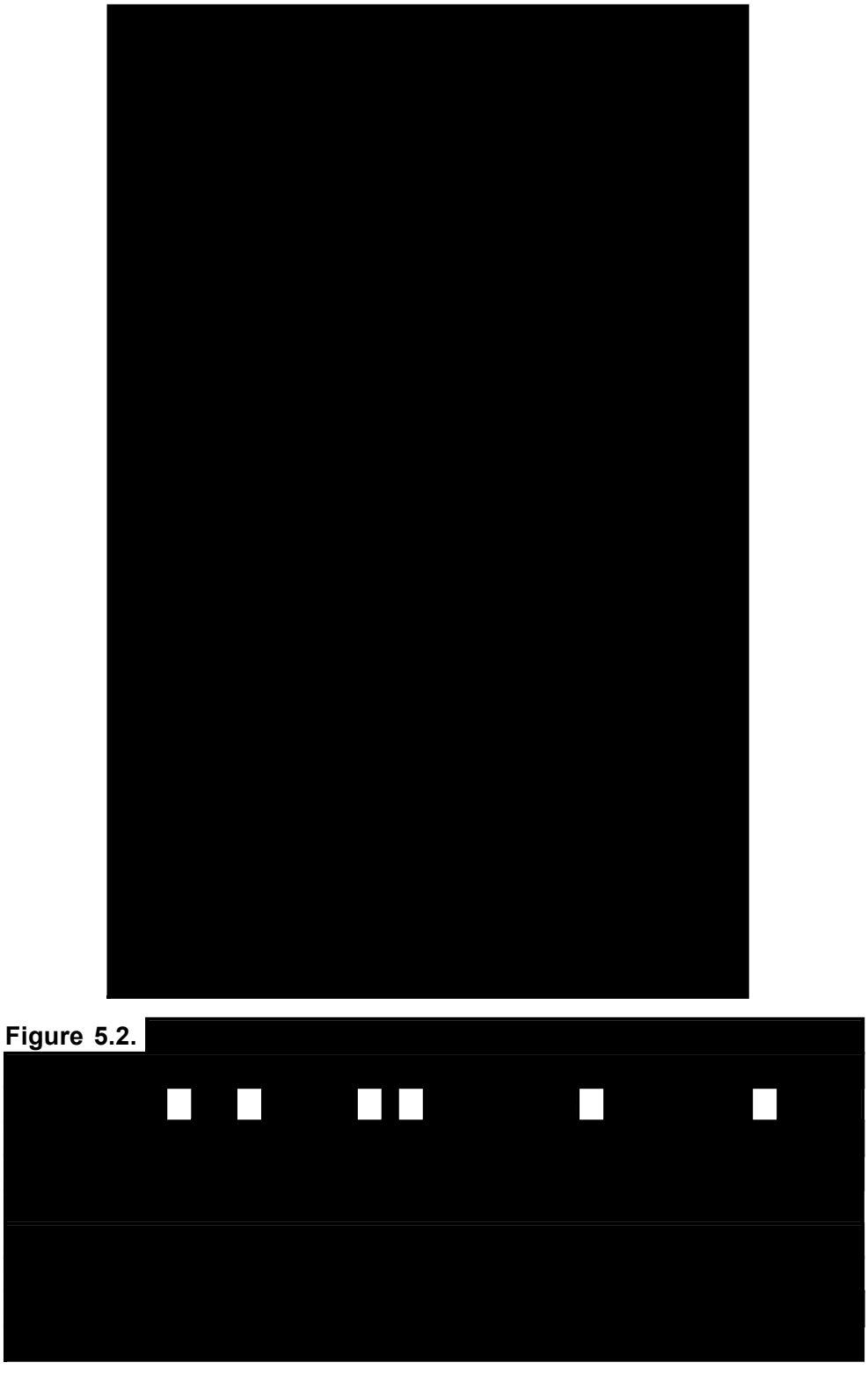

Figure 5.2.

Different transcription start sites in spectraplakin genes result in at least four different N-termini in BPAG1, while at least three start sites are present in the gene encoding MACF1/ACF7 (Leung *et al*, 1999; Röper *et al*, 2002; Suozzi *et al*, 2012). The alternate start sites, in addition to altering cytoskeletal associations, confer tissue specificity. BPAG1e is specific to skin epidermis (forming links between hemidesmosomes and keratin intermediate filaments; Mueller *et al*, 1989), whereas BPAG1a1/BPAG1n4 is highly expressed in the peripheral nervous system, and BPAG1b is specific to the muscle (Groves *et al*, 2010; Leung *et al*, 2001; Steiner-Champliaud *et al*, 2010; Yang *et al*, 1996). Mammalian MACF1/ACF7 is also expressed broadly, including the central nervous system and the epidermis (Karakesisoglou *et al*, 2000).

5.2. MACF1/ACF7 Functions

MACF1/ACF7 has been shown to interact with both microtubules and actin in cultured mammalian cells (Leung *et al*, 1999). It is a microtubule plus-end tracking protein (+TIP) that mediates cortical interactions via the association of microtubule ends with the actin cytoskeleton and the plasma membrane (Akhmanova and Steinmetz, 2008; see 3.5. Microtubule Plus-End Tracking Proteins [+TIPs]). Furthermore, it directly binds EB1 (another +TIP) and demonstrates EB1-dependent plus-end-tracking of microtubules *in vivo* (Slep *et al*, 2005).

In *MACF1*/*ACF7*-null primary endodermal cells, Kodama *et al* (2003) demonstrate that extending microtubules fail to co-align with F-actin at the plasma membrane. In HeLa cells, MACF1/ACF7 was shown to regulate the cortical localisation of CLASP2 (another +TIP), which suggests it plays a role in the stabilisation of microtubules and cell motility (Drabek *et al*, 2006). The loss of MACF1/ACF7 results in less-stable, long microtubules with skewed

cytoplasmic trajectories. This is devastating for the developing mouse embryo, in which full *MACF1/ACF7* knockout causes pre-implantation lethality (Kodama *et al*, 2003).

In mammalian cells, the bundling of actin filaments provides stabilising forces for the capture, growth and guidance of microtubules (Kodama *et al*, 2003). Intriguingly, MACF1/ACF7 deficiency compromises the targeting of microtubules along F-actin to focal adhesions and consequently impairs focal adhesion dynamics (Wu *et al*, 2008). In epidermal cells, the effect of MACF1/ACF7 on focal adhesion dynamics is dependent on polarised microtubules, which are stabilised by underlying actin fibres. At focal adhesion sites, microtubules are thought to serve as macromolecular tracks, which enable the delivery of factors that promote focal adhesion turnover (Ezratty *et al*, 2005; Kaverina *et al*, 1998; Kaverina *et al*, 1999; Krylyshkina *et al*, 2002; Krylyshkina *et al*, 2003). The loss of MACF1/ACF7, therefore, impedes the convergence of microtubule ends at peripheral focal adhesions and, as a result, focal adhesions become highly stabilised and refractile to the normal dynamics necessary for efficient cell migration (Wu *et al*, 2008).

It is not fully understood how MACF1/ACF7 functions in targeting plus-ended microtubule growth along F-actin to polarised focal adhesions. Wu *et al* (2008) have shown that MACF1/ACF7's binding domains for actin filaments, microtubules, and microtubule plus-end proteins are not sufficient to rescue the defects in focal adhesion-cytoskeletal dynamics and migration functions of *MACF1*/*ACF7*-null keratinocytes. They also uncovered an intrinsic actin-dependent ATPase domain in MACF1/ACF7 that is required for the regulation of focal adhesions and also might help to maintain essential +TIP proteins at the plus ends of microtubules during their coordinated growth along actin filaments (Suozzi *et al*, 2012; Wu *et al*, 2008).

Kakinuma *et al* (2004) have shown that the transport of vesicles from the trans-Golgi network (TGN) also depends on MACF1/ACF7. Their results indicate that the TGN protein p230 (which is anchored to TGN membranes) interacts with MACF1/ACF7, providing the molecular link for the transport of glycophosphatidylinositol (GPI)-anchored proteins along microtubule and

actin cytoskeletal tracks from the TGN to the plasma membrane/cell periphery (Kakinuma *et al*, 2004).

The generation of a conditional knockout (cKO) mouse has highlighted the importance of MACF1/ACF7 in nervous system development (Goryunov *et al*, 2010). *MACF1* cKO brains showed a disorganised cerebral cortex with a mixed layer structure, heterotopia of the hippocampal pyramidal layer, disorganized thalamocortical and corticofugal fibres, and aplastic anterior and hippocampal commissures (Goryunov *et al*, 2010).

The function of MACF1/ACF7 in mammalian skin has been clarified owing to the specific deletion of *MACF1/ACF7* in skin epidermal cells (Wu *et al*, 2008, 2011). Unlike mice that lack BPAG1, which show skin blistering and sensory neuron and muscle degeneration (with each cell type manifesting gross defects in cytoskeletal organisation; Brown *et al*, 1995; Guo *et al*, 1995), *MACF1/ACF7* cKO mice display no gross morphological changes in their skin or hair coat (Wu *et al*, 2008). Possibly because MACF1/ACF7s function in development can also be performed by BPAG1. When challenged to respond to injury, however, *MACF1/ACF7* cKO skin cells display a significant delay in migration and wound closing. The delayed response is rooted in impaired epidermal migration, as also shown by monolayer scratch assays implemented on cultured primary keratinocytes (isolated from cKO back skin and wild type littermate controls). The aberrant migration seen in *MACF1/ACF7*-null keratinocytes is due to the absence of microtubule-induced focal adhesion turnover (i.e. more stable focal adhesions) and increased adherence to the underlying extracellular matrix substratum (Wu *et al*, 2011). The findings of Wu *et al* (2008, 2011) thus indicate that MACF1/ACF7, through its ability to coordinate microtubule-actin dynamics, regulates migration by promoting focal adhesion dynamics (Suozzi *et al*, 2012).

Recently, a link between MACF1/ACF7 and GSK3β has been illustrated. Wu *et al* (2011) have shown that, during wound healing in mammals, GSK3β controls microtubule architecture and polarised movement of skin stem cells through the regulation of MACF1/ACF7 (see 6.5. GSK3β Regulates

MACF1/ACF7 in Cell Migration). They propose that this data may further substantiate a link between MACF1/ACF7 and Wnt signalling.

5.3. MACF1/ACF7 and its Role in Wnt Signalling

In mouse embryos, MACF1/ACF7 is ubiquitously expressed (Bernier *et* al, 2000; Leung *et al*, 1999). High expression has been shown in neuronal tissues and the foregut of embryonic day 8.5 (E8.5) embryos and the head fold and primitive streak of E7.5 embryos (Chen *et al*, 2006). MACF1/ACF7 heterozygous mice were shown to develop normally, while homozygous knockout mice died early during gastrulation and displayed developmental retardation at E7.5: with defects in the formation of the primitive streak, node, and mesoderm (Chen *et al*, 2006). Since this phenotype is reminiscent of *Wnt-3*$^{-/-}$ mice (Lui *et al*, 1999) and *LRP5/6* double-knockout mice (Kelly *et al*, 2004), Chen *et al* (2006) hypothesised and tested for a role of MACF1/ACF7 in Wnt signalling. Using coimmunoprecipitation assays, MACF1/ACF7 was found to be in a cytosolic complex with Axin, GSK3β, β-catenin, and APC. In cultured cells, reduction of MACF1/ACF7 (via siRNA) was shown to increase the cytosolic levels of Axin and inhibit canonical Wnt signalling (i.e. decrease the amount of β-catenin in the nucleus). Intriguingly, MACF1/ACF7 was seen to translocate with Axin to the plasma membrane in a Wnt-dependent manner, and both a wild type and a dominant negative form of MACF1/ACF7 were shown to bind to LRP6 and Axin simultaneously (Chen *et al*, 2006).

Chen *et al* (2006) have proposed a model for the involvement of MACF1/ACF7 in the Wnt/β-catenin signalling pathway. In the presence of Wnt, frizzled and LRP5/6 (receptor and coreceptor respectively) are activated. MACF1/ACF7 is then thought to be involved in the translocation of a complex containing Axin, β-catenin, and GSK3β (but not APC) from the cytosol to the cell membrane, where Axin and MACF1/ACF7 bind to LRP5/6. As a result, GSK3β is inactivated by phosphorylation, Axin is degraded, and β-catenin is released. This then enters the nucleus and activates Wnt-responsive genes. Conversely, in the absence of Wnt, MACF1/ACF7 binds to a complex containing Axin, APC, β-catenin, and GSK3β. There is then no

expression of the TCF controlled genes owing to the degradation of β-catenin after phosphorylation by GSK3β (see figure 5.3; Chen *et al*, 2006).

Figure 5.3.

Aims

- To generate an RNA probe against the expressed sequence tag clone ChEST16M13, which is thought to correspond to MACF1/ACF7, and perform *in situ* hybridisation experiments to establish an expression pattern for MACF1/ACF7 in chick. This may help determine a role, if any, for MACF1/ACF7 in chick gastrulation and/or somitogenesis.
- To knockdown MACF1/ACF7 (using siRNAs directed against mouse MACF1/ACF7) in murine C2C12 cells to reveal effects, if any, on the microtubule cytoskeleton.

Results

5.4. Characterisation of ChEST16M13 (MACF1/ACF7)

An expressed sequence tag (EST; ChEST16M13, supplied by Ark-Genomics) that was thought to correspond to MACF1/ACF7 was identified. In chick, only one MACF1/ACF7 transcript (ENSGALT00000005857) has been annotated. Analysis has shown that ChEST16M13 recognises exons 89-93 of this transcript (figure 5.4A). In human, however, 37 alternative MACF1/ACF7 transcripts (20 of which are protein coding) have been annotated. ChEST16M13 recognises exons 80-84 in human transcript MACF1-031 (figure 5.4B).

Figure 5.4.

In addition to the human MACF1-031 transcript, further analyses reveals that this EST (ChEST16M13) also recognises the human MACF1-204, MACF1-028, MACF1-203, MACF1-201, MACF1-001, MACF1-032, MACF1-003, and MACF1-005 transcripts (figure 5.4B).

5.5. MACF1/ACF7 Chick Expression Pattern

An RNA probe was synthesised using the ChEST16M13 clone (i.e. against a fragment of the chick *MACF1/ACF7* gene) and used for *in situ* hybridisation experiments. In early chick embryos, *MACF1/ACF7* appears to be expressed in the primitive streak; figure 5.5A shows strong expression at HH Stage 2, which appears to decrease at HH Stage 3 and Stage 4 (figure 5.5B and C respectively). At HH Stage 11 expression is apparent in the forebrain, hindbrain, pre-segmented mesoderm and in the somites (figure 5.5D and E).

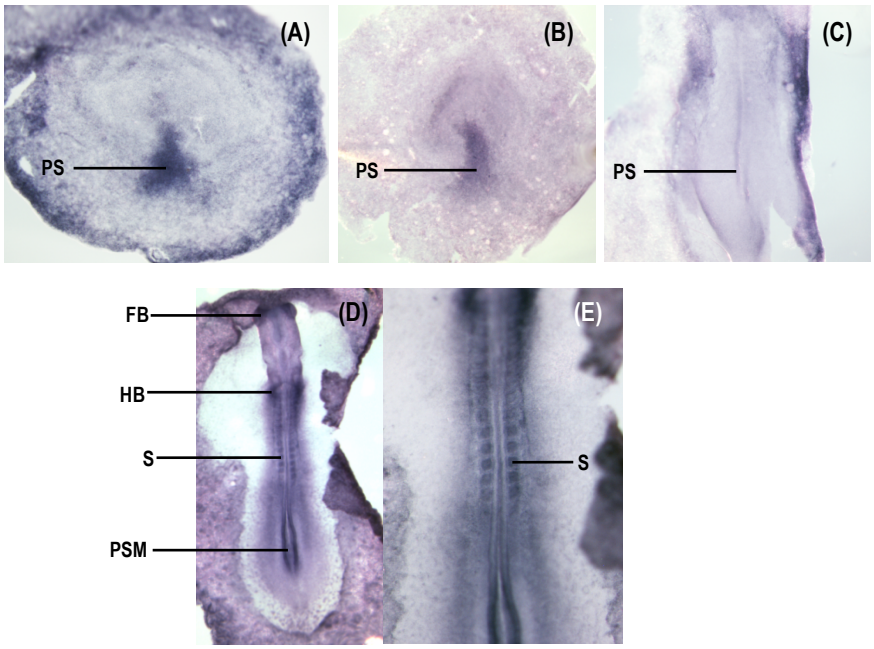

Figure 5.5. The expression pattern of *MACF1/ACF7* in early chick embryos. *MACF1/ACF7* appears to be expressed in the primitive streak: **(A)** shows strong expression at HH Stage 2, which appears to decrease at HH Stage 3 and HH Stage 4, **(B)** and **(C)** respectively. **(D)** At HH Stage 11 expression is apparent in the forebrain, hindbrain, pre-segmented mesoderm and in the somites. **(E)** Higher magnification of somite expression in embryo shown in **(D)**. ***PS**: primitive streak, **FB**: forebrain, **HB**: hindbrain, **S**: somite, **PSM**: pre-segmented mesoderm

At HH Stage 17 *MACF1/ACF7* expression is evident in the somites, forelimbs and heart (figure 5.6A and B). A section through the trunk of the embryo (just above the hind limb in this instance) reveals expression in the dermomyotome and dorsomedial lip of the somite (figure 5.6C).

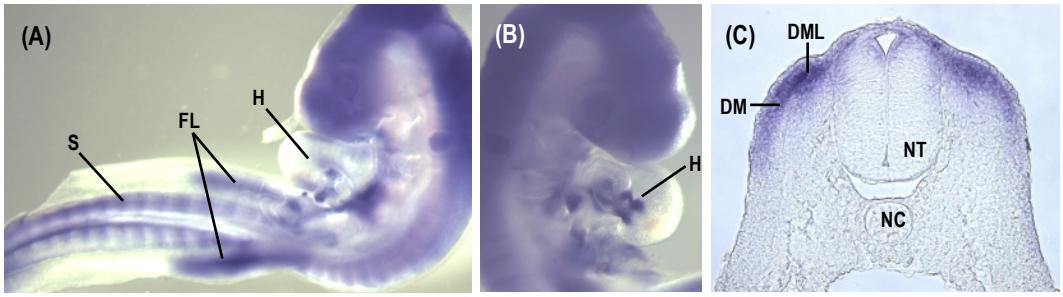

Figure 5.6. The expression pattern of *MACF1/ACF7* in a HH Stage 17 chick embryo. Expression is apparent in the somites (**A**), forelimbs (**A**), and the heart (**A**, **B**). A section through the embryo trunk (just above the hind limb in this instance) reveals that MACF1/ACF7 expression is evident in the dermomyotome and dorsomedial lip (DML) of the somites (**C**). ***FL**: forelimb, **H**: heart, **S**: somite, **NT**: neural tube, **NC**: notochord, **DM**: dermomyotome, **DML**: dorsomedial lip.

At HH Stage 20 *MACF1/ACF7* expression is apparent in the fore and hindlimbs (figure 5.7A, F, G, and H), the first pharyngeal arch (figure 5.7A, B, C, D, and E), the olfactory placode (figure 5.7A, B, C, D, and E), and the heart (figure 5.7E and F). There also appears to be very weak expression in the optic vesicle (figure 5.7B, C, D, and E) and the otic vesicle (figure 5.7A).

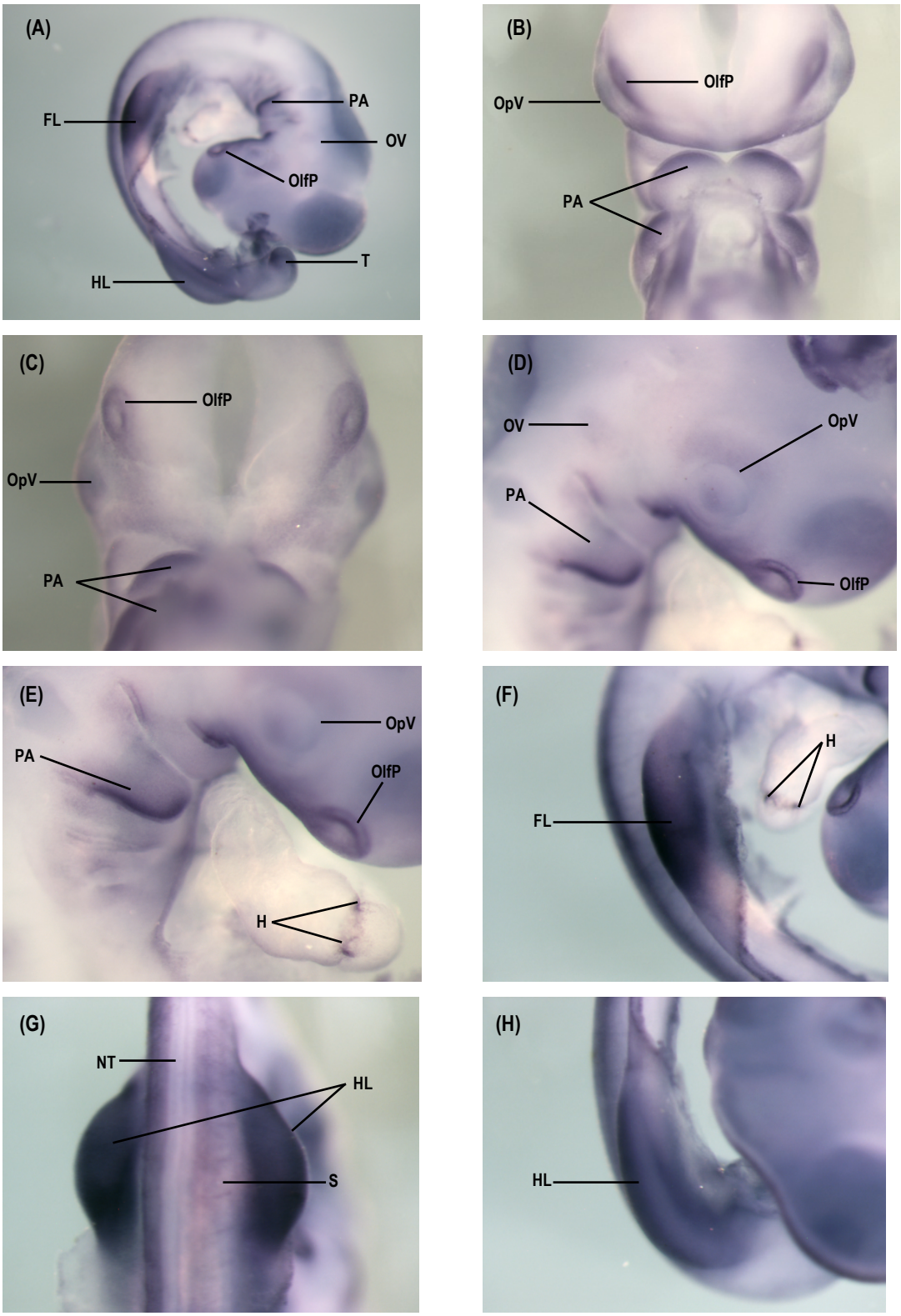

Figure 5.7. The expression pattern of *MACF1/ACF7* in a HH Stage 20 embryo. Expression is apparent in the fore and hindlimbs (**A**, **F**, **G**, and **H**), the first pharyngeal arch (**A**, **B**, **C**, **D**, and **E**), the olfactory placode (**A**, **B**, **C**, **D**, and **E**), and the heart (**E** and **F**). There also appears to be very weak expression in the optic vesicle (**B**, **C**, **D**, and **E**) and the otic vesicle (**A**). ***FL**: forelimb, **PA**: pharyngeal arch, **OV**: otic vesicle, **OlfP**: olfactory placode, **HL**: hindlimb, **T**: tail, **OpV**: optic vesicle, **H**: heart, **S**: somite, **NT**: neural tube.

At HH Stage 31 *MACF1/ACF7* expression is evident in the forelimbs, hindlimbs, the formed beak (with a single egg tooth), and the tail (figure 5.8A) Expression also appears to be ubiquitous in the heart (including the auricles) of a day 7 (HH Stage 31) embryo (figure 5.8B).

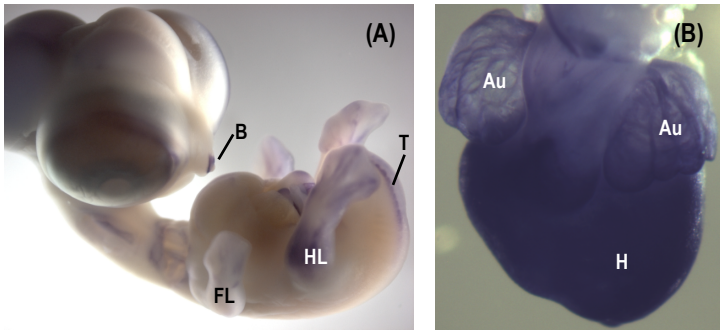

Figure 5.8. The expression pattern of *MACF1/ACF7* in a HH Stage 31 embryo. (**A**) Expression is apparent in the forelimbs, hindlimbs, the formed beak (with a single egg tooth), and the tail. (**B**) Expression also appears to be ubiquitous in the heart (including the auricles) of a day 7 (HH Stage 31) embryo. ***FL**: forelimb, **HL**: hindlimb, **T**: tail, **B**: beak, **H**: heart, **Au**: auricle.

5.6. MACF1/ACF7 Immunofluorescence Staining

To characterise the localisation of MACF1/ACF7 with regard to the microtubule cytoskeleton, murine C2C12 cells, following 3 days in differentiation medium, were fixed with ice-cold methanol-MES and immunostained with α-tubulin antibody and MACF1/ACF7 antibody (see table 2.1). Figure 5.9 demonstrates the cross-reactivity of the α-tubulin antibody with mouse (cells), and also methanol-MES as an adequate fixative. As expected, α-tubulin antibody illustrates microtubule expression (figure 5.9B). MACF1/ACF7 antibody shows a ubiquitous expression for MACF1/ACF7, but this pattern/antibody remains to be verified (figure 5.9A).

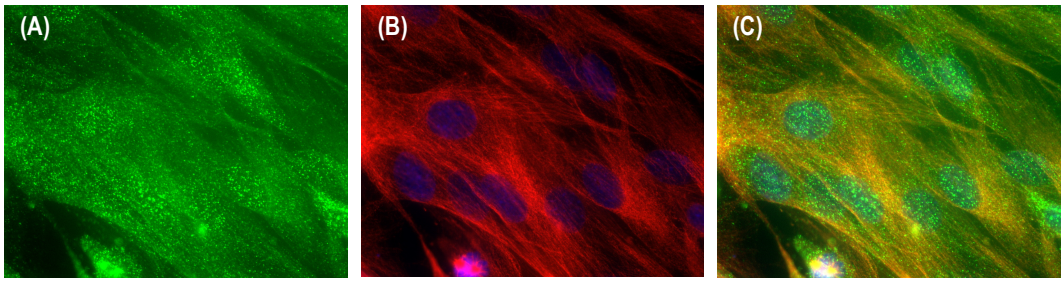

Figure 5.9. MACF1/ACF7 and microtubule immunostaining in murine C2C12 cells. C2C12 cells, following 3 days in differentiation medium, were fixed with ice-cold methanol-MES and immunostained with α-tubulin antibody and MACF1/ACF7 antibody. MACF1/ACF7 antibody shows a ubiquitous expression for MACF1/ACF7 in green (A) and α-tubulin antibody illustrates microtubule expression in red (B). (C) Merged image of (A) and (B), DNA is visualised via DAPI staining (blue).

To characterise the localisation of MACF1/ACF7 with regard to the actin cytoskeleton, C2C12 cells were immunostained with phalloidin and MACF1/ACF7. Cells were fixed with PFA and permeabilized with TritonX-100 (see materials and methods for further details). Phalloidin staining reveals actin filaments (figure 5.10A) and, again, MACF1/ACF7 appears to be abundant throughout the cells (although, as abovementioned this antibody needs to be verified; figure 5.10B).

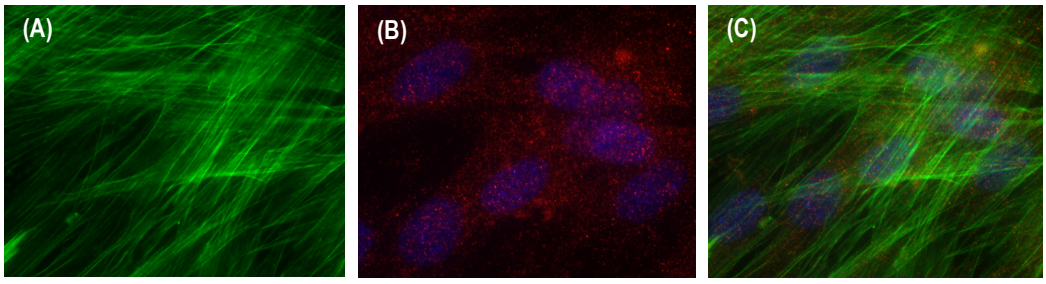

Figure 5.10. MACF1/ACF7 and actin immunostaining in murine C2C12 cells. C2C12 cells, following 3 days in differentiation medium, were fixed with PFA, permeabilized with TritonX-100 and immunostained with MACF1/ACF7 antibody and phalloidin. Phalloidin staining illustrates F-actin expression in green (A) and MACF1/ACF7 antibody shows a ubiquitous expression for MACF1/ACF7 in red (B). (C) Merged image of (A) and (B), DNA is visualised via DAPI staining (blue).

5.7. MACF1/ACF7 siRNA transfection in C2C12 cells

To confirm any MACF1/ACF7 knockdown in C2C12 cells transfected with siRNAs directed against mouse MACF1/ACF7 a western blot was performed. C2C12 cells were transfected on day 0 (of differentiation) with a combination of pre-designed siRNAs directed against mouse MACF1/ACF7 (supplied from Applied Biosystems, LifeTechnologies; see 2.21 Cell Transfection). Protein lysate was harvested following 48 hours growth in differentiation medium and a western blot was stained against MACF1/ACF7. MACF1/ACF7 antibody reveals several bands in control cells (i.e. non-transfected day 2 cells), including a particularly strong band at approximately 50kDa (figure 5.11A, lane 1). This strong band, however, almost completely disappears in cells that were transfected with siRNA1, siRNA2, or a combination of siRNA1 and siRNA2 (figure 5.11A, lanes 2 - 4).

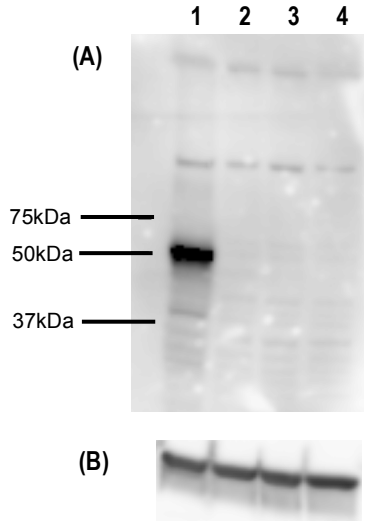

Figure 5.11. MACF1/ACF7 knockdown in C2C12 cells. Protein lysate was harvested from C2C12 cells grown in differentiation medium for 2 days. A western blot was stained against MACF1/ACF7 (**A**), and actin as a loading control (**B**). MACF1/ACF7 antibody reveals several bands in control wild type (i.e. non-transfected) cells (lane 1). The strong band that appears at approximately 50kDa, however, almost completely disappears in those cells transfected with siRNA1, siRNA2, or a combination of siRNA1 and siRNA2 (lanes 2, 3, and 4 respectively). Notably, the same MACF1/ACF7 siRNAs failed to affect the two upper molecular weight proteins detected by the MACF1/ACF7 antibody. The domain composition of these bands (or potential isoforms) is unknown (western blot and siRNA transfection performed by and courtesy of Dr. Katarzyna Goljanek-Whysall).

Discussion and Future Work

In chick, only one MACF1/ACF7 transcript (ENSGALT00000005857) has been annotated. ChEST16M13 has been shown to recognise exons 89-93 of this transcript (figure 5.4A). In human, however, 37 alternative MACF1/ACF7 transcripts (20 of which are protein coding) have been annotated. ChEST16M13 recognises exons 80-84 in the human transcript MACF1-031 (figure 5.4B). This EST also recognises, in addition to the human MACF1-031 transcript, the human MACF1-204, MACF1-028, MACF1-203, MACF1-201, MACF1-001, MACF1-032, MACF1-003, and MACF1-005 transcripts. It is not unreasonable, therefore, to posit that in chick, other transcripts (which may exist and are yet to be annotated) may also be recognised by this EST clone.

An RNA probe, synthesised using ChEST16M13, was used for *in situ* hybridisation experiments to determine the expression pattern of the *MACF1/ACF7* gene in a variety of HH Stage chicken embryos (figures 5.5-5.8). Expression is apparent in both the primitive streak of early chick embryos and in the somites of HH Stage 11 and 17 embryos, further suggesting that this gene may have a role in gastrulation and/or also in somitogenesis. The mouse knockout generated by Chen *et al* (2006) had a gastrulation phenotype, which is consistent with the expression in the primitive streak. Furthermore, a section through the trunk of the embryo (just above the hind limb) reveals expression in the dermomyotome and dorsomedial lip of the somite. Interference of *MACF1/ACF7* in early chick embryos or in early somites could, therefore, test the effects (if any) of this gene on the development of the primitive streak and the formation and/or differentiation of somites (see 6.8 MACF1/ACF7 and Early Muscle Fibres). Of particular interest would be any effects on the cytoskeletal architecture during gastrulation and/or somitogenesis. *MACF1/ ACF7* expression is also evident in other structures at different stages of development (see figures 5.5-5.8).

In chick, the full *MACF1/ACF7* expression pattern has not been previously shown, so to confirm these results it would be worthwhile repeating the above *in situ* hybridisation experiments with a sense mRNA probe as a

control. Further *in situ* hybridisation experiments are also required to complete the *MACF1/ACF7* expression pattern for all chick HH Stages and cryosectioning is also essential for comprehensive analysis. *In situ* hybridisation experiments were replicated more than once with a minimum of 3 embryos for each HH Stage. However, while the expression pattern shown here for each HH Stage is a majority example it ought to be noted that in some embryos the expression varied. The reason for this might be that the EST is longer than what was sequenced (i.e. sequencing is generally only efficient for approximately 1kb and EST was only sequenced in one orientation) and if the temperature varied slightly between experiments the end of the probe may have bound differently giving slightly varied results?

It is also worth noting that a slightly different expression pattern (for HH stage 17 chick embryos) has been shown for MACF1/ACF7 on the *Gallus* Expression *in Situ* Hybridization Analysis (GEISHA) database (available at: http://geisha.arizona.edu/geisha/). BLAST (Basic Local Alignment Search Tool) analysis shows that the probe (5' sequence) used in the generation of the GEISHA data corresponds to ChEST558D1 (Contig number 341352.2). Interestingly, sequence alignment of the 5' probe against the chicken genome reveals alignment to a region of chromosome 23 that is 195bp downstream of the MACF1/ACF7 stop codon and 493bp upstream of BMP8a. No exons are currently annotated within this intergenic region. However, sequence alignment of the 5' probe against the human *MACF1/ACF7* 3' UTR (untranslated region) reveals short regions of homology. Thus it is likely that the probe used to generate the data on GEISHA corresponds to a chicken 3' UTR. To be certain, however, it would be necessary to clone the chicken 3'UTR of *MACF1/ACF7*. Further analyses of the probe used to collect the GEISHA data also suggests that it can recognise, in addition to all the human transcripts recognised by ChEST16M13, human MACF1-010, MACF1-011, and MACF1-007 (figure 5.4). The recognition of these additional transcripts may also result in a varied expression pattern.

In 2000, Bernier *et al* described the developmental expression profile for mouse *MACF1/ACF7*. RNA *in situ* hybridisation experiments illustrated

MACF1/ACF7 transcripts in the dermomyotome and neural fold of day 8.5 mouse embryos and, later in development, expression was predominant in neural and muscle tissues (of particular interest, at day 10.5, expression appeared restricted to the myotome of the somite). Interestingly, just before birth, expression was strongly upregulated in type II alveolar lung cells (Bernier *et al*, 2000). Bernier *et al* (1996) had previously reported the identification of three different *MACF1/ACF7* isoforms. Two of these isoforms were reported to have putative actin binding domains (ABDs) at their N-termini, which were later shown to be functional (Leung *et al*, 1999). The three different isoforms were shown to contain alternative exons at their 5' ends (Bernier *et al*, 1996), a similar transcript diversity to BPAG1 (Brown *et al*, 1995). Bernier *et al* (2000) performed RNase protection assays (using a riboprobe that could distinguish between transcripts for isoforms 1 and 2) to determine the tissue distribution of isoforms 1 and 2 in postnatal day 3 mice. They also determined the distribution of isoform 3 (which lacks a functional ABD domain) using RT-PCR (reverse transcription-polymerase chain reaction). High levels of *MACF1/ACF7* transcripts for isoform 2 were detected in the brain, spinal cord, and lung, while expression was lower in the kidney, heart and skeletal muscle (with none detected in the skin, liver, stomach, and spleen). Conversely, isoform 1 transcripts were detected in all tissues tested and were predominant in skin, kidney, and stomach. Transcripts for isoform 3 were mainly detected in the brain and spinal cord, with moderate levels in skin, lung, and kidney (and no detection in the heart, skeletal muscle and liver).

Evidently, transcripts for all three isoforms have different tissue distribution (Bernier *et al*, 2000). RNase protection assays were also performed on RNA from mouse embryos at day 7.5 to day 10.5 and these illustrated that *MACF1/ACF7* is expressed early in embryogenesis (Bernier *et al*, 2000). *MACF1-1/ACF7-1* mRNA was detected in day 7.5 to day 10.5 embryos, while *MACF1-2/ACF7-2* mRNA only became detectable at day 10.5 (Bernier *et al*, 2000). Bernier *et al* (2000) suggest that the alternate isoforms of MACF1/ACF7 may have differential functions based on the cell types in which they are expressed and the partners with which they interact.

The isoforms of BPAG1, the only other known mammalian spectraplakin, have also been shown to be tissue specific (see 5.1. MACF1/ACF7 Structure and Isoforms). Thus it is not unreasonable to speculate that MACF1/ACF7 isoforms exist in chick and that these would also be tissue specific. As abovementioned, the ChEST16M13 clone recognises the only annotated chick MACF1/ACF7 transcript and nine of the thirty-seven alternative human MACF1/ACF7 transcripts. It is difficult to determine if these particular transcripts correlate to any of the known mammalian isoforms and thus determine if this particular EST is isoform specific (i.e. is the expression pattern for chick, shown here [using an RNA probe against this EST], relative to one or more isoform?). BLAST analysis of the ChEST16M13 sequence shows that this EST corresponds to a predicted chick MACF1/ACF7 isoform 4-like, but how/if this corresponds to known mammalian isoforms remains to be elucidated. Furthermore, it is difficult in the current literature to define the named isoforms in mammals. For instance, how do the mouse MACF1/ACF7 isoforms described by Bernier *et al* (1996; see above) correlate to those mammalian isoforms described in the review by Suozzi *et al* (2012; see 5.1. MACF1/ACF7 Structure and Isoforms)? One could speculate that the mouse isoform, which lacks a functional ABD domain (i.e. isoform 3), reported by Bernier *et al* (1996), corresponds to the MACF1c isoform (which has a predicted domain structure and lacks an ABD domain) reviewed by Suozzi *et al* (2012) but this would need to be confirmed (as with all the other isoforms). Nonetheless, it is evident that, in mammals, MACF1/ACF7 and BPAG1 are expressed in multiple isoforms in different tissues, and this is likely to be the case in chick.

BPAG1 knockout mice (*BPAG*$^{-/-}$) display sensory neuronal defects, skin blistering, and muscle degeneration (dying at 3-5 weeks of age). The neuronal defects are due to the absence of BPAG1a in the nervous system. Degeneration is only seen in certain tissues even though BPAG1 is ubiquitously expressed. This suggests that MACF1/ACF7 might compensate for BPAG1 in other regions (Brown *et al*, 1995; Guo *et al*, 1995). *MACF1/ACF7* knockout mice, however, die at gastrulation (Chen *et al*, 2006), indicating that the function of MACF1/ACF7 may be different from that of

BPAG1 in some tissues essential for development (or that BPAG1 is not expressed in those tissues). Intriguingly, *MACF1/ACF7* cKO mice display no gross morphological changes in their skin or hair coat (Wu *et al*, 2008), which suggests that MACF1/ACF7s function later in development may be performed by BPAG1. Together, these data suggest that there is likely to be some redundancy between MACF1/ACF7 and BPAG1. As aforementioned, the spectraplakin family also comprises a single gene in zebrafish, *Magellan*, a single gene in *Drosophila melanogaster*, *short stop* (*shot*)/*Kakapo*, and a single *Caenorhabditis elegans* gene, *vab-10* (reviewed by Suozzi *et al*, 2012). *Vab-10* mutants display elongation and body morphology defects (Bosher *et al*, 2003). Mutations of *short stop* (*shot*)/*Kakapo* result in defects in epidermal integrity, epidermal muscle attachment, muscle-dependent tendon cell differentiation, anastomosis of the tracheal branches, axonal outgrowth and guidance, and dendritic morphogenesis (see review by Röper and Brown, 2003). As *short stop* (*shot*)/*Kakapo* is the only spectraplakin gene in *Drosophila melanogaster* it is not surprising that mutations in this gene have a stronger phenotype than mutations in *BPAG1* (owing to possible redundancy between BPAG1 and MACF1; Röper *et al*, 2002).

Preliminary experiments to establish if MACF1/ACF7 knockdown in C2C12 cells affects the microtubule cytoskeleton have been illustrated (figures 5.9-5.11). Immunostaining of murine C2C12 cells, following 3 days in differentiation medium, with a MACF1/ACF7 antibody has demonstrated a ubiquitous expression for MACF1/ACF7 (figures 5.9A and 5.10B). The accuracy of this antibody, however, is yet to be confirmed. Additionally, negative control experiments should be performed (i.e. staining without primary antibody). That said, the stain appears stronger in cells fixed with methanol-MES (figure 5.9A) compared to those fixed in PFA and TritonX-100 (figure 5.10B), however, this may also be a result of the secondary antibody that was utilised (i.e. anti-mouse Alexa fluor 568 [red] fades much more quickly than anti-mouse Alexa fluor 488 [green]). To note, some C2C12s were fixed with PFA and TritonX-100 to accommodate the staining conditions of phalloidin. As expected, phalloidin staining reveals F-actin (figure 5.10A)

and α-tubulin staining illustrates the expression of microtubules (figure 5.9B) in wild type C2C12s. A western blot was performed to confirm any MACF1/ACF7 knockdown in C2C12 cells transfected with siRNAs directed against mouse MACF1/ACF7 (figure 5.11). The MACF1/ACF7 antibody revealed several bands in control cells (non-transfected cells), including a particularly strong band at approximately 50kDa (figure 5.11A, lane 1). This strong band, however, almost completely disappeared in cells that were transfected with siRNA1, siRNA2, or siRNA1 and siRNA2 together (figure 5.11A, lanes 2 - 4). Notably, the same MACF1/ACF7 siRNAs failed to affect the two upper molecular weight proteins detected by the MACF1/ACF7 antibody (figure 5.11). The domain composition of any of the detected bands is unknown. There is a possibility that the band that disappears following siRNA transfection is a specific isoform, or perhaps, more likely, it is a cleavage (degradation) product. Further experiments are needed to validate this.

Sanchez-Soriano *et al* (2009) have shown that it is possible (using a MACF1/ACF7 antibody) to detect a protein appearing as a ~600 kDa band on a western blot: before transferring proteins to a polyvinylidene difluoride (PVDF) membrane, cell lysates from Neuro 2A cells (from a mouse neural crest-derived cell line) were resolved by sodium dodecyl sulfate polyacrylamide gel electrophoresis (SDS-PAGE) using a 3-8% Tris-acetate gradient gel (Invitrogen). The detected band was shown to correspond in size to the Shot-LA isoform implicated in axon extension in *Drosophila* (Lee and Kolodziej, 2002). Owing to it's size, this band could represent the full-length MACF1/ACF7 or a large ~600kDa isoform. It may, therefore, be worthwhile repeating the western blot technique described above for C2C12 cell lysate (following siRNA transfection) to see if there is any decrease in the larger MACF1/ACF7 bands (not detected on the western shown here, figure 5.11). It would also be interesting to repeat the immunostaining described above (figures 5.9 and 5.10) but this time following transfection of the C2C12 myoblasts with different combinations of siRNAs (directed against MACF1/ACF7) to see if there are any affects on the microtubule and actin cytoskeleton. As the loss of MACF1/ACF7 in primary endodermal cells has

been shown to result in less-stable, long microtubules with skewed cytoplasmic trajectories, when compared to control cells (Kodama *et al*, 2003), it is anticipated that following siRNA transfection, not only would there be a reduction in MACF1/ACF7 (confirmation of MACF1/ACF7 knockdown via immunostaining would first require verification of the MACF1/ACF7 antibody) but also a disruption to the microtubule cytoskeleton.

In C2C12 cells immunostaining for MACF1/ACF7 has not been previously shown. Staining for other +TIPS (EB1 and EB3 for example), however, has been previously reported (Mimori-Kiyosue and Tsukita; Straube and Merdes, 2007). Interestingly, Young *et al* (2003) have illustrated the localisation of muscle/neuronal, BPAG1a/b, isoforms and the epithelial, BPAG1e, isoform within C2C12 myoblasts. An antibody specific to BPAG1a/b isoform 2 was shown to detect protein co-aligning with actin stress fibres, and additionally, the same antibody and two BPAG1e antibodies predominantly detected protein in the nuclei. A BPAG1a/b isoform 2 N-terminal fusion protein containing the plakin domain was also shown to localise to actin stress fibres and to nuclei (Young *et al*, 2003). Young *et al* (2003) subsequently demonstrated that a functional nuclear localisation signal exists within the plakin domain and is responsible for localisation of the fusion protein to the nucleus. Furthermore, BPAG1a/b isoform 1 N-terminal fusion proteins were shown to differ in their interaction with actin filaments and their ability to localise to the nucleus, indicating BPAG1 isoforms with different N-termini have differing roles (Young *et al*, 2003).

The immunostaining for MACF1/ACF7 in C2C12s shown here could indicate a similar pattern to that depicted for BPAG1, in that the stain appears to be in the nucleus and possibly along actin filaments (figures 5.9A, 5.10B and 5.10C). However as aforementioned, the MACF1/ACF7 antibody that was utilised has to be verified and optimal cell fixing conditions need to be established. If the epitope against which the MACF1/ACF7 antibody is directed was known, it would also be interesting to determine what MACF1/ACF7 protein isoforms are being recognised in the mouse, chick, and human, and compare this to the isoforms that are being recognised by the ChEST16M13 clone in the *in situ* hybridisation experiments (i.e. are the

antibody and EST highlighting the same isoforms?). It would also be interesting to see the localisation of the recognition site (i.e. is the epitope of the antibody in the N-terminal or C-terminal?).

Chapter 6: Wnt Signalling in Somitogenesis and Myogenesis

Introduction

Somite development is a rhythmic process that involves a series of steps, which include paraxial mesoderm segmentation, epithelialisation, somite formation, somite patterning, somite maturation, and differentiation of somitic cells into different lineages (Geetha-Loganathan *et al*, 2008). Wnt signalling has been shown to play vital roles in several of these steps of development. Wnts are signalling molecules that regulate numerous developmental processes, including proliferation, asymmetric division, patterning, and cell fate determination (Wodarz and Nusse, 1998), they function as signals via either the canonical pathway or the noncanonical pathways (see 1.5. Wnt Signalling).

6.1. Somite Patterning and Wnt Signalling

The formation of the dermomyotome is a result of dorsoventral patterning whereby the ventromedial epithelial somite undergoes EMT to form the sclerotome, which leaves behind a dorsally located epithelial sheet termed the dermomyotome. The epithelial state of the dermomyotome is regulated by signals that originate from dorsal structures such as the surface ectoderm and dorsal neural tube. These dorsalising signals work in contrast to the ventral signals from the notochord and floor plate, which promote de-epithelialisation and mesenchymal fate. The patterning and fate determination of somitic cells thus occurs in response to the extrinsic signals from the adjacent tissues (Brand-Saberi *et al*, 1996; Brent and Tabin, 2002; Kalcheim and Ben-Yair, 2005; Scaal and Christ, 2004; Williams and Ordahl, 1997). Wnts are acknowledged as key players in the establishment of the dorsal epithelial dermomyotome, while the paracrine factors Sonic Hedgehog

(Shh) and Noggin are the major ventralising signals. Shh and Noggin, produced and secreted by the notochord (and Shh also by the floor plate of the neural tube), are necessary for induction (and maintenance) of the sclerotome (Brand-Saberi *et al*, 1993; Borycki *et al*, 1998; Christ *et al*, 1992; Dietrich *et al*, 1997; Dockter and Ordahl, 2000; Fan and Tessier-Lavigne, 1994). The formation of the medial half of the dermomyotome is attributed to Wnt1 and Wnt3a signalling from the dorsal neural tube, whereas ectodermal Wnt4, Wnt6, and Wnt7a signalling influences the lateral half of the dermomyotome (Christ *et al*, 1992; Münsterberg *et al*, 1995a; Olivera-Martinez *et al*, 2001). Galli *et al* (2004) have also shown that Wnt3a stimulates cell proliferation in the dermomyotome. Intriguingly, soon after the sclerotome and dermomyotome are established, the dorsal Wnt signals and the ventral Shh signals synergise to promote and develop the intermediate myotome (Dietrich *et al*, 1997).

The dermomyotome is patterned along the mediolateral axis into medial, central, and lateral regions, which contain progenitors of epaxial muscle, dermis, and hypaxial muscle, respectively. At the level of the segmental plate and the epithelial somites, Wnt6 is expressed throughout the entire ectoderm, which overlies the neural tube, the paraxial mesoderm and the lateral plate mesoderm. As the somite matures, however, its expression becomes restricted to the lateral ectoderm, which covers the ventrolateral lip of the dermomyotome and the lateral plate mesoderm (Geetha-Loganathan *et al*, 2006). Geetha-Loganathan *et al* (2006) have shown that Wnt11 is an epithelialisation factor that, upon induction by the neural tube (Marcelle *et al*, 1997), maintains the epithelial state of the dorsomedial lip while restricting the expression of *Wnt6* to the ectoderm overlying the ventrolateral lip. Wnt11 and Wnt6 thus maintain the epithelial nature of the dorsomedial and ventrolateral lips, respectively, allowing the central region of the dermomyotome to de-epithelialise to form dermis and muscle (Gros *et al*, 2005), which indicates a role of Wnt signalling in the patterning of the dermomyotome along its mediolateral axis (Geetha-Loganathan *et al*, 2006; Geetha-Loganathan *et al*, 2008).

Bone morphogenetic proteins (BMPs) also have a significant role in somite patterning. *BMP4* is expressed in the dorsal neural tube, where it induces *Wnt1* (which in turn induces *Wnt11* expression in the dorsomedial lip of the dermomyotome [Marcelle *et al*, 1997]), and in the lateral plate mesoderm. BMPs block *MyoD* expression (and thus have a negative influence on myogenesis), so to ensure proper formation of the myotome their action is controlled by the early expression of their antagonist *Noggin* in the medial somite (Reshef *et al*, 1998).

The signals that govern somite patterning also influence cell fate determination. Wnt signals from the surface ectoderm and the dorsal neural tube, for example, do not just favour a dorsal somitic fate (i.e. the dermomyotome) but in connection they also promote myogenesis. Wagner *et al* (2000) have shown, via implantation of Wnt1, Wnt3a, and Wnt4 secreting cells, that not only was the ventral region of the somite compromised but also that myotome formation was enhanced (noted by an increase of the *MyoD* expression domain).

6.2. Wnt Signalling and Skeletal Muscle Development

In vertebrates, most skeletal muscles (excluding certain head muscles) develop from somites (Bryson-Richardson and Currie, 2008). Maturing somites develop the ventrally located mesenchymal sclerotome, which forms cartilage scaffold of the bony skeleton, and the dorsally located epithelial dermomyotome, which develops into the dermis and the skeletal muscles of the trunk and limbs. Originating in the dermomyotome, myogenic precursor cells (MPCs) are identified by the expression of the paired-box transcription factors Pax3 and Pax7 (Kassar-Duchossoy *et al*, 2005). Cells that delaminate from the dermomyotome express myogenic regulatory factors (MRFs) and ultimately downregulate Pax3/Pax7 to produce the first skeletal muscle tissue (the myotome). At limb level, myogenic progenitor cells with long-range migratory capability delaminate from the somite and will later form muscles in the extremities (Buckingham *et al*, 2003).

Embryonic myogenesis is coordinated via a complex signalling network of temporally regulated morphogenetic cues from structures that surround the developing muscle tissue. These extrinsic signalling molecules, as abovementioned, include Wnts, Sonic Hedgehog (Shh), and bone morphogenetic proteins (BMPs). The following will focus on the roles of Wnt family members in regulating the development of embryonic muscle (figure 6.1).

Figure 6.1.

Wnt1, Wnt3a, and Wnt4 are expressed in the dorsal half of the neural tube and, in cooperation with Shh signalling from the notochord, have been shown to induce myogenesis in presegmented mesoderm explants (Münsterberg *et al*, 1995a). However, Wnt7a and Wnt7b, which do not induce somitic myogenesis *in vitro*, are mainly expressed in the ventral half of the neural tube (Parr *et al*, 1993). Wnt signalling has additionally been demonstrated to influence the expression of myogenic regulatory factors (MRFs), which are essential transcriptional regulators of myogenic lineage progression and

differentiation. In explant cultures of paraxial mesoderm from mouse embryos, Wnt1, produced in the dorsal neural tube, was shown to induce myogenesis via activation of the MRF Myf5, whereas Wnt7a or Wnt6, produced in the dorsal ectoderm, preferentially activates the MRF MyoD (Tajbakhsh *et al*, 1998). Wnt7a activates MyoD via a PKC-dependent β-catenin-independent non-canonical pathway (Brunelli *et al*, 2007). Wnt1 signals through two Frizzled receptors (Fzd1 and Fzd6) in the epaxial domain of the somite, to regulate the expression of Myf5 via the canonical Wnt/β-catenin pathway (Borello *et al*, 2007).

During mouse somitogenesis the Fzd7 receptor is expressed in the hypaxial region of the somite, which suggests an interaction with Wnt7a (Borello *et al*, 1999a). Correspondingly, as mentioned above, the Fzd1 and Fzd6 receptors are expressed in the epaxial region, which correlates with the expression of Myf5. In addition, transplacental delivery of sFRP3 (a soluble Wnt antagonist) reduces skeletal myogenesis in a dose-dependent fashion, which demonstrates that Wnt signalling is indispensable during embryonic myogenic development (Borello *et al*, 1999b).

Otto *et al* (2006) have illustrated that, within the dorsal somite, Wnt1, Wnt3a, Wnt4, and Wnt6 can upregulate and expand Pax3 and Pax7 expression. In addition, Wnt6 can mimic the effect of the dorsal ectoderm in maintaining the expression of Pax3 and Pax7. Wnt-induced expression of Myf5, MyoD, and Pax3, in the mouse somite, is mediated by PKA and cAMP response element-binding protein (CREB; Chen *et al*, 2005). Furthermore, Abu-Elmagd *et al* (2010) have shown that Wnt signals that directly affect Lef1 transcriptional activator and Pitx2 transcription factor activity affect the number of premyogenic Pax3/Pax7 cells.

Knockout studies performed in mouse embryos have revealed the importance of Wnt signalling in dermomyotome formation. Embryos lacking both Wnt1 and Wnt3a do not form the medial region of the dermomyotome, which is accompanied with a reduction in the expression of Myf5 (Ikeya and Takada, 1998). Also, Linker *et al* (2005) have demonstrated that Wnt6 β-catenin-dependent signalling from the dorsal ectoderm is necessary for the

maintenance of epithelial organisation in somites and dermomyotome formation. Moreover, conditional deletion of β-catenin (driven by Pax3-Cre or Pax7-Cre) revealed that β-catenin is required within the somite for the formation of the dermomyotome and the myotome and for the determination of the number of foetal progenitors and myofibres in the limb (Hutcheson *et al*, 2009).

6.3. Wnt11 and Early Muscle Fibres

Gros *et al* (2009) have shown that the sequential action of the Wnt/PCP and the Wnt/β-catenin pathways is essential for the formation of fully functional chick embryonic muscle fibres. Their studies revealed that *Wnt11* expression in the epaxial dermomyotome acts as a local cue to direct and organise the elongation of primitive myofibres in the myotome. Their results demonstrate that the effect of Wnt11 is mediated through the evolutionary conserved planar cell polarity (PCP) pathway, downstream of the Wnt/β-catenin pathway that is required to initiate the myogenic program of myocytes and the expression of *Wnt11* itself.

The neural tube, which drives *Wnt11* expression in the dorsomedial lip of the dermomyotome (Marcelle *et al*, 1997), was shown to be necessary and sufficient to orient myocyte elongation. Half of the neural tube was removed at the level of the presomitic mesoderm, where myocytes have not yet formed. One day after ablation, myocytes that had formed during incubation (stained for myosin heavy chain) were disorganised when compared to those on the control side of the embryo (figure 6.2a, b). When the neural tube was removed at an embryonic level where myocytes had already formed, the myotome was almost normal following one day of incubation. Additionally, as myosin heavy chain antibodies only reveal fully elongated myocytes, dorsomedial lip cells were electroporated with a GFP reporter gene (before neural tube ablation), to show all cell shape changes induced by the absence of the neural tube. One day later, in addition to disoriented fully elongated myocytes, Gros *et al* (2009) observed GFP-positive cells that had elongated

in the either the wrong direction, in many directions, or had failed to elongate altogether when compared to the control (figure 6.2c, d).

Figure 6.2.

To test if Wnt11 plays a role during the polarised elongation of myocytes, small interfering RNAs (siRNAs), directed against chick *Wnt11*, were also electroporated. This lead to partially elongated electroporated cells within the myotome in addition to mis-oriented myocytes, a phenotype that was not seen in GFP- or control siRNA-electroporated embryos (Gros *et al*, 2009). These experiments show that Wnt11 is necessary to control myocyte orientation and indicate that the action of the neural tube on the polarised elongation of myocytes is mediated, somewhat, by Wnt11.

In vertebrates, during convergence extension movements, Wnt11 has been reported to act through the PCP pathway (Heisenberg *et al*, 2000; Wallingford *et al*, 2000) and Djiane *et al* (2000) and Witzel *et al* (2006) have

shown that Fzd7 mediates its activity. To ascertain if Wnt11 is acting through the PCP pathway in chick somites, Gros *et al* (2009) electroporated a secreted form of Fzd7, which acts as a competitive inhibitor of Fzd7 function (Bhanot *et al*, 1996). Electroporated cells failed to elongate and, correspondingly, when a full-length *Fzd7* was overexpressed myocytes were shown to elongate aberrantly. The overexpression and knockdown (via siRNAs) of chick *Prickle1*, a core PCP molecule expressed in the myotome (Cooper *et al*, 2008) that has no known role in β-catenin-dependent Wnt signalling but is required for PCP in vertebrates and invertebrates (Seifert and Mlodzik, 2007), also resulted in the disorganised elongation of myocytes (Gros *et al*, 2009). Dishevelled (Dvl), the downstream effector of frizzled, mediates the activity of both the β-catenin-dependent and the PCP pathways and several *dvl* constructs have been shown to interfere with one or both of these pathways in *Drosophila* or *Xenopus* (Axelrod *et al*, 1998; Heisenberg *et al*, 2000; Rothbacher *et* al, 2000; Wallingford *et al*, 2000). The full-length *dvl* and *dvl-*Δ*PDZ* and *dvl-*Δ*DEP* (constructs that lack the PDZ or the DEP domain respectively) have been shown to interfere with the Wnt/PCP pathway during vertebrate gastrulation (Heisenberg *et al*, 2000; Rothbacher *et al*, 2000; Wallingford *et al*, 2000). Gros *et al* (2009) demonstrate that expression of all three of these constructs in the dorsomedial lip results in failure of electroporated cells to elongate correctly within the myotome. Rho and Rac (small GTPases) are downstream effectors of the PCP pathway. The overexpression of Rock (Rho-associated, coiled-coil containing protein kinase) in the dorsomedial lip resulted in the formation of mis-oriented or multipolar myocytes. Additionally the overexpression of *Wnt11* brought about a robust phosphorylation of JNK (c-Jun N-terminal kinase, the kinase associated with Rac) within the transition zone, which suggests that Wnt11 is able to activate this WNT/PCP target. Together, these data infer that Wnt11 regulates the polarised elongation of myocytes via the PCP pathway (Gros *et al*, 2009).

As Wnt11 has also been shown to activate the canonical, β-catenin-dependent pathway (during *Xenopus* axis formation for example; Tao *et al*, 2005), Gros *et al* (2009) next determined if Wnt11 regulates the polarised

elongation of myocytes via activation of the PCP pathway only or the canonical pathway as well. In mice, initiation of the expression of Myf5 in the dorsomedial lip was demonstrated to depend on Wnt/β-catenin-dependent signalling (Borello *et al*, 2006). Correspondingly, electroporation of full-length Dvl or an activated form of β-catenin (both of which activate the Wnt/β-catenin-dependent pathway) resulted in overexpression of Myf5. Electroporation of dominant-negative forms of β-catenin or Lef1 (which repress the Wnt/β-catenin-dependent pathway), however, led to inhibition of Myf5 expression, confirming that the Wnt/β-catenin-dependent pathway is essential for muscle fate (Abu-Elmagd *et al* 2010; Gros *et al*, 2009). *Myf5* expression was neither upregulated nor downregulated following electroporation (in the dorsomedial lip) of *Wnt11*, secreted *Fzd7*, siRNAs against chick *Wnt11*, *dvl-ΔPDZ* or *dvl-ΔDEP*. This indicates that, within the transition zone, these constructs do not modulate the Wnt/β-catenin-dependent pathway and that the elongation defects generated by these constructs are due to a modulation of the PCP pathway only (Gros *et al*, 2009). Inhibition of Wnt/β-catenin-dependent signalling also affected elongation in electroporated cells. Those cells, however, did not activate the expression of *Myf5*, yet they retained Pax7 expression. Gros *et al* (2009) suggest that blockage of the β-catenin-dependent pathway maintains the cells in an undifferentiated ($Pax7^{+}$ $Myf5^{-}$) state, which inhibits their maturation into polarised and elongating myocytes. Together with the observation that canonical Wnt signalling regulates the expression of *Wnt11* (see Gros *et al*, 2009), this implies that β-catenin-dependent Wnt signalling is required upstream of muscle fibre polarised elongation, which is itself controlled by the Wnt11/PCP pathway (figure 6.3).

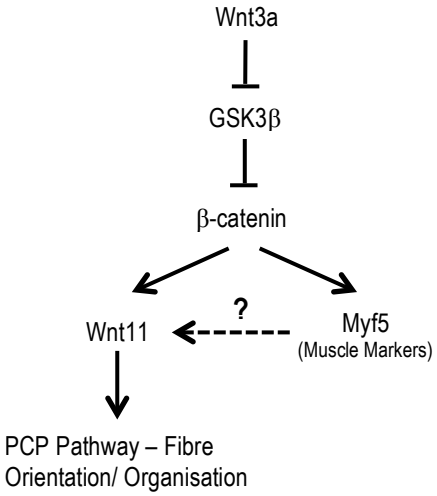

Figure 6.3. The sequential action of the Wnt/PCP and the Wnt/β-catenin pathways is essential for the formation of fully functional chick embryonic muscle fibres (Gros *et al*, 2009). *Wnt11* expression in the epaxial dermomyotome acts as a local cue to direct and organise the elongation of primitive myofibres in the myotome. The effect of Wnt11 is mediated through the PCP pathway, downstream of the Wnt/β-catenin pathway that is required to initiate the myogenic program of myocytes and the expression of *Wnt11* itself.

To conclude, Gros *et al* (2009) exposed differentiating myocytes to localised exogenous sources of Wnt11 to test whether *Wnt11* (expressed by the dorsomedial lip cells) provides an instructive or a permissive signal to the elongating myocytes in the transition zone. Wnt11-expressing cells were placed between two adjacent, newly formed somites and myocytes that formed under these conditions elongated parallel to the grafted cells (figure 6.4b,e). Myocytes elongated normally, however, in embryos grafted with control cells (figure 6.4a, d). Furthermore, when small aggregates of cells expressing Wnt11 were positioned within the somite, myocytes were observed swirling around the injected cells (figure 6.4c, f).

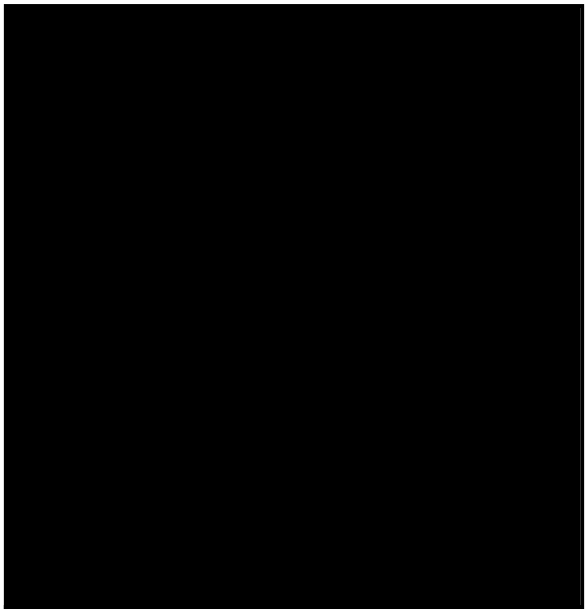

Figure 6.4.

In a reverse experiment, myocytes were shown to elongate in a disorganised manner in somites uniformly expressing Wnt11 (homogenously infected with RCAS-Wnt11 retroviruses). Together, these data indicate the importance of a localised source of Wnt11 for the oriented elongation of myocytes and they reveal that Wnt11 acts as an instructive cue interpreted by myocytes to determine the orientation of their elongation (Gros *et al*, 2009).

6.4. Wnt Signalling and the Cytoskeleton

The cytoskeleton, as aforementioned, is highly dynamic and undergoes continuous reorganisation. This reorganisation allows cells to change shape, to divide, and to participate in directed migration. In order to achieve such complex cellular functions cytoskeletal elements must be co-ordinately

regulated. Numerous studies have revealed key cytoplasmic molecules that regulate the organisation and dynamic of the cytoskeleton. Furthermore, several extracellular factors have been shown to trigger signalling cascades that directly modulate the cytoskeleton (Salinas, 2007).

Embryonic morphogens, such as Wnts, influence the fate of cells during early embryonic patterning, cell movement, and cell polarity (Wodarz and Nusse, 1998), processes in which the cytoskeleton is noticeably modified. It has frequently been assumed that these morphogens, and many other growth factors, regulate the cytoskeleton indirectly by inducing changes in gene expression. More recent studies, however, have shown that signalling pathways (activated by morphogens) directly modulate the cytoskeleton by altering the activity, destination and stability of cytoskeletal regulators (reviewed by Salinas, 2007).

The canonical Wnt pathway is mostly associated with β-catenin and transcriptional regulation (see 1.5. Wnt Signalling). However, canonical Wnt signalling has been shown to directly regulate the cytoskeleton without transcriptional activity (Ciani *et al*, 2004; Schlesinger *et al*, 1999; Walston *et al*, 2004). Various components of the canonical Wnt pathway have been shown to associate with the cytoskeleton (table 6.1). These associations suggest two possible outcomes. First, that Wnt signalling can be locally activated within specific cellular compartments. Second, local alterations to the cytoskeleton could induce the release or sequestration of Wnt components associated with the cytoskeleton resulting in the activation or repression of the Wnt cascade in specific cellular compartments. Wnt signalling, therefore, can be confined to specific cellular regions and as a consequence influence cell behaviour without necessarily affecting nuclear function (Salinas, 2007).

Table 6.1. [redacted]

Numerous studies in *Caenorhabditis elegans*, *Drosophila*, and vertebrates have demonstrated a role for Wnt signalling in the regulation of the microtubule cytoskeleton. In addition to regulating microtubule stability, Wnts regulate the organisation of the microtubule network by modulating the tethering of the microtubules to the cell cortex. Capture of microtubules at the cell cortex is essential for correct alignment of the mitotic spindle (and thus segregation of chromosomes during cell division), for cell migration, and for oriented cell growth such as axon elongation (for a comprehensive review see Salinas, 2007).

Miller *et al* (1999) and Krylova *et al* (2000) illustrated that, in mammalian cells, Dvl is tightly associated with microtubules. This was the first

demonstration that canonical Wnt signalling might directly regulate the cytoskeleton. In developing neurons, endogenous Dvl preferentially associates with stable microtubules (Krylova *et al*, 2000). Wnt pathway activation (through Dvl) increases microtubule stability as microtubules become resistant to depolymerisation by nocodazole (Ciani *et al*, 2004; Krylova *et al*, 2000). Ciani *et al* (2004) have shown that microtubule stability is achieved via inhibition of GSK3β but through a transcription-independent pathway. In addition they also illustrated that endogenous Axin (a negative regulator of the Wnt cascade) binds to and stabilises microtubules, which may suggest that Axin is a modulator rather than an inhibitor of the Wnt pathway or that perhaps it plays a dual role. Thus, a canonical Wnt pathway that diverges downstream of GSK3β regulates microtubules, which results in profound changes in cell behaviour (Salinas, 2007).

The inhibition of GSK3β directly affects the behaviour of microtubules by altering the phosphorylation of specific cytoskeletal targets. GSK3β phosphorylates many MAPs including MAP1B, MAP2 and APC. Wnt pathway activation, in axons, results in a significant decrease in MAP1B phosphorylation, at a site phosphorylated by GSK3β (Ciani *et al*, 2004; Lucas *et al*, 1998). Intriguingly, GSK3β phosphorylation of MAP1B maintains microtubules in a dynamic state (Goold *et al*, 1999), while decreased phosphorylation (via inhibition of GSK3β) results in increased microtubule stability (Lucas *et al*, 1998). Though the effects of Wnts on axon behaviour and the stability of microtubules can be explained by alterations in the phosphorylation of MAP1B, other GSK3β targets may also contribute to changes in the microtubule cytoskeleton. Together this data shows that canonical Wnt signalling regulates microtubule stability by directly targeting cytoskeletal proteins (Salinas, 2007).

6.5. GSK3β Regulates MACF1/ACF7 in Cell Migration

Wu *et al* (2011) have recently reported that GSK3β orchestrates polarisation and reorganisation of microtubules in hair follicle stem cells during wound healing. This report, along with another study by Zaoui *et al* (2010), has

shown that GSK3β governs the elongation of microtubules through its control of the +TIP protein MACF1/ACF7 (Previewed by Yucel and Oro, 2011; for more information about MACF1/ACF7 see Chapter 5). Wu *et al* (2011) demonstrate that there is a significant delay in wound closure in mice with mutations in the *MACF1/ACF7* gene. They illustrate that GSK3β directly phosphorylates the C-terminus of MACF1/ACF7, which diminishes MACF1/ACF7's binding to microtubules (i.e. attenuating the interaction between the acidic C-terminal tubulin tails and MACF1/ACF7's GSR domain). Using a phospho-specific antibody, Wu *et al* (2011) also show that phospho-MACF1/ACF7 localises to the cytoplasm but not to microtubules, corroborating that MACF1/ACF7 phosphorylation uncouples the +TIP from microtubules (figure 6.5). The authors subsequently show that a phosphorylation-refractile MACF1/ACF7 (a mutant version of MACF1/ACF7 that is refractory to phosphorylation by GSK3β) can rescue certain elements of the MACF1/ACF7 mutant phenotype (overall microtubule architecture for example; Previewed by Yucel and Oro, 2011).

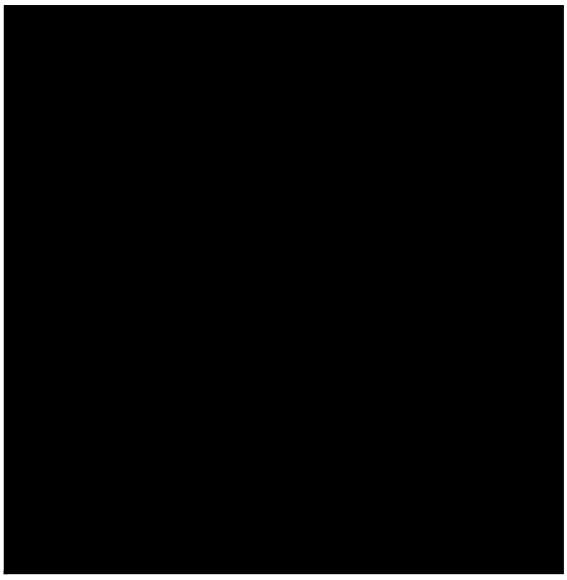

Figure 6.5.

Comparably, Zaoui *et al* (2010) have studied the role of GSK3β in the migration of breast carcinoma cells responding to Heregulin (the epidermal growth factor [EGF] ligand) via stimulation of the tyrosine kinase receptor ErbB2. Previously, Zaoui and colleagues had shown that, at the leading edge of the cell, Heregulin induces directed cell protrusions by triggering the Memo (mediator of ErbB2 motility) membrane complex. They had also demonstrated that APC and CLASP2 mediate the formation of microtubules at cell protrusions during these cells' migration (Marone *et al*, 2004; Zaoui *et al*, 2008). More recently they show that Memo inactivates GSK3β, which in turn targets APC and CLASP2 to the plasma membrane. Furthermore, Heregulin activity localises MACF1/ACF7 to the membrane and microtubules, and this localisation depends on GSK3β and APC (Previewed by Yucel and Oro, 2011; Zaoui *et al*, 2010).

Taken together, the abovementioned data convincingly link the activity of GSK3β and the phosphorylation status of MACF1/ACF7 with cell migration and MACF1/ACF7 association with microtubules (Yucel and Oro, 2011). The biochemical mechanism of the regulation of MACF1/ACF7 by GSK3β, however, remains to be elucidated. Wu *et al* (2011) illustrate that neither the kinase-refractile nor the phospho-mimetic mutants of MACF1/ACF7 could rescue the directional mutant and polarity defects in MACF1/ACF7 mutant hair follicle stem cells. Thus, unpredictably, GSK3β regulation of MACF1/ACF7 must be more complex than simply inhibition by phosphorylation, which implies that subsets of the multiple MACF1/ACF7 phosphorylation sites might have distinct functions. Kumar *et al* (2009) have previously observed such behaviour for CLASP2. Alternatively, prolonged microtubule elongation may require the cycling of MACF1/ACF7 phosphorylation (Yucel and Oro, 2011).

Aim

- To further examine the effects of Wnts on myofibre orientation, which may reveal a direct role for the canonical Wnt pathway in fibre orientation that is independent of Wnt11.

Results

6.6. Wnt11 and Early Muscle Fibres

To visualise myofibres in somites, HH Stage 20 chick embryos were immunostained in wholemount with MF20, a monoclonal antibody that recognises the heavy chain of myosin II. As expected, myosin heavy chain is apparent in both the somites and in the heart (figure 6.6).

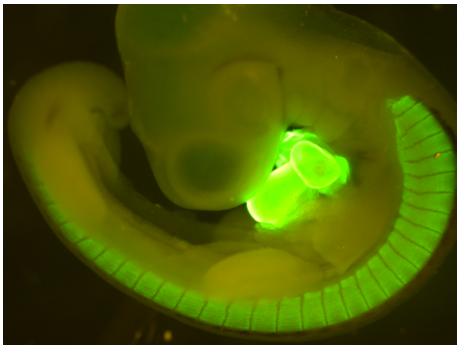

Figure 6.6. Myosin heavy chain expression in a HH Stage 20 Chick embryo. Embryo was immunostained in wholemount with MF20 antibody and, as expected, myosin heavy chain appears in the somites and in the heart.

To test the effects of Wnt11 on myofibre orientation, Wnt11 secreting rat fibroblast cells (a kind gift from Dr. Chen-Ming Fan, Carnegie Institution of Washington, Baltimore, MD 21218) were stained with DiI and injected either within the myotome (somite IV) or between two somites (somites III and IV, or somites IV and V) of HH Stage 16 chick embryos. Embryos were re-

incubated for 14-16 hours and then subjected to *in situ* hybridisation experiments, to detect *Wnt11*, and immunostaining for myosin heavy chain (see figure 6.7 for an example).

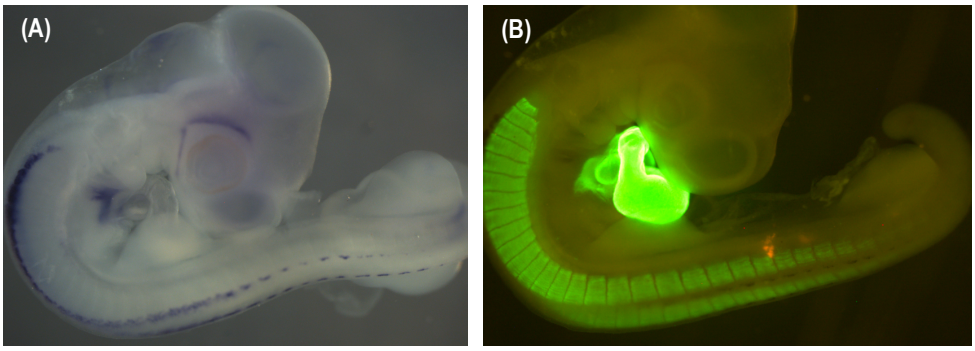

Figure 6.7. *Wnt11* and myosin heavy chain expression in a HH Stage 20 Chick embryo following targeted fibroblast injection. Wnt11 secreting rat fibroblasts (stained red with DiI) were injected between somites IV and V at HH Stage 16. The embryo was re-incubated for 14 h and subsequently hybridised with an RNA probe for *Wnt11* (A) and immunostained in wholemount with MF20 to reveal myosin heavy chain in green (B).

Again, as anticipated myosin heavy chain is apparent in the heart and somites of the HH Stage 20 embryo (figure 6.7B). *Wnt11* is strongly expressed in the dorsomedial lip of the somite as previously described by Tanda *et al* (1995) and Marcelle *et al* (1997). Interestingly, expression is also evident in what appears to be eye muscle (figure 6.7A). To observe the effects of the exogenous Wnt11 on myofibres, the somites positioned on either side of the injected fibroblasts were excised and prepared for widefield inverted microscopy (figure 6.8; see materials and methods for more details about slice cultures).

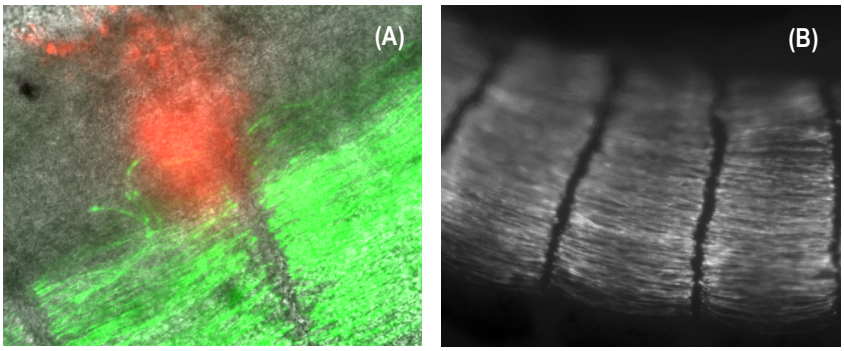

Figure 6.8. Effects of an exogenous source of Wnt11 on early myofibres. (A) Dorsal view of somites where DiI labelled Wnt11-expressing cells (red) were positioned between the two somites at HH Stage 16. Following re-incubation for 14 h the embryo was immunostained for myosin heavy chain (green), which illustrates aberrant myotome organisation. (B) Dorsal view of somites illustrating myotome organisation (myosin heavy chain) in the absence of any injected exogenous cells.

The injected fibroblasts were sometimes 'pushed out' to the lateral side of the somite as in figure 6.8A. Nonetheless, in agreement with Gros *et al* (2009), the early myofibres appear to be orienting toward the Wnt11 secreting cells (figure 6.8A, n=3). This disorientation of myofibres was never seen in somites that were not cell injected (figure 6.8B, n=4).

6.7. Wnt3a and Early Muscle Fibres

To test if canonical Wnt orients the myofibres independently of Wnt11, Wnt3a-expressing rat fibroblasts (a kind gift from Dr. Jan Kitajewski, Columbia University, New York, 10032) were also injected either within the myotome (somite IV) or between two somites (somites III and IV, or somites IV and V) of HH Stage 16 chick embryos. Embryos were subsequently re-incubated for 14-16 hours and then hybridised with an RNA probe for *Wnt3a* and immunostained for myosin heavy chain (see figure 6.9 for an example).

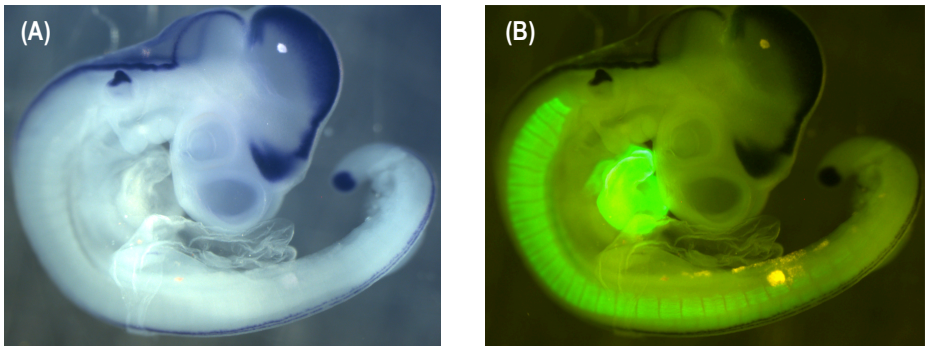

Figure 6.9. *Wnt3a* and myosin heavy chain expression in a HH Stage 20 Chick embryo following targeted fibroblast injection. Wnt3a secreting rat fibroblasts (stained red with DiI) were injected into somite IV at HH Stage 16. The embryo was re-incubated for 14 h and subsequently hybridised with an RNA probe for *Wnt3a* (A) and immunostained in wholemount with MF20 to reveal myosin heavy chain in green (B).

In agreement with previous studies (see GEISHA database available at: http://geisha.arizona.edu/geisha/ for more details), *Wnt3a* is strongly expressed in the developing spinal cord, the tail bud, the otic placode, and in the midbrain (figure 6.9A). As before, myosin heavy chain is in the heart and somites of the HH Stage 20 embryo (figure 6.9B).

To observe the effects of the exogenous Wnt3a on myofibres, the somites positioned nearest to the injected cells were isolated and prepared for widefield-inverted microscopy (figure 6.10; see materials and methods for more details about slice cultures).

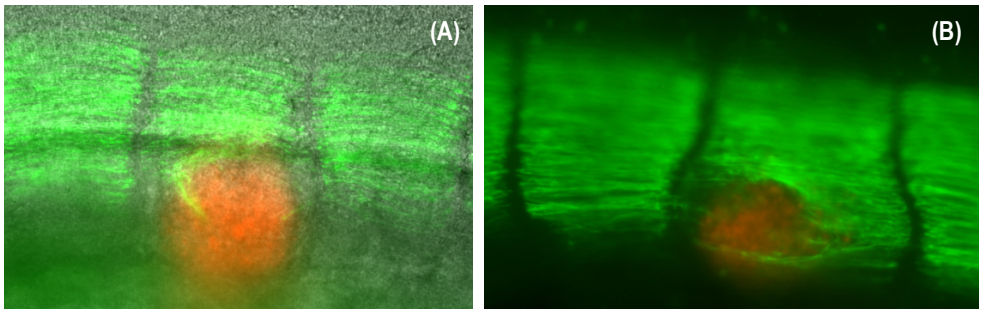

Figure 6.10. Effects of an exogenous source of Wnt3a on early myofibres. (A) Dorsal view of somites where DiI labelled Wnt3a-expressing cells (red) were positioned within the myotome of somite IV at HH Stage 16. Following re-incubation for 14 h the embryo was immunostained for myosin heavy chain (green), which illustrates aberrant myotome organisation. (B) Dorsal view of somites where DiI labelled LNCX2 control cells (red) were injected within the

myotome of somite IV at HH Stage 16. Following re-incubation for 14 h the embryo was immunostained for myosin heavy chain (green).

As shown in figure 6.10A, myofibres appear to be orienting toward the Wnt3a secreting cells (n=8), not dissimilar to those myofibres orienting toward exogenous Wnt11 shown above. In the somites injected with control cells, although the cells often displayed obstruction to the myofibres (as shown in figure 6.10B), the myofibres never appeared to be orienting in their direction (n=4).

Wnt3a and Wnt1 signalling from the neural tube are known to drive the expression of *Wnt11* in the dorsomedial lip of the dermomyotome (Marcelle *et al*, 1997). Thus embryos injected with Wnt3a-expressing cells were hybridised with an RNA probe for *Wnt11* to examine whether the effect on the myofibres was a direct response to Wnt3a and not because of any upregulation of *Wnt11* in the lateral region of the somite (see figure 6.11 for an example).

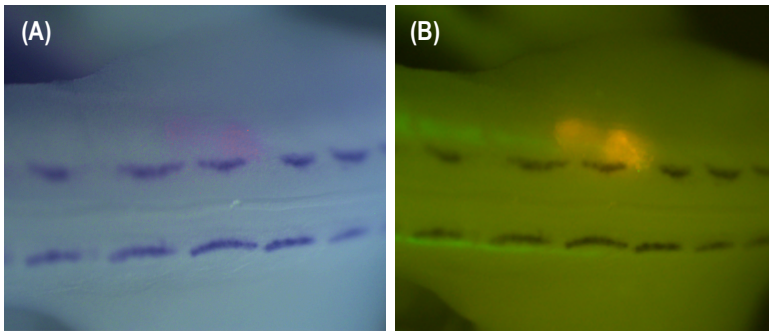

Figure 6.11. Exogenous Wnt3a in the myotome and lateral regions of the somite does not upregulate *Wnt11*. Wnt3a-expressing fibroblasts (stained red with DiI) were injected between somites III and IV at HH Stage 16. The embryo was re-incubated for 14 h and subsequently hybridised with an RNA probe for *Wnt11* (A) and immunostained in wholemount for myosin heavy chain in green (B).

Evidently, excluding the endogenous *Wnt11*, no additional *Wnt11* expression is apparent near the Wnt3a-expressing fibroblasts. Nor is there any upregulation of endogenous *Wnt11* (i.e. in the dorsomedial lip) in the cell

injected somite compared to the non-injected side (figure 6.11, n=9). This suggests that a canonical Wnt ligand (Wnt3a), independent of *Wnt11*, has a role in the orientation of embryonic myofibres.

6.8. MACF1/ACF7 and Early Muscle Fibres

Wnts are known to inhibit GSK3β. GSK3β has been shown to govern the elongation of microtubules through its control of MACF1/ACF7: active GSK3β phosphorylates the +TIP protein, thus uncoupling it from microtubules and inhibiting their growth, while inactive GSK3β allows the extension of microtubules by +TIPs, which helps to polarise the cytoskeleton and direct cellular movement (Wu *et al*, 2011; Zaoui *et al*, 2010). Wu *et al* (2008) have demonstrated that in *MACF1/ACF7*-null mouse keratinocytes there is aberrant and delayed cell migration. It is posited, therefore, that MACF1/ACF7 (downstream of GSK3β) has a role in the cell migration and orientation necessary for correct myotome formation/myofibre organisation. This may provide a direct link between canonical Wnt and the orientation of chick embryonic myofibres via GSK3β and its regulation of MACF1/ACF7 (figure 6.12).

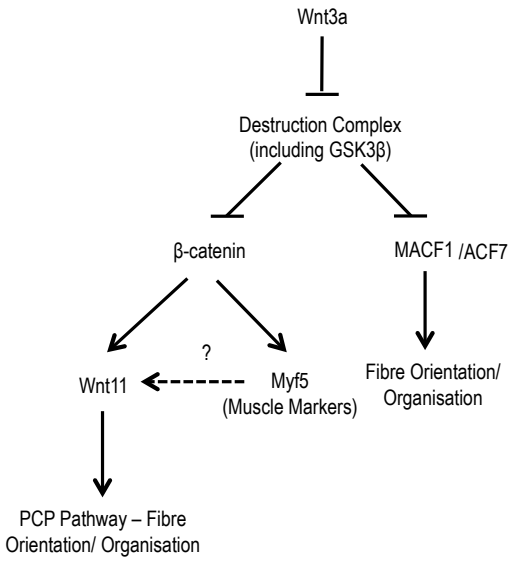

Figure 6.12. Proposed additional pathway suggesting a role for MACF1/ACF7, downstream of GSK3β, in the organisation of chick embryonic muscle fibres. For further details on the Wnt11-PCP pathway that is depicted see figure 6.3.

To test if MACF1/ACF7 is required for correct myofibre organisation, somites I-V of HH Stage 16 chick embryos were injected with a morpholino that targets the first translation start site of MACF1/ACF7. Following electroporation, embryos were re-incubated for 12-16 hours and then immunostained for myosin heavy chain. Electroporated somites, now interlimb, were isolated and prepared for inverted confocal two-photon microscopy (see figure 6.13 for an example).

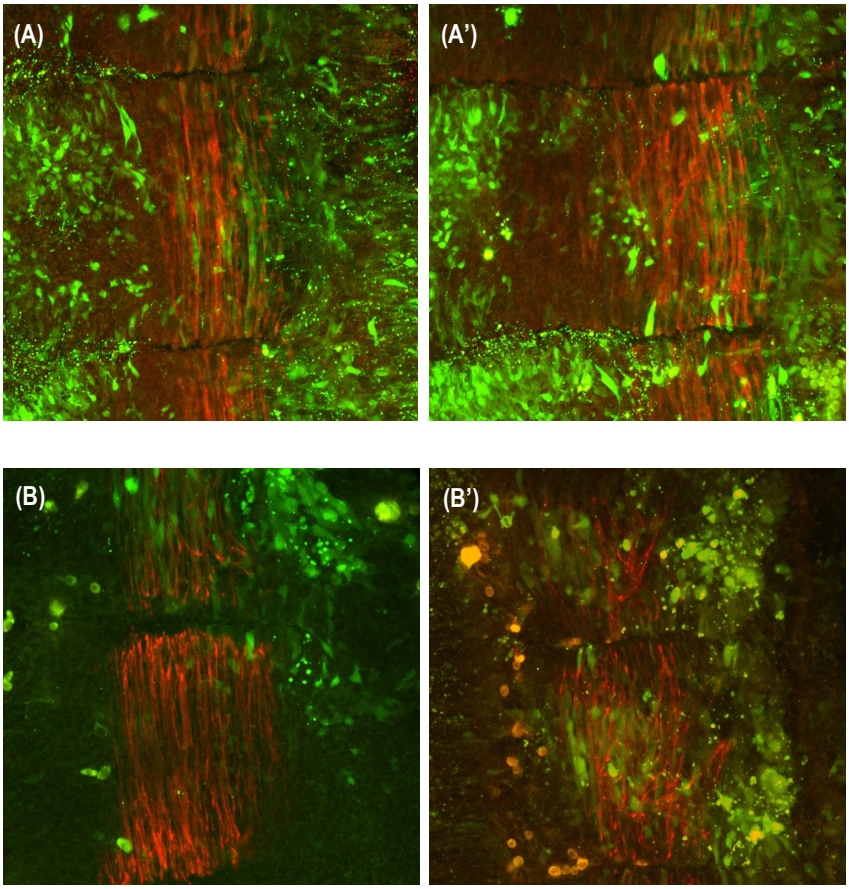

Figure 6.13. Attempted MACF1/ACF7 knockdown in somites and its effects on myofibre organisation. (**A**, **A**') Control morpholino (green) was injected and electroporated into somites I-V of a HH Stage 16 chick embryo, following 15 h re-incubation the embryo was immunostained for myosin heavy chain (red). **A** and **A'** represent 2 different interlimb somites from the same electroporated embryo. (**B**, **B**') A morpholino (green) against the translation start site of MACF1/ACF7 was injected and electroporated into somites I-V of a HH Stage 16 chick embryo, following 15 h re-incubation the embryo was immunostained for myosin heavy chain (red). **B** and **B'** represent 2 different interlimb somites from the same electroporated embryo.

As anticipated, electroporation of a control morpholino appears to have no overall influence on the organisation of myofibres (figure 6.13A, A', n=2). Intriguingly however, in the example shown here, following electroporation of a MACF1/ACF7 morpholino the myofibres appear to be relatively normal in one somite but somewhat aberrant, with disrupted fibre orientation, in a neighbouring somite of the same embryo (figure 6.13B, B', n=1).

In addition to the morpholino electroporations, an overexpression and rescue experiment was designed (but not completed, see below) to test if MACF1/ACF7 is required for correct myofibre organisation. The electroporation of hGSK3β into early somites resulted in normal myofibre organisation (data not shown). This suggested that, despite the additional GSK3β, there were not enough β-catenin destruction complexes to inhibit the function of β-catenin and, that there was not enough active GSK3β to phosphorylate MACF1/ACF7 and uncouple it from microtubules (i.e. inhibit its proposed function in myofibre organisation). An alternative experimental approach considered was the overexpression of Axin2. It is hypothesised that overexpression of Axin2 will prevent the diassociation of β-catenin destruction complexes (as the 'free' Axin will saturate the appropriate receptors) and, therefore, perturb normal fibre organisation, validating both pathways (i.e. β-catenin will be downregulated and as a consequence so will the activation of Wnt11). Although it ought to be noted that the 'free' Axin may not preferably bind to the receptor over the destruction complexes, and that, although overexpression of Axin2 should result in more Axin there might not necessary be enough of all the other components required to form destruction complexes. Nonetheless, this experiment could be complemented by rescue of β-catenin downstream of the destruction complex (i.e. constitutively active β-catenin is electroporated at the same time as Axin2). In this scenario the Wnt11-PCP pathway should be rescued and normal myofibre organisation should ensue. If this is the case then this pathway is sufficient for organisation. However, if correct orientation is not observed this might suggest that the proposed parallel MACF1/ACF7 pathway is also necessary.

To enable such a complex experiment it was necessary to first test if an assay involving simultaneous cell injection and electroporation was possible. Somites I-V of HH Stage 16 embryos were injected and electroporated with GFP-GPI and subsequently LNCX2 control fibroblasts stained red with DiI were injected between two somites. Following overnight incubation, electroporated somites on either side of the injected cells were excised and prepared for inverted confocal two-photon microscopy (see figure 6.14 for an example).

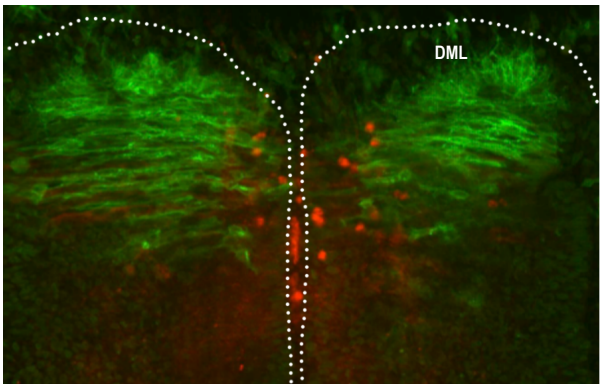

Figure 6.14. Simultaneous cell injection and electroporation is possible in early chick somites. Electroporated GFP-GPI (green) is evident in the myofibres and LNCX2 rat fibroblast cells (stained red with DiI) are apparent within the border of the two somites. Dashed lines outline individual somites. ***DML**: dorsomedial lip.

Evidently, it is possible to inject and electroporate an embryo with a construct and, at the same time, inject cells in suspension (figure 6.14, n=2). Based on previous experience, embryo survival rate and development appeared to be very similar to that of embryos following electroporation only (Scaal *et al*, 2004).

Next, somites I-V of HH Stage 16 embryos were injected and electroporated with either GFP-GPI only or Axin2 and GFP-GPI. Subsequently, Wnt3a-expressing fibroblasts stained red with DiI were injected between two somites. Following overnight incubation, electroporated somites on either

side of the injected cells were isolated and prepared for inverted confocal two-photon microscopy (figure 6.15).

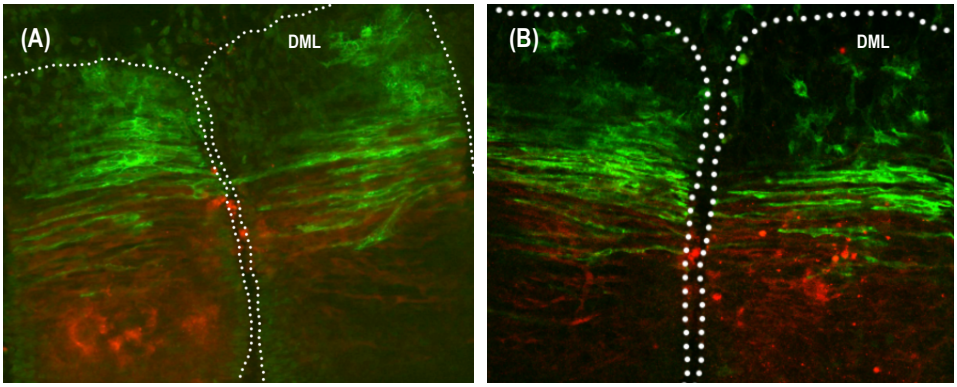

Figure 6.15. Preliminary experiments to test if Axin2 overexpression can perturb the myofibres response/orientation towards exogenous Wnt3a (shown earlier). (**A**) Dorsal view of somites that were electroporated with GFP-GPI only (green) and simultaneously injected, between the two somites, with Wnt3a-expressing cells (stained red with DiI). (**B**) Dorsal view of somites that were electroporated with GFP-GPI and Axin2 (green) and at the same time injected, between the two somites, with Wnt3a-expressing cells (stained red with DiI). Dashed lines outline individual somites. ***DML**: dorsomedial lip.

As anticipated, the myofibres electroporated with Axin2 (overexpressing Axin2) and GFP-GPI appear to be relatively normal, in that they are not orienting toward the Wnt3a secreting cells (which are apparent not just in the border between the two somites but also within the somites; figure 6.15B, n=1). That said the myofibres electroporated with GFP-GPI only (figure 6.15A, n=2) are not responding/orienting toward the Wnt3a cells as expected (shown earlier with myosin heavy chain staining, figure 6.10). To show that it was not the electroporation itself that was affecting the previously observed response (see figure 6.10), protein lysate was harvested from the same passage of Wnt3a-secreting fibroblasts used in this experiment and from newly thawed cells. A western blot was stained against Wnt3a and while the newly thawed cells were secreting Wnt3a in abundance, only a very faint band was detected in the cells that were utilised (even though they were under antibiotic selection; data not shown). This is likely to be the reason why GFP-GPI electroporated cells are not responding to the ectopic fibroblasts,

as there is very little Wnt3a being secreted (in earlier experiments i.e. figure 6.10, the Wnt3a-expressing fibroblasts were at a much earlier passage and, at this point in time, the expression had been verified by western).

It is worth noting that the above morpholino experiments and the Axin2 overexpression experiments are only preliminary. Repeat experiments (with newly thawed cells (with confirmed Wnt3a secretion via western blot), in the case of Axin2 overexpression experiment) remain to be performed. The β-catenin rescue experiments are also yet to be performed.

Discussion and Future Work

As previously described by Tanda *et al* (1995) and Marcelle *et al* (1997), strong *Wnt11* expression has been illustrated in the dorsomedial lip of the chick somite (figure 6.7A). Expression is also evident in what appears to be eye muscle. In agreement with Gros *et al* (2009), the injection of Wnt11-expressing fibroblasts into the developing somites of chick embryos has shown that Wnt11 influences the orientation of myofibres (figure 6.8). The disorientation of fibres was not seen in non-cell-injected somites; however, control cells (containing the same plasmid backbone without Wnt11) should also be injected to verify that the phenotype is a result of the secreted Wnt11 and not the cells themselves. Interestingly, subsequent hybridisation with an RNA probe for *Wnt11* did not appear to detect these cells. The cells utilised expressed mouse Wnt11, while the probe was against chick: thus the identity between chick and mouse Wnt11 is apparently not sufficient for the probe to cross-react. In addition quenching may disguise a weak signal if any.

Wnt3a, in agreement with previously reported studies (see GEISHA database available at: http://geisha.arizona.edu/geisha/ for more details), has been shown to be expressed in the developing spinal cord, the tail bud, the otic placode, and in the midbrain of HH Stage 20 chick embryos (figure 6.9A). To test if the canonical Wnt ligand, Wnt3a, orients embryonic myofibres, Wnt3a-secreting rat fibroblasts were also injected into the developing somites of chick embryos. Myofibres were shown to orient toward the Wnt3a cells

(figure 6.10A), in a similar vein to those myofibres shown to be influenced by Wnt11 (shown in figure 6.8A and by Gros *et al*, [2009]). The disorientation of fibres was not seen in somites injected with control cells (i.e. LNCX2 rat fibroblasts). However, as aforementioned, there did appear to be some obstruction to the fibres due to the localisation of the exogenous control cells (figure 6.10B).

As Wnt3a and Wnt1 signalling from the neural tube have been shown to drive the expression of *Wnt11* in the dorsomedial lip of the dermomyotome (Marcelle *et al*, 1997), embryos injected with Wnt3a-expressing cells were subsequently hybridised with an RNA probe for *Wnt11* to examine whether the effect on the myofibres was a direct response to Wnt3a and not because of any upregulation of *Wnt11* in the lateral region of the somite (figure 6.11). No additional *Wnt11* expression (i.e. excluding endogenous *Wnt11*) was seen near the Wnt3a-expressing fibroblasts. In addition, no upregulation of endogenous *Wnt11* in the cell-injected somite was observed, compared to the non-injected side (figure 6.11), which suggests that (canonical) Wnt3a, independently of *Wnt11*, has a role in the orientation of embryonic myofibres. The wholemount embryos remain to be sectioned to show conclusively that there is no upregulation of *Wnt11*.

Intriguingly, Geetha-Loganathan *et al* (2006) state that implantation of Wnt3a-producing cells into the somites does lead to the upregulation of *Wnt11.* They imply that cells implanted in what appears to be the lateral portion of the somite upregulate the endogenous expression of *Wnt11* (i.e. the expression in the dorsomedial lip) but no expression is seen in the vicinity of the ectopic cells. While the latter agrees with what is shown here, upregulation of endogenous *Wnt11* (in somites injected with Wnt3a-secreting fibroblasts), however, was never seen suggesting that in fact Wnt3a alone is not sufficient. Additionally, Gros *et al* (2009) have shown that grafting of an ectopic neural tube perpendicular to the antero-posterior embryonic axis between two newly formed somites induces the ectopic expression of *Wnt11* (in somites in contact with the graft). They suggest that this is due to the action of Wnt1 and/or Wnt3a from the dorsal neural tube. Perhaps, therefore,

no upregulation of *Wnt11* was seen subsequent to the injection of Wnt3a-secreting cells, as Wnt1 is also required?

To test if MACF1/ACF7, which is regulated by GSK3β (Wu *et al*, 2011), has a role in the cell migration and orientation necessary for correct myofibre organisation, a fluorescein isothiocyanate (FITC) labelled morpholino that targets the first translation (ATG) start site of MACF1/ACF7 was injected and electroporated into developing chick somites. Following overnight re-incubation, it was anticipated that cells containing the MACF1/ACF7 morpholino would be disorganised compared to either non-electroporated cells or those electroporated with a control morpholino. Unfortunately, as shown in figure 6.13 it is difficult to identify individual cells electroporated with morpholino and thus compare them with the non-electroporated cells. It is presumed that non-electroporated fibres would show a normal phenotype.

However, there is a possibility that any disorganised fibres (i.e. those expressing the MACF1/ACF7 morpholino, if this indeed causes disorientation) could influence them. That said, overall, electroporation of a control morpholino appears to have no influence on the organisation of myofibres (stained for myosin heavy chain; figure 6.13A, A'). Yet, the electroporation of a MACF1/ACF7 morpholino shows what appears to be relatively normal myofibres in one somite but somewhat aberrant (with disrupted fibre orientation) myofibres in a neighbouring somite of the same embryo (figure 6.13B, B'). The difference in phenotype between the two somites could be a result of the volume of injected/electroporated morpholino. Using FITC as a guide for the volume of morpholino electroporated, it appears that there is more morpholino in the somite shown in figure 6.13B' compared to that shown in figure 6.13B, which suggests that higher amounts of electroporated morpholino may have a stronger phenotype. It ought to be noted that this is preliminary data and repeat experiments are necessary before any real conclusions can me made. Furthermore the morpholino needs to be validated (i.e. is it specific?). Unfortunately, as described previously, the specificity of the MACF1/ACF7 antibody used in the abovementioned immunostaining/western blot experiments (Chapter 5) is also yet to be confirmed and, therefore, cannot be

used to validate the morpholino. Thus *in vitro* translation may be an appropriate method to confirm its accuracy. However, given that there are likely multiple isoforms produced in the chick (which are not yet annotated), this may also be quite challenging.

The *MACF1*/*ACF7* gene contains multiple translation initiation codons, which are separated by extended stretches of DNA (Karakesisglou *et al*, 2000; Leung *et al*, 1999). Thus it is possible that some of the MACF1/ACF7 isoforms (see chapter 5 for more information) do not contain the translation start site that is targeted by the MACF1/ACF7 morpholino abovementioned. This might suggest that, alone, this morpholino is inadequate to knockdown enough MACF1/ACF7 to see a significant phenotype. Perhaps simultaneous electroporation of this morpholino and a splice morpholino would result in greater knockdown and consequently a stronger phenotype? Following successful knockdown (with one or more morpholinos), it is hypothesised that the subsequent injection of Wnt3a-expressing cells will show that cells/fibres expressing MACF1/ACF7 morpholino(s) are not only disorganised but also unresponsive to the ectopic Wnt3a.

In 2010, Goryunov *et al* knocked out MACF1a in the developing mouse nervous system using Cre/loxP technology. To avoid (the improbability of) targeting MACF1/ACF7's multiple translation initiation codons with a single construct, they decided to specifically target the actin-binding domain of MACF1/ACF7, which at the time of their study was present in both known isoforms of MACF1/ACF7, MACF1a and MACF1b. Embryos carrying two fully recombined alleles in all tissues (i.e. *MACF1*R/R embryos) were shown to have a phenotype as severe as that described by Chen *et al* (2006) and Kodama *et al* (2003) in *MACF1*/*ACF7* knockout embryos (i.e. mice died within 24–36 h after birth of apparent respiratory distress). *MACF1* cKO brains showed a disorganised cerebral cortex with a mixed layer structure, heterotopia of the hippocampal pyramidal layer, disorganized thalamocortical and corticofugal fibres, and aplastic anterior and hippocampal commissures. Further analysis of the expression of MACF1/ACF7 in the cKO mice brains highlighted the existence of a novel isoform, which they termed MACF1c. This isoform lacked the actin-binding domain and was not affected by the

conditional knockout, which suggests it has a separate initiation codon downstream of the actin-binding domain. The *MACF1/ACF7* cKO mice generated by Goryunov *et al* (2010), thus exemplify a nervous-system-specific knockout of MACF1a, which appears crucial for normal brain development. The MACF1c isoform, which was shown to be identical to MACF1a except for the absence of an actin-binding domain (i.e. it is still expected to contain a microtubule-binding domain), did not compensate for the loss of MACF1a, which argues that the actin-binding capacity of MACF1/ACF7 is essential in the developing brain (Goryunov *et al*, 2010). Of further interest, BPAG1 (the other mammalian spectraplakin and MACF1/ACF7 homologue, see Chapter 5) has also been shown to contain an initiation codon downstream of the actin-binding domain, though the resulting transcript, BPAG1e is only expressed in epithelia (Sonnenberg and Liem, 2007).

It is also worth mentioning that numerous attempts were made to inject and electroporate the somites of HH Stage 16 embryos with the same constructs used for the published Wu *et al* (2011) data (a kind gift from Prof. Elaine Fuchs, The Rockefeller University, New York, 10065). Specifically, their engineered mammalian expression vectors encoding human influenza hemagglutinin epitope (HA)-tagged full-length ACF7, as well those with point mutations that converted GSK3β phosphorylation sites at P1 (phosphorylation site cluster 1) and P2 (phosphorylation site cluster 2) to either a kinase refractile version harbouring Ser-Ala mutations (S:A mutant) or a phosphomimetic version, containing Ser-Asp mutations (S:D mutant). However, these electroporation's were never successful and, unfortunately, the same result occurred following attempts to transfect C2C12 cells. It is speculated that this could be due to the extremely large size (>20kb) of the plasmids. Therefore, it might be worthwhile cloning smaller MACF1/ACF7 domains for overexpression experiments (the microtubule binding or the actin-binding domains for example), to see this has any effects on chick somite development/myofibre orientation. Expression of a specific domain may give a dominant negative effect: for example, overexpression of the microtubule-binding domain may prevent the endogenous full length

MACF1/ACF7 from binding to microtubules and may induce some phenotype.

As previously mentioned, the possibility that Wnt3a might influence chick embryonic myofibres, independently of *Wnt11* (see figures 6.10A and 6.11), led to the hypothesis that MACF1/ACF7 might be the link between Wnt3a and fibre orientation (see proposed model, figure 6.12). An overexpression/rescue experiment was designed (in addition to MACF1/ACF7 morpholino experiments) to prove/disprove this theory (please see the above results section for experimental design, reasoning and some discussion). It ought to be noted that this experiment remains to be completed, attempts at Axin2 overexpression for example were only attempted once (figure 6.15), thus the data shown here is preliminary. The completion of these experiments, however, might show that MACF1/ACF7 does have a role to play in chick myofibre orientation. If so, it is posited that the link between MACF1/ACF7 and GSK3β would be similar to that shown by Wu *et al* (2011) in hair follicle stem cells. However, the link between Wnt3a and GSK3β remains elusive. While it is widely accepted that Wnt signalling inhibits GSK3β, how this occurs is not completely understood. It might also be valuable to perform an in situ hybridisation experiment against *MACF1/ACF7* on embryos injected with Wnt3a secreting cells, to see if Wnt3a itself directly upregulates *MACF1/ACF7*.

On a final note, an assay involving simultaneous cell injection and electroporation has been demonstrated (figure 6.14), which may prove useful for experiments that require live visualisation of myofibres (i.e. not fixed and immunostained for myosin heavy chain) following cell injection into the somite (i.e. time-lapse).

Chapter 7: Overall Summary

Using the chick as a model system, experiments presented in this thesis have demonstrated the difficulty of observing cytoskeletal proteins (and any interacting proteins) in tissues/embryos (*in vivo*), when compared to cells in culture (*in vitro*). In particular, fixing and immunostaining of young primitive streak stage (HH 3-4) chicken embryos was problematic owing to both their fragility and the dependency on good quality eggs. Unfortunately, it proved too challenging to further characterise the cytoskeleton (and any interacting proteins) and successively examine the formation and resolution of the rosette structures that had been previously reported (Wagstaff *et al*, 2008).

Additionally, observation of the microtubule cytoskeleton in avian somites in real time was difficult as it was not possible to distinguish the microtubules following GFP-tubulin overexpression. That said the electroporation technique utilised for overexpression experiments was extremely successful. While it was not possible to visualise the microtubules themselves, this technique in combination with time-lapse microscopy revealed a somite structure congruent with that previously published (Gros *et al,* 2009). It was also anticipated that targeted electroporation (i.e. electroporation of the medial portion of the somite to transfect the medial lip of the dermomyotome) of reporter constructs into developing somites would enable the visualisation, in real time, of cells which have been reported to translocate from the dorsomedial lip to the transition zone and subsequently to the myotome (Gros *et al*, 2009; Rios *et al*, 2011; Scaal *et al*, 2004). However, though electroporation and microscopy were both successful, the successive analysis proved to be much more difficult than expected.

Nonetheless, microtubule immunostaining of fixed somites has been demonstrated. These stains highlighted dividing cells within both the dermomyotome and the lips of somites, which appear to be dividing in the plane of the epithelial dermomyotomal sheet. This corresponds with previously published data by Venters and Ordahl (2005) and Yusuf and Brand-Saberi (2006). However, to date, analysis has not revealed any rosette structures like those that were previously seen in the primitive streak

(Wagstaff *et al*, 2008). Although still in its infancy, the fixation method used for these stains looks promising and once optimised it may be used to characterise additional cytoskeletal proteins.

On a separate note, an expression pattern for the *MACF1/ACF7* (microtubule-actin cross-linking factor 1/actin cross-linking factor 7) gene has been illustrated in a variety of HH Stage chicken embryos. Expression is apparent in both the primitive streak of early stage embryos and in the somites of HH Stage 11 and 17 embryos. This, in addition to data published by Chen *et al* (2006), further suggests a role for MACF1/ACF7 in gastrulation but more intriguingly it also suggests a possible role for MACF1/ACF7 in somitogenesis. Preliminary experiments to knockdown *MACF1/ACF7* in somites, using a morpholino that targets the first translation (ATG) start site of MACF1/ACF7, have shown some promising results with regard to myofibre orientation. There will be worth to further optimise and repeat these experiments.

Finally, in agreement with Gros *et al* (2009), the injection of Wnt11-expressing fibroblasts into the developing somites of chicken embryos has shown that Wnt11 influences the orientation of myofibres. Furthermore, a similar effect has been shown following the injection of Wnt3a-expressing fibroblasts into the somites (experiments presented in this thesis). This effect on myofibres was shown to be independent of *Wnt11* and suggests that canonical Wnt (Wnt3a) has a role in the orientation of myofibres. An overexpression/rescue experiment to further validate this was designed, but unfortunately owing to time constraints remains to be completed.

In summary, the cytoskeleton is vital throughout development: playing an important role in intracellular transport, cellular division, cell polarisation, cell shape changes and cell migration. Surprisingly, although much is known about the cytoskeleton of eukaryotic cells *in vitro*, little has been illustrated during early development, particularly during gastrulation and somite morphogenesis. Techniques established here have enabled preliminary examination of the cytoskeleton *in vivo* and when used further they may begin to unravel the importance of the cytoskeleton and how it is regulated.

References

Abu-Elmagd, M., Robson, L., Sweetman, D., Hadley, J., Francis-West, P. and Münsterberg, A. (2010) Wnt/Lef1 signaling acts via Pitx2 to regulate somite morphogenesis. *Developmental Biology*, **337**: 211-219

Affolter, M. and Weijer, C. J. (2005) Signaling to Cytoskeletal Dynamics during Chemotaxis. *Developmental Cell*, **9**: 19-34

Akhmanova, A. and Hoogenraad, C. C. (2005) Microtubule plus-end-tracking proteins: mechanisms and functions. *Current opinion in cell biology*, **17**: 47-54

Akhmanova, A., Hoogenraad, C. C., Drabek, K., Stepanova, T., Dortland, B., Verkerk, T., Vermeulen, W., Burgering, B. M., De Zeeuw, C. I., Grosveld, F. and Galjart, N. (2001) Clasps are CLIP-115 and -170 associating proteins involved in the regional regulation of microtubule dynamics in motile fibroblasts. *Cell*, **104**: 923-935

Akhmanova, A. and Steinmetz, M. O. (2008) Tracking the ends: a dynamic protein network controls the fate of microtubule tips. *Nature Reviews Molecular Cell Biology*, **9**: 309-322

Akhmanova, A. and Steinmetz, M. O. (2010) Microtubule +TIPs at a glance. *Journal of Cell Science*, **123**: 3415-3419

Alberts, B., Johnson, A., Lewis, J., Raff, M., Roberts, K. and Walter, P. (2002) Molecular Biology of the Cell Fourth Edition, Chapter 16. Garland Science

Andries, L., Harrisson, F., Hertsens, R. and Vakaet, L. (1985) Cell junctions and locomotion of the blastoderm edge in gastrulating chick and quail embryos. *Journal of Cell Science*, **78**: 191-204

Aoyama, H. and Asamoto, K. (1988) Determination of somite cells: independence of cell differentiation and morphogenesis. *Development*, **104** (1): 15-28

Applewhite, D.A., Grode, K. D., Keller, D., Zadeh, A. D., Slep, K. C., and Rogers, S. L. (2010) The spectraplakin Short stop is an actin-microtubule cross-linker that contributes to organization of the microtubule network. *Molecular Biology of the Cell*, **21**: 1714-1724

Axelrod, J. D., Miller, J. R., Shulman, J. M., Moon, R. T. and Perrimon, N. (1998) Differential recruitment of Dishevelled provides signaling specificity in the planar cell polarity and Wingless signaling pathways. *Genes & Development*, **12**: 2610-2622

Bachvarova, R. F., Skromne, I. and Stern, C. D. (1998) Induction of primitive streak and Hensen's node by the posterior marginal zone in the early chick embryo. *Development*, **125**: 3521-3534

Bai, S. W., Herrera-Abreu, M. T., Rohn, J. L., Racine, V., Tajadura, V., Suryavanshi, N., Bechtel, S., Wiemann, S., Baum, B. and Ridley, A. J. (2011) Identification and characterization of a set of conserved and new regulators of cytoskeletal organization, cell morphology and migration. *BMC Biol*. **9**: 54

Bellairs, R. (1963) The development of the somites in the chick embryo. *Journal of Embryology and Experimental Morphology*, **11**: 697-714

Bellairs, R. (1979) The mechanism of somite segmentation in the chick embryo. *Journal of Embryology and Experimental Morphology*, **51**: 227-243

Bellairs, R. (1986) The Primitive Streak. *Anatomy and Embryology*, **174**: 1-14

Ben-Yair, R. and Kalcheim, C. (2005) Lineage analysis of the avian dermomyotome sheet reveals the existence of single cells with both dermal and muscle progenitor fates. *Development*, **132**: 689-701

Bernier, G., Mathieu, M., De Repentigny, Y., Vidal, S. M. and Kothary, R. (1996) Cloning and characterization of mouse ACF7, a novel member of the dystonin subfamily of actin binding proteins. *Genomics*, **38**: 19-29

Bernier, G., Pool, M., Kilcup, M., Alfoldi, J., De Repentigny, Y. and Kothary, R. (2000) Acf7 (MACF) is an actin and microtubule linker protein whose expression predominates in neural, muscle, and lung development. *Developmental Dynamics*, **219**: 216-225

Bettencourt-Dias, M., and Glover, D. M. (2007) Centrosome biogenesis and function: centrosomics brings new understanding. *Nature Reviews. Molecular Cell Biology*, **8**: 451-463

Bieling, P., Laan, L., Schek, H., Munteanu, E. L., Sandblad, L., Dogterom, M., Brunner, D. and Surrey, T. (2007) Reconstitution of a microtubule plus-end tracking system in vitro. *Nature*. **450**: 1100-1105

Blankenship, J. T., Backovic, S. T., Sanny, J. S., Weitz, O. and Zallen, J. A. (2006) Multicellular Rosette Formation Links Planar Cell Polarity to Tissue Morphogenesis. *Developmental Cell*, **11**: 459-470

Blau, H. M., Chiu, C. P. and Webster, C. (1983) Cytoplasmic activation of human nuclear genes in stable heterocaryons. *Cell*, **32**: 1171-1180

Boardman, P. E., Sanz-Ezquerro, J., Overton, I. M., Burt, D. W., Bosch, E., Fong, W. T., Tickle, C., Brown, W. R. A., Wilson, S. A. and Hubbard, S. J. (2002) A comprehensive collection of chicken cDNAs. *Current Biology*, **12**: 1965-1969

Boettger, T., Knoetgen, H., Wittler, L. and Kessel, M. (2001) The avian organiser. *Int. J. Dev. Biol.*, **45**: 281-287

Borello, U., Buffa, V., Sonnino, C., Melchionna, R., Vivarelli, E. and Cossu, G. (1999a) Differential expression of the Wnt putative receptors Frizzled during mouse somitogenesis. *Mechanisms of Development*, **89**: 173-177

Borello, U., Coletta, M., Tajbakhsh, S., Leyns, L., De Robertis, E. M., Buckingham, M. and Cossu, G. (1999b) Transplacental delivery of the Wnt antagonist Frzb1 inhibits development of caudal paraxial mesoderm and skeletal myogenesis in mouse embryos. *Development*, **126**: 4247-4255

Borello, U., Berarducci, B., Murphy, P., Bajard, L., Buffa, V., Piccolo, S., Buckingham, M. and Cossu, G. (2006) The Wnt/beta-catenin pathway regulates Gli-mediated Myf5 expression during somitogenesis. *Development*, **133**: 3723-3732

Borycki, A. G., Mendham, L. and Emerson, C. P. Jr. (1998) Control of somite patterning by Sonic hedgehog and its downstream signal response genes. *Development*, **125** (4): 777-790

Brand-Saberi, B., Ebensperger, C., Wilting, J., Balling, R. and Christ, B. (1993) The ventralizing effect of the notochord on somite differentiation in chick embryos. *Anat. Embryol.*, **188**: 239-245

Brand-Saberi, B., Wilting, J., Ebensperger, C. and Christ, B (1996) The formation of somite compartments in the avian embryo. *Int. J. Dev. Biol.* **40** (1): 411-420

Brauner, I., Spicer, D. B., Krull, C. E. and Venuti, J. M. (2010) Identification of Responsive Cells in the Developing Somite Supports a Role for β-Catenin-Dependent Wnt signaling in Maintaining the DML Myogenic Progenitor Pool. *Developmental Dynamics*, **239**: 222-236

Brent, A. E. and Tabin, C. J. (2002) Developmental regulation of somite derivatives: muscle, cartilage and tendon. *Current Opinion in Genetics & Development*, **12**: 548–557

Brent, A. E., Schweitzer, R. and Tabin, C. J. (2003) A somitic compartment of tendon progenitors. *Cell*, **113** (2): 235-48

Brown, A., Bernier, G., Mathieu, M., Rossant, J. and Kothary, R. (1995) The mouse dystonia musculorum gene is a neural isoform of bullous pemphigoid antigen 1. *Nature Genetics*, **10**: 301-306

Brown, N. H. (2008) Spectraplakins: the cytoskeleton's Swiss army knife. *Cell*, **135**: 16-18

Brunelli, S., Relaix, F., Baesso, S., Buckingham, M. and Cossu, G. (2007) Beta catenin-independent activation of MyoD in presomitic mesoderm requires PKC and depends on Pax3 transcriptional activity. *Developmental Biology*, **304**: 604-614

Brunner, D. and Nurse, P. (2000) CLIP170-like tip1p spatially organizes microtubular dynamics in fission yeast. *Cell*, **102**: 695-704

Bryson-Richardson, R. J. and Currie, P. D. (2008) The genetics of vertebrate myogenesis. *Nature Reviews Genetics*, **9**: 632-646

Burattini, S., Ferri, P., Battistelli, M., Curci, R., Luchetti, F. and Falcieri, E. (2004) C2C12 murine myoblasts as a model of skeletal muscle development: morpho-functional characterization. *European Journal of Histochemistry*, **48**: 223-233

Busch, K. E., Hayles, J., Nurse, P. and Brunner, D. (2004) Tea2p kinesin is involved in spatial microtubule organization by transporting tip1p on microtubules. *Developmental Cell*, **6**: 831-843

Buttrick, G. J. and Wakefield, J. G. (2008) PI3-K and GSK-3: Akt-ing together with microtubules. *Cell Cycle*, **7**: 2621-2625

Carvalho, P., Gupta, Jr., M. L., Hoyt, M. A. and Pellman, D. (2004) Cell cycle control of kinesin-mediated transport of Bik1 (CLIP-170) regulates microtubule stability and dynein activation. *Developmental Cell*, **6**: 815-829

Cayouette, M. and Raff, M. (2003) The orientation of cell division influences cell-fate choice in the developing mammalian retina. *Development*, **130**: 2329-2339

Chapman, S. C., Collignon, J., Schoenwolf, G. C. and Lumsden, A. (2001) Improved method for chick whole-embryo culture using a filter paper carrier. *Dev Dyn*, **220**: 284-289

Chapman, S. C., Brown, R., Lees, L., Schoenwolf, G. C. and Lumsden, A. (2004) Expression analysis of chick Wnt and frizzled genes and selected inhibitors in early chick patterning. *Dev. Dyn*, **229**: 668-676

Chen, A. E., Ginty, D. D. and Fan, C. M. (2005) Protein kinase A signalling via CREB controls myogenesis induced by Wnt proteins. *Nature*, **433**: 317-322

Chen, H. J., Lin, C. M., Lin, C. S., Perez-Olle, R., Leung, C. L. and Liem, R. K. H. (2006) The role of microtubule actin cross-linking factor 1 (MACF1) in the Wnt signaling pathway. *Genes and Development*, **20**: 1933-1945

Chretien, D., Jainosi, I., Taveau, J. C. and Flyvbjerg, H. (1999) Microtubule's conformational cap. *Cell Struct Funct.*, **24**: 299-303

Christ, B., Jacob, H. J. and Jacob, M. (1972) Experimentelle Untersuchungen zur Somitenentstehung beim Hühnerembryo. *Anatomy and Embryology*, **138**: 82-97

Christ, B., Jacob, M. and Jacob, H. J. (1973) Weitere Befunde zur Differenzierung des achsennahen Mesoderms junger Hühnerembryonen. *Anat. Anz. Ergänz-H. zum Bd.,* **134**: 175-182

Christ, B., Brand-Saberi, B., Grim, M. and Wilting, J. (1992) Local signalling in dermomyotomal cell type specification. *Anat. Embryol*., **186** (5): 505-510

Christ, B. and Ordahl, C. P. (1995) Early stages of chick somite development. *Anatomy and Embryology*, **191**: 381-396

Chuai, M., Zeng, W., Yang, X., Boychenko, V., Glazier, J. A. and Weijer, C. J. (2006) Cell movement during primitive streak formation. *Developmental Biology*, **296**: 137-149

Chuai, M. and Weijer, C. J. (2008) The Mechanisms Underlying Primitive Streak Formation in the Chick Embryo. *Current Topics in Developmental Biology*, **81**: 135-156

Ciani, L., Krylova, O., Smalley, M. J., Dale, T. C. and Salinas, P. C. (2004) A divergent canonical WNT-signaling pathway regulates microtubule dynamics: dishevelled signals locally to stabilize microtubules. *Journal of Cell Biology*, **164**: 243-253

Cinnamon, Y., Kahane, N. and Kalcheim, C. (1999) Characterization of the early development of specific hypaxial muscles from the ventrolateral myotome. *Development*, **126**: 4305–4315

Cinnamon, Y., Kahane, N., Bachelet, I. and Kalcheim, C. (2001) The sub-lip domain - a distinct pathway for myotome precursors that demonstrate rostral-caudal migration. *Development* **128**: 341–351

Clevers, H. (2006) Wnt/beta-catenin signaling in development and disease. *Cell*, **127**: 469-480

Cooke, J. and Zeeman, E. C. (1976) A clock and wavefront model for control of the number of repeated structures during animal morphogenesis. *Journal of Theoretical Biology*, **58**: 455-476

Cooper, O., Sweetman, D., Wagstaff, L. and Münsterberg, A. (2008) Expression of avian prickle genes during early development and organogenesis. *Developmental Dynamics*, **237**: 1442-1448

Cossu, G., Kelly, R., Tajbakhsh, S., Di Donna, S., Vivarelli, E. and Buckingham, M. (1996) Activation of different myogenic pathways: myf-5 is induced by the neural tube and MyoD by the dorsal ectoderm in the mouse paraxial mesoderm. *Development*, **122** (2): 429-437

Cui, C., Yang, X., Chuai, M., Glazier, J. A. and Weijer, C. J. (2005) Analysis of tissue flow patterns during primitive streak formation in the chick embryo. *Developmental Biology*, **284**: 37-47

Dale, R. M., Sisson, B. E. and Topczewski, J. (2009) The emerging role of Wnt/PCP signaling in organ formation. *Zebrafish*, **6**: 9-14

Davidson, G., Wu, W., Shen, J., Bilic, J., Fenger, U., Stannek, P., Glinka, A. and Niehrs, C. (2005) Casein kinase 1 gamma couples Wnt receptor activation to cytoplasmic signal transduction. *Nature*, **438**: 867-872

Denetclaw, W. F. Jr., Christ, B. and Ordahl, C. P. (1997) Location and growth of epaxial myotome precursor cells. *Development*, **124**: 1601–1610

Denetclaw, W. F. and Ordahl, C. P. (2000) The growth of the dermomyotome and formation of early myotome lineages in thoracolumbar somites of chicken embryos. *Development*, **127**: 893-905

Denetclaw, W. F. Jr., Berdougo, E., Venters, S. J. and Ordahl, C. P. (2001) Morphogenetic cell movements in the middle region of the dermomyotome dorsomedial lip associated with patterning and growth of the primary epaxial myotome. *Development*, **128**: 1745–1755

Dietrich, S., Schubert, F. R. and Lumsden, A. (1997) Control of dorsoventral pattern in the chick paraxial mesoderm. *Development*, **124**: 3895-3908

Dietrich, S., Schubert, F. R., Healy, C., Sharpe, P. T. and Lumsden, A. (1998) Specification of hypaxial musculature. *Development*, **125**: 2235–2249

Dikovskaya, D., Newton, I. P. and Nathke, I. S. (2004) The adenomatous polyposis coli protein is required for the formation of robust spindles formed in CSF Xenopus extracts. *Mol Biol Cell*, **15**: 2978-2991

Djiane, A., Riou, J., Umbhauer, M., Boucaut, J. and Shi, D. (2000) Role of frizzled 7 in the regulation of convergent extension movements during gastrulation in Xenopus laevis. *Development*, **127**: 3091-3100

Dockter, J. and Ordahl, C. P. (2000) Dorsoventral axis determination in the somite: a re-examination. *Development*, **127** (10): 2201-2206

Dominguez, I., Itoh, K. and Sokol, S.Y. (1995) Role of glycogen synthase kinase 3 beta as a negative regulator of dorsoventral axis formation in Xenopus embryos. *Proc Natl Acad Sci U S A*, **92**: 8498-8502

Dormann, D. and Weijer, C. J. (2003) Chemotactic cell movement during development. *Current Opinion in Genetics and Development*, **13**: 358-364

dos Remedios, C. G., Chhabra, D., Kekic, M., Dedova, I. V., Tsubakihara, M., Berry, D. A. and Nosworthy, N. J. (2003) Actin binding proteins: regulation of cytoskeletal microfilaments. *Physiological Reviews*, **83**: 433-473

Drabek, K., van Ham, M., Stepanova, T., Draegestein, K., van Horssen, R., Sayas C. L., Akhmanova, A., Ten Hagen, T., Smits, R., Fodde, R., Grosveld, F. and Galjart, N. (2006) Role of CLASP2 in microtubule stabilization and the regulation of persistent motility. *Current Biology*, **16**: 2259-2264

Duband, J. L., Dufour, S., Hatta, K., Takeichi, M., Edelman, G. M. and Thiery, J. P. (1987) Adhesion molecules during somitogenesis in the avian embryo. *J. Cell Biol.*, 104: 1361-1374

Dubrelle, J., McGrew, M. J. and Pourquié, O. (2001) FGF signaling controls somite boundary position and regulates segmentation clock control of spatiotemporal Hox gene activation. *Cell*, **106**: 219-232

Etienne-Manneville, S. (2010) From signaling pathways to microtubule dynamics: the key players. *Current Opinion in Cell Biology*, **22**: 104-111

Etienne-Manneville, S. (2004) Actin and Microtubules in Cell Motility: Which one is in control? *Traffic*, **5**: 470-477

Etienne-Manneville, S. and Hall, A. (2002) Rho GTPases in cell biology. *Nature*, **420**: 629-635

Ezratty, E. J., Partridge, M. A. and Gundersen, G. G. (2005) Microtubule-induced focal adhesion disassembly is mediated by dynamin and focal adhesion kinase. *Nature Cell Biology*, **7**: 581-590

Fan, C. M. and Tessier-Lavigne, M. (1994) Patterning of mammalian somites by surface ectoderm and notochord: evidence for sclerotome induction by a hedgehog homolog. *Cell*, **79** (7): 1175-1186

Folker, E. S., Baker, B. M. and Goodson, H. V. (2005) Interactions between CLIP-170, tubulin, and microtubules: implications for the mechanism of CLIP-170 plus-end tracking behaviour. *Molecular Biology of the Cell*, **16**: 5373-5384

Fukata, M., Nakagawa, M. and Kaibuchi, K. (2003) Roles of Rho-family GTPases in cell polarisation and directional migration. *Current Opinion in Cell Biology*, **15**: 590-597

Fukata, M., Watanabe, T., Noritake, J., Nakagawa, M., Yamaga, M., Kuroda, S., Matsuura, Y., Iwamatsu, A., Perez, F. and Kaibuchi, K. (2002) Rac1 and Cdc42 capture microtubules through IQGAP1 and CLIP-170. *Cell*, **109**: 873-885

Galli, L. M., Willert, K., Nusse, R., Yablonka-Reuveni, Z., Nohno, T., Denetclaw, W. and Burrus, L. W. (2004) A proliferative role for Wnt-3a in chick somites. *Developmental Biology*, **269**: 489-504

Gardner, M. K., Hunt, A. J., Goodson, H. V. and Odde, D. J. (2008) Microtubule assembly dynamics: new insights at the nanoscale. *Current Opinion in Cell Biology*, **20**: 64-70

Geetha-Loganathan, P., Nimmagadda, S., Huang, R., Christ, B. and Scaal, M. (2006) Regulation of ectodermal Wnt6 expression by the neural tube is transduced by dermomyotomal Wnt11: a mechanism of dermomyotomal lip sustainment. *Development*, **133**: 2897-2904

Geetha-Loganathan, P., Nimmagadda, S., Scaal, M., Huang, R. and Christ, B. (2008) Wnt Signaling in somite development. *Annals of Anatomy*, **190**: 208-222

Gilbert, S. F. (2006) Developmental Biology Eighth Edition: Chapter 14. Sinauer Associates, Inc., Publishers. Sunderland, Massachusetts USA

Goodson, H. V., Skube, S. B., Stalder, R., Valetti, C., Kreis, T. E., Morrison, E. E. and Schroer, T. A. (2003) CLIP-170 interacts with dynactin complex and the APC-binding protein EB1 by different mechanisms. *Cell Motility and the Cytoskeleton*. **55**:156-173

Goold, R. G., Owen, R. and Gordon-Weeks, P. R. (1999) Glycogen synthase kinase 3beta phosphorylation of microtubule-associated protein 1B regulates the stability of microtubules in growth cones. *Journal of Cell Science*, **112** (19): 3373-3384

Goryunov, D., He, C. Z., Lin, C. S., Leung, C. L. and Liem, R. K. (2010) Nervous-tissue-specific elimination of microtubule-actin crosslinking factor 1a results in multiple developmental defects in the mouse brain. *Molecular and Cellular Neurosciences*, **44**: 1-14

Gournier, H., Goley, E. D., Niederstrasser, H., Trinh, T. and Welch, M. D. (2001) Reconstitution of human Arp2/3 complex reveals critical roles of individual subunits in complex structure and activity. *Molecular Cell*, **8**: 1041-1052

Graeper, L. (1929) Die Primitiventwicklung des Huehnchens nach sterokinematographischen Untersuchungen kontorlliert durch vitle Farbmarkierung und verglichen mit der Entwicklung anderer Wirbeltiere. [Chick primitive streak stage development following vital dye labelling and videomicroscopy studies and comparison to the development of other vertebrates.] *Wilhelm Roux Arch. Entwicklungsmech*, **116**: 382-429

Gros, J., Scaal, M. and Marcelle, C. (2004) A two-step mechanism for myotome formation in chick. *Developmental Cell*, **6**: 875-882

Gros, J., Manceau, M., Thomé, V., and Marcelle, C. (2005) A common somitic origin for embryonic muscle progenitors and satellite cells. *Nature*, **435**: 954-958

Gros, J., Serralbo, O. and Marcelle, C. (2009) WNT11 acts as a directional cue to organize the elongation of early muscle fibres. *Nature*, **457**: 589-594

Groves, R. W., Liu, L., Dopping-Hepenstal, P. J., Markus, H. S., Lovell, P. A., Ozoemena, L., Lai-Cheong, J. E., Gawler, J., Owaribe, K., Hashimoto, T., Mellerio, J. E., Mee, J. B. and McGrath, J. A. (2010) A homozygous nonsense mutation within the dystonin gene coding for the coiled-coil domain of the epithelial isoform of BPAG1 underlies a new subtype of autosomal recessive epidermolysis bullosa simplex. *The Journal of Investigative Dermatology*, **130**: 1551-1557

Guo, J. X., Jacobson, S. L. and Brown, D. L. (1986) Rearrangement of tubulin, actin, and myosin in cultured ventricular cardiomyocytes of the adult rat. *Cell Motility and the Cytoskeleton*, **6**: 291-304

Guo, L., Degenstein, L., Dowling, J., Yu, Q. C., Wollmann, R., Perman, B. and Fuchs, E. (1995) Gene targeting of BPAG1: abnormalities in mechanical strength and cell migration in stratified epithelia and neurologic degeneration. *Cell*, **81**: 233-243

Habas, R. and Dawid, I. B. (2005) Dishevelled and Wnt signaling: is the nucleus the final frontier? *Journal of Biology*, **4**: 2

Hamburger, V. and Hamilton, H. L. (1951) A series of normal stages in the development of the chick embryo. *J Morphol* **88**: 49-92

Hartwig, J. H. (1995) Actin-binding proteins. 1: Spectrin super family. *Protein Profile*. **2**: 703-800

Hayashi, I. and Ikura, M. (2003) Crystal structure of the amino-terminal microtubule-binding domain of end-binding protein 1 (EB1). *The Journal of Biological Chemistry*, **278**: 36430-36434

He, X., Saint-Jeannet, J. P., Woodgett, J. R., Varmus, H. E. and Dawid, I. B. (1995) Glycogen synthase kinase-3 and dorsoventral patterning in Xenopus embryos. *Nature*, **374**: 617-622

Heisenberg, C. P., Tada, M., Rauch, G. J., Saude, L., Concha, M. L., Geisler, R., Stemple, D. L., Smith, J. C. and Wilson, S. W. (2000) Silberblick/Wnt11 mediates convergent extension movements during zebrafish gastrulation. *Nature*, **405**: 76-81
Higgs, H. N. and Pollard, T. D. (2001) Regulation of actin filament network formation through ARP2/3 complex: activation by a diverse array of proteins. *Annual Review of Biochemistry*, **70**: 649-676

Hirsinger, E., Malapert, P., Dubrulle, J., Delfini, M. C., Duprez, D., Henrique, D., Ish-Horowicz, D. and Pourquie, O. (2001) Notch signalling acts in postmitotic avian myogenic cells to control MyoD activation. *Development*, **128**: 107-116

Hogan, P. G., Chen, L., Nardone, J. and Rao, A. (2003) Transcriptional regulation by calcium, calcineurin, and NFAT. *Genes Dev*. **17**: 2205-2232

Hollenbeck, P. (2001) Cytoskeleton: Microtubules get the signal. *Current Biology*, **11**: 820-823

Hollway, G. E. and Currie, P. D. (2003) Myotome meanderings: Cellular morphogenesis and the making of the muscle. *EMBO reports*, **4** (9): 855-860

Horwitz, R. and Webb, D. (2003) Cell Migration. *Current Biology*, **13** (19): 756-759

Howard, J. and Hyman, A. A. (2003) Dynamics and mechanics of the microtubule plus end. *Nature*, **422**: 753-758

Hutcheson, D. A., Zhao, J., Merrell, A., Haldar, M. and Kardon, G. (2009) Embryonic and fetal limb myogenic cells are derived from developmentally distinct progenitors and have different requirements for beta-catenin. *Genes & Development*, **23**: 997-1013

Ikeya, M., and Takada, S. (1998) Wnt signaling from the dorsal neural tube is required for the formation of the medial dermomyotome. *Development*, **125**: 4969-4976

Inoue, Y. H., Savoian, M. S., Suzuki, T., Mathe, E., Yamamoto, M. T. and Glover, D. M. (2004) Mutations in orbit/mast reveal that the central spindle is comprised of two microtubule populations, those that initiate cleavage and those that propagate furrow ingression. *Journal of Cell Biology*, 166: 49-60

James, R. G., Conrad, W. H. and Moon, R. T. (2008) Beta-catenin-independent Wnt pathways: signals, core proteins, and effectors. *Methods Mol. Biol.,* 468: 131-44

Jaworski, J., Hoogenraad, C. C. and Akhmanova, A. (2008) Microtubule plus-end tracking proteins in differentiated mammalian cells. *International journal of biochemistry and cell biology*, **40**: 619-637

Jefferson, J. J., Leung, C. L. and Liem, R. K. (2004) Plakins: goliaths that link cell junctions and the cytoskeleton. *Nature Reviews. Molecular Cell Biology*, **5**: 542-553

Kahane, N. and Kalcheim, C. (1998) Identification of early postmitotic cells in distinct embryonic sites and their possible roles in morphogenesis. *Cell Tissue Res*, **294**: 297–307

Kahane, N., Cinnamon, Y. and Kalcheim, C. (1998a) The cellular mechanism by which the dermomyotome contributes to the second wave of myotome development. *Development*, **125**: 4259–4271

Kahane, N., Cinnamon, Y. and Kalcheim, C. (1998b) The origin and fate of pioneer myotomal cells in the avian embryo. *Mech. Dev.*, **74** (12): 59-73

Kahane, N., Cinnamon, Y., Bachelet, I. and Kalcheim, C. (2001) The third wave of myotome colonization by mitotically competent progenitors: regulating the balance between differentiation and proliferation during muscle development. *Development*, **128**: 2187–2198

Kahane, N., Cinnamon, Y. and Kalcheim, C. (2002) The roles of cell migration and myofiber intercalation in patterning formation of the postmitotic myotome. *Development*, **129**: 2675–2687

Kakinuma, T., Ichikawa, H., Tsukada, Y., Nakamura, T. and Toh, B. H. (2004) Interaction between p230 and MACF1 is associated with transport of a glycosyl phosphatidyl inositol-anchored protein from the Golgi to the cell periphery. *Experimental Cell Research*, **298**: 388-398

Kalcheim, C. and Ben-Yair, R. (2005) Cell rearrangements during development of the somite and its derivatives. *Curr Opin Genet Dev*, **15**: 371-380

Karakesisoglou, I., Yang, Y. and Fuchs, E. (2000) An epidermal plakin that integrates actin and microtubule networks at cellular junctions. *Journal of Cell Biology*, **149**: 195-208

Kassar-Duchossoy, L., Giacone, E., Gayraud-Morel, B., Jory, A., Gomes, D. and Tajbakhsh, S. (2005) Pax3/Pax7 mark a novel population of primitive myogenic cells during development. *Genes and Development*, **19**: 1426-1431

Kaverina, I., Rottner, K. and Small, J. V. (1998) Targeting, capture, and stabilization of microtubules at early focal adhesions. *Journal of Cell Biology*, **142**: 181-190

Kaverina, I., Krylyshkina, O. and Small, J. V. (1999) Microtubule targeting of substrate contacts promotes their relaxation and dissociation. *Journal of Cell Biology*, **146**: 1033-1044

Keller, R., Davidson, L., Edlund, A., Elul, T., Ezin, M., Shook, D. and Skoglund, P. (2000) Mechanisms of Convergence and Extension by Cell Intercalation. *Philos. Trans. R. Soc. Lond. B Biol. Sci*, **355**: 897-922

Keller, R. (2005) Cell Migration during Gastrulation. *Current Opinion in Cell Biology*, **17**: 533-541

Kelly, O. G., Pinson, K. I. and Skarnes, W. C. (2004) The Wnt co-receptors Lrp5 and Lrp6 are essential for gastrulation in mice. *Development*, **131**: 2803-2815

Kieny, M., Mauger, A. and Sengel, P. (1972) Early regionalization of the somitic mesoderm as studied by the development of the axial skeleton of the chick embryo. *Developmental Biology*, **28** (1): 142-161

Kirscner, M. and Mitchison, T. (1986) Beyond self-assembly: from microtubules to morphogenesis. *Cell*, **45**: 329-342

Kita, K., Wittmann, T., Nathke, I. S. and Waterman-Storer, C. M. (2006) Adenomatous polyposis coli on microtubule plus ends in cell extensions can promote microtubule net growth with or without EB1. *Molecular Biology of the Cell*. **17**: 2331-2345

Kodama, A., Karakesisoglou, I., Wong, E., Vaezi, A. and Fuchs, E. (2003) ACF7: an essential integrator of microtubule dynamics. *Cell*, **115**: 343-354

Kohler, T., Prols, F. and Brand-Saberi, B. (2005) PCNA in situ hybridization: a novel and reliable tool for detection of dynamic changes in proliferative activity. *Histochemistry and Cell Biology*, **123**: 315-327

Komarova, Y. A., Akhmanova, A. S., Kojima, S., Galjart, N. and Borisy, G. G. (2002) Cytoplasmic linker proteins promote microtubule rescue in vivo. *Journal of cell biology*, **159**: 589-599

Komarova, Y., De Groot, C. O., Grigoriev, I., Gouveia, S. M., Munteanu, E. L., Schober, J. M., Honnappa, S., Buey, R. M., Hoogenraad, C. C., Dogterom, M., Borisy, G. G., Steinmetz, M. O. and Akhmanova, A. (2009) Mammalian end binding proteins control persistent microtubule growth. *Journal of cell biology*, **184**: 691-706

Komarova, Y., Lansbergen, G., Galjart, N., Grosveld, F., Borisy, G. G. and Akhmanova, A. (2005) EB1 and EB3 control CLIP dissociation from the ends of growing microtubules. *Molecular Biology of the Cell*, **16**: 5334-5345

Kopan, R., Nye, J. S. and Weintraub, H. (1994) The intracellular domain of mouse Notch: a constitutively activated repressor of myogenesis directed at the basic helix-loop-helix region of MyoD. *Development*, **120**: 2385-2396

Krylova, O., Messenger, M. J. and Salinas, P. C. (2000) Dishevelled-1 regulates microtubule stability: a new function mediated by glycogen synthase kinase-3beta. *Journal of Cell Biology*, **151**: 83-94

Krylyshkina, O., Anderson, K. I., Kaverina, I., Upmann, I., Manstein, D. J., Small, J. V. and Toomre, D. K. (2003) Nanometer targeting of microtubules to focal adhesions. *Journal of Cell Biology*, **161**: 853-859

Krylyshkina, O., Kaverina, I., Kranewitter, W., Steffen, W., Alonso, M. C., Cross, R. A. and Small, J. V. (2002) Modulation of substrate adhesion dynamics via microtubule targeting requires kinesin-1. *Journal of Cell Biology*, **156**: 349-359

Kumar, P., Lyle, K. S., Gierke, S., Matov, A., Danuser, G. and Wittmann, T. (2009) GSK3beta phosphorylation modulates CLASP-microtubule association and lamella microtubule attachment. *Journal of Cell Biology*, **184** (6): 895-908

Kuroda, K., Tani, S., Tamura, K., Minoguchi, S., Kurooka, H. and Honjo, T. (1999) Delta-induced Notch signaling mediated by RBP-J inhibits MyoD expression and myogenesis. *J Biol Chem*, **274**: 7238-7244

Langman, J. (1981) *Medical Embryology,* 4th Ed. Williams & Wilkins, Baltimore

Lansbergen, G. and Akhmanova, A. (2006a) Microtubule plus end: a hub of cellular activities. *Traffic*, **7**: 499-507

Lansbergen, G., Grigoriev, I., Mimori-Kiyosue, Y., Ohtsuka, T., Higa, S., Kitajima, I., Demmers, J., Galjart, N., Houtsmuller, A. B., Grosveld, F. and Akhmanova, A. (2006b) CLASPs attach microtubule plus ends to the cell cortex through a complex with LL5beta. *Developmental Cell*, **11**: 21-32

Lansbergen, G., Komarova, Y., Modesti, M., Wyman, C., Hoogenraad, C. C., Goodson, H. V., Lemaitre, R. P., Drechsel, D. N., van Munster, E., Gadella, T. W., Jr., Grosveld, F., Galjart, N., Borisy, G. G. and Akhmanova, A. (2004) Conformational changes in CLIP-170 regulate its binding to microtubules and dynactin localization. *Journal of cell biology*, **166** (7): 1003-1014

Lauffenburger, D. A. and Horwitz, A. F. (1996) Cell migration: A physically integrated molecular process. *Cell*, **84**: 359-369

Lawson, A. and Schoenwolf, G. C. (2001a) New insights into critical events of avian gastrulation. *The Anatomical Record*, **262**: 221-226

Lawson, A. and Schoenwolf, G. C. (2001b) Cell populations and morphogenetic movements underlying formation of the avian primitive streak and organizer. *Genesis*, **29**: 188-195

Lecaudey, V., Cakan-Akdogan, G., Norton, W. H. J. and Gilmour, D. (2008) Dynamic Fgf signaling couples morphogenesis and migration in the zebrafish lateral line primordium. *Development*, **135**: 2695-2705

Lee, H., Engel, U., Rusch, J., Scherrer, S., Sheard, K. and Van Vactor, D. (2004). The microtubule plus end tracking protein Orbit/MAST/CLASP acts downstream of the tyrosine kinase Abl in mediating axon guidance. *Neuron*, **42**: 913-926

Lee, S. and Kolodziej, P. A. (2002) Short Stop provides an essential link between F-actin and microtubules during axon extension. *Development*, **129**: 1195-1204

Leonova, E. V. and Lomax, M. I. (2002) Expression of the mouse Macf2 gene during inner ear development. *Brain Research. Molecular Brain Research*, **105**: 67-78

Leung, C. L., Sun, D., Zheng, M., Knowles, D. R. and Liem, R. K. (1999) Microtubule actin cross-linking factor (MACF): A hybrid of dystonin and dystrophin that can interact with the actin and microtubule cytoskeletons. *Journal of Cell Biology*, **147**: 1275-1286

Leung, C. L., Zheng, M., Prater, S. M. and Liem, R. K. (2001) The BPAG1 locus: Alternative splicing produces multiple isoforms with distinct cytoskeletal linker domains, including predominant isoforms in neurons and muscles. *The Journal Cell of Biology*, **154**: 691-697

Leung, C. L., Green, K. J. and Liem, R. K. (2002) Plakins: a family of versatile cytolinker proteins. *Trends in Cell Biology*, **12**: 37-45

Levayer, R. and Lecuit, T. (2008) Breaking down EMT. *Nature Cell Biology*, **10** (7): 757-759

Levy, J. R. and Holzbaur, E. L. (2007) Special delivery: dynamic targeting via cortical capture of microtubules. *Developmental Cell*, **12**: 320-322

Lin, C. M., Chen, H. J., Leung, C. L., Parry, D. A. and Liem, R. K. (2005) Microtubule actin crosslinking factor 1b: a novel plakin that localizes to the Golgi complex. *J Cell Sci*. **118**: 3727-3738

Linker, C., Lesbros, C., Gros, J., Burrus, L. W., Rawls, A. and Marcelle, C. (2005) β-Catenin-dependent Wnt signalling controls the epithelial organisation of somites through the activation of *paraxis*. *Development*, **132**: 3895-3905

Logan, C. Y., and Nusse, R. (2004) The Wnt signaling pathway in development and disease. *Annual Review of Cell and Developmental Biology*, **20**: 781-810

Lomakin, A. J., Semenova, I., Zaliapin, I., Kraikivski, P., Nadezhdina, E., Slepchenko, B. M., Akhmanova, A. and Rodionov, V. (2009) CLIP-170-dependent capture of membrane organelles by microtubules initiates minus-end directed transport. *Developmental Cell*, **17**: 323-333

Lopez-Sanchez, C., Puelles, L., Garcia-Martinez, V. and Rodriguez-Gallardo. (2005) Morphological and Molecular Analysis of the Early Developing Chick Requires an Expanded Series of Primitive Streak Stages. *Journal of Morphology*, **264**: 105-116

Lucas, F. R., Goold, R. G., Gordon-Weeks, P. R. and Salinas, P. C. (1998) Inhibition of GSK-3beta leading to the loss of phosphorylated MAP-1B is an early event in axonal remodelling induced by WNT-7a or lithium. *Journal of Cell Science*, **111** (10): 1351-1361

Lui, P., Wakamiya, M., Shea, M. J., Albrecht, U., Behringer, R. R. and Bradley, A. (1999) Requirement for Wnt3 in vertebrate axis formation. *Nature Genetics*, **22**: 361-365

Maiato, H., Sampaio, P., and Sunkel, C. E. (2004) Microtubule-associated proteins and their essential roles during mitosis. *International Review of Cytology*, **241**: 53-153

Manceau, M., Gros, J., Savage, K., Thomé, V., McPherron, A., Paterson, B. and Marcelle, C. (2008) Myostatin promotes the terminal differentiation of embryonic muscle progenitors. *Genes and Development*, **22**: 668-681

Marcelle, C., Stark, M.R. and Bronner-Fraser, M. (1997) Coordinate actions of BMPs, Wnts, Shh and noggin mediate patterning of the dorsal somite. *Development*, **124**: 3955-3963

Marone, R., Hess, D., Dankort, D., Muller, W. J., Hynes, N. E. and Badache, A. (2004) Memo mediates ErbB2-driven cell motility. *Nature Cell Biology*, **6**: 515-522

Maroto, M. and Pourquié, O. (2001) A molecular clock involved in somite segmentation. *Curr. Top. Dev. Biol.*, **51**: 221-248

Mathe, E., Inoue, Y. H., Palframan, W., Brown, G. and Glover, D. M. (2003) Orbit/Mast, the CLASP orthologue of Drosophila, is required for asymmetric stem cell and cystocyte divisions and development of the polarised microtubule network that interconnects oocyte and nurse cells during oogenesis. *Development*, **130**: 901-915

Mikawa, T., Poh, A. M., Kelly, K. A., Ishii, Y. and Reese, D. E. (2004) Induction and Patterning of the Primitive Streak, an Organizing center of Gastrulation in the Amniote. *Developmental Dynamics*, **229**: 422-432

Miller, J. R., Rowning, B. A., Larabell, C. A., Yang-Snyder, J. A., Bates, R. L. and Moon, R. T. (1999) Establishment of the dorsal-ventral axis in Xenopus embryos coincides with the dorsal enrichment of dishevelled that is dependent on cortical rotation. *Journal of Cell Biology*, **146**: 427-437

Mimori-Kiyosue, Y. and Tsukita, S. (2003) "Search-and-capture" of microtubules through plus-end-binding proteins (+TIPs). *Journal of Biochemistry*, **134**: 321-326

Mitchison, T. and Kirschner, M. (1984) Dynamic instability of microtubule growth. *Nature*, **312**: 237-242

Montcouquiol, M., Rachel, R. A., Lanford, P. J., Copeland, N. G., Jenkins, N. A. and Kelley, M. W. (2003) Identification of Vangl2 and Scrb1 as planar polarity genes in mammals. *Nature*, **423**: 173-177

Morrison, S. J. and Kimble, J. (2006) Asymmetric and symmetric stem-cell divisions in development and cancer. *Nature*, **441**: 1068-1074

Mueller, S., Klaus-Kovtun, V. and Stanley, J. R. (1989) A 230-kD basic protein is the major bullous pemphigoid antigen. *Journal of Investigative Dermatology*, **92**: 33-38

Mumm, J. S. and Kopan, R. (2000) Notch signaling: from the outside in. *Dev Biol*, **228**: 151-165

Münsterberg, A. E. and Lassar, A. B. (1995a) Combinatorial signals from the neural tube, floor plate and notochord induce myogenic bHLH gene expression in the somite. *Development*, **121** (3): 651-660

Münsterberg, A. E., Kitajewski, J., Bumcrot, D. A., McMahon, A. P. and Lassar, A. B. (1995b) Combinatorial signaling by Sonic hedgehog and Wnt family members induces myogenic bHLH gene expression in the somite. *Genes and Development*, **9** (23): 2911-2922

Musa, H., Orton, C., Morrison, E. E. and Peckham, M. (2003) Microtubule assembly in cultured myoblasts and myotubes following nocodazole induced microtubule depolymerisation. *Journal of Muscle Research and Cell Motility*, **24**: 301-308

Nakaya, Y., Kuroda, S., Katagiri, Y. T., Kaibuchi, K. And Takahashi, Y. (2004) Mesenchymal-Epithelial Transition during Somitic Segmentation Is Regulated by Differential Roles of Cdc42 and Rac1. *Developmental Cell*, **7**: 425-438

Nakaya, Y., Sukowati, E. W., Wu, Y. and Sheng, G. (2008) RhoA and microtubule dynamics control cell-basement membrane interaction in EMT during gastrulation. *Nature Cell Biology*, **10** (7): 765-775

Nakaya, Y. and Sheng, G. (2009) An amicable separation- Chick's way of doing EMT. *Cell Adhesion and Migration*, **3** (2): 160-163

Nofziger, D., Miyamoto, A., Lyons, K. M. and Weinmaster, G. (1999) Notch signaling imposes two distinct blocks in the differentiation of C2C12 myoblasts. *Development*, **126**: 1689-1702

Nusse, R. and Varmus, H. E. (1982) Many tumors induced by the mouse mammary tumor virus contain a provirus integrated in the same region of the host genome. *Cell*, **31**: 99-109

Olivera-Martinez, I., Thelu, J., Teillet, M. A. and Dhouailly, D. (2001) Dorsal dermis development depends on a signal from the dorsal neural tube, which can be substituted by Wnt-1. *Mech. Dev.*, **100**: (2) 233-244

Ordahl, C. P. and Le Douarin, N. M. (1992) Two myogenic lineages within the developing somite. *Development*, **114**: 339-353

Ordahl, C. P. (1993). Myogenic lineages within the developing somite. *Molecular Basis of Morphogenesis*, pp. 165-176. Wiley-Liss, Inc.

Ordahl, C. P., Berdougo, E., Venters, S. J. and Denetclaw, W. F. (2001) The dermomyotome dorsomedial lip drives growth and morphogenesis of both the primary myotome and dermomyotome epithelium. *Development*, **128**: 1731–1744

Otto, A., Schmidt, C. and Patel, K. (2006) Pax3 and Pax7 expression and regulation in the avian embryo. *Anatomy and Embryology (Berl)*, **211**: 293-310

Ovechkina, Y. and Wordeman, L. (2003) Unconventional motoring: an overview of the Kin C and Kin I kinesins. *Traffic*, **4**: 367-375

Packard, D. S. Jr. (1978) Chick somite determination: the role of factors in young somites and the segmental plate. *J. Exp. Zool.*, **203**: 295-306

Palmeirim, I., Henrique, D., Ish-Horowicz, D. and Pourquié, O. (1997) Avian hairy gene expression identifies a molecular clock linked to vertebrate segmentation and somitogenesis. *Cell*, **91**: 639-648

Parr, B. A., Shea, M. J., Vassileva, G. and McMahon, A. P. (1993) Mouse Wnt genes exhibit discrete domains of expression in the early embryonic CNS and limb buds. *Development*, **119**: 247-261

Peifer, M., Pai, L. M. and Casey, M. (1994) Phosphorylation of the Drosophila adherens junction protein Armadillo: roles for wingless signal and zeste-white 3 kinase. *Dev Biol*, **166**: 543-556

Perez, F., Diamantopoulos, G. S., Stalder, R. and Kreis, T. E. (1999) CLIP-170 highlights growing microtubule ends in vivo. *Cell*, **96**: 517-527

Pierce, S. B. and Kimelman, D. (1995) Regulation of Spemann organizer formation by the intracellular kinase Xgsk-3. *Development*, **121**: 755-765

Pierre, P., Scheel, J., Rickard, J. E. and Kreis, T. E. (1992) CLIP-170 links endocytic vesicles to microtubules. *Cell*, **70**: 887-900

Pizon, V., Gerbal, F., Diaz, C. C. and Karsenti, E. (2005) Microtubule-dependent transport and organization of sarcomeric myosin during skeletal muscle differentiation. *The Embo Journal*, **24**: 3781-3792

Pollard, T. D. and Borisy, G. G. (2003) Cellular Motility Driven by Assembly and Disassembly of Actin Filaments. *Cell*, **112**: 453-465

Pollitt, A. Y. and Insall, R. H. (2009) WASP and SCAR/WAVE proteins: the drivers of actin assembly. *Journal of Cell Science*, **122**: 2575-2578

Pourquié, O., Fan, C. M., Coltey, M., Hirsinger, E., Watanabe, Y., Bréant, C., Francis-West, P., Brickell, P., Tessier-Lavigne, M. and LeDouarin, N. M. (1996) Lateral and axial signals involved in avian somite patterning: a role for BMP4. *Cell*, **84**: 461–471

Pourquié, O. (2003) The segmentation clock: converting embryonic time into spatial pattern. *Science*, **301**: 328-330

Pourquié, O. (2004) The chick embryo: a leading model in somitogenesis studies. *Mech. Dev.*, **121**: 1069-1079

Relaix, F., Rocancourt, D., Mansouri, A. and Buckingham, M. (2005) A Pax3/Pax7-dependent population of skeletal muscle progenitor cells. *Nature*, **435**: 948-953

Reshef, R., Maroto, M. and Lassar, A. B. (1998) Regulation of dorsal somitic cell fates: BMPs and Noggin control the timing and pattern of myogenic regulator expression. *Genes & Development*, **12**: 290-303

Rice, L. M., Montabana, E. A. and Agard, D. A. (2008) The lattice as allosteric effector: structural studies of alphabeta- and gamma-tubulin clarify the role of GTP in microtubule assembly. *Proc Natl Acad Sci U S A*., **105**: 5378-5383

Ridley, A. J. (2001) Rho GTPases and cell migration. *Journal of Cell Science*, **114**: 2713-2722

Ridley, A. J. (2011) Life at the Leading Edge. *Cell*, **145** (7): 1012-1022

Ridley, A. J., Schwartz, M. A., Burridge, K., Firtel, R. A., Ginsberg, M. H., Borisy, G., Parsons, J. T. and Horwitz, A. R. (2003) Cell Migration: Integrating Signals from Front to Back. *Science*, **302**: 1704-1709

Rios, A. C., Serralbo, O., Salgado, D. and Marcelle, C. (2011) Neural crest regulates myogenesis through the transient activation of NOTCH. *Nature*, **473**: 532-535

Röper, K., Gregory, S. L. and Brown, N. H. (2002) The 'spectraplakins': cytoskeletal giants with characteristics of both spectrin and plakin families. *Journal of Cell Science*, **115**: 4215-4225

Röper, K. and Brown, N. H. (2003) Maintaining epithelial integrity: a function for gigantic spectraplakin isoforms in adherens junctions. *Journal of Cell Biology*, **162**: 1305-1315

Röper, K. and Brown, N. H. (2004) A spectraplakin is enriched on the fusome and organizes microtubules during oocyte specification in Drosophila. *Current Biology*, **14**: 99-110

Rørth, P. (2007) Collective guidance of collective cell migration. *Trends in Cell Biology*, **17** (12): 575-579

Rothbacher, U., Laurent, M. N., Deardorff, M. A., Klein, P. S., Cho, K. W. and Fraser, S. E. (2000) Dishevelled phosphorylation, subcellular localization and multimerization regulate its role in early embryogenesis. The *EMBO Journal*, **19**: 1010-1022

Saitoh, O., Arai, T. and Obinata, T. (1988) Distribution of microtubules and other cytoskeletal filaments during myotube elongation as revealed by fluorescence microscopy. *Cell and Tissue Research*, **252**: 263-273

Salinas, P. C. (2007) Modulation of the microtubule cytoskeleton: a role for a divergent canonical Wnt pathway. *Trends in Cell Biology*, **17** (17): 333- 342

Sanchez-Soriano, N., Travis, M., Dajas-Bailador, F., Goncalves-Pimentel, C., Whitmarsh, A. J. and Prokop, A. (2009) Mouse ACF7 and drosophila short stop modulate filopodia formation and microtubule organisation during neuronal growth. *Journal of Cell Biology*, **122**: 2534-2542

Scaal, M. and Christ, B. (2004) Formation and differentiation of the avian dermomyotome. *Anat Embryol (Berl)*, **208**: 411-424

Scaal, M., Gros, J., Lesbros, C. and Marcelle, C. (2004) In Ovo Electroporation of Avian Somites. *Developmental Dynamics*, **229**: 643-650

Schlesinger, A., Shelton, C. A., Maloof, J. N., Meneghini M. and Bowerman, B. (1999) Wnt pathway components orient a mitotic spindle in the early Caenorhabditis elegans embryo without requiring gene transcription in the responding cell. *Genes and Development*, **13**: 2028-2038

Seifert, J. R. and Mlodzik, M. (2007) Frizzled/PCP signalling: a conserved mechanism regulating cell polarity and directed motility. *Nature Reviews Genetics*, **8**: 126-138

Sharma, R. P. (1973) Wingless, a new mutant in *D. melanogaster*, *Drosoh. Inf. Serv.*, **50**: 134

Shawber, C., Nofziger, D., Hsieh, J. J., Lindsell, C., Bogler, O., Hayward, D. and Weinmaster, G. (1996) Notch signaling inhibits muscle cell differentiation through a CBF1-independent pathway. *Development*. 122:3765-3773

Siegrist, S. E. and Doe, C. Q. (2007) Microtubule-induced cortical cell polarity. *Genes and Development*, **21**: 483-496

Slep, K. C., Rogers, S. L., Elliott, S. L., Ohkura, H., Kolodziej, P. A. and Vale, R. D. (2005) Structural determinants for EB1-mediated recruitment of APC and spectraplakins to the microtubule plus end. *Journal of Cell Biology*, **168**: 587-598

Small, J. V. and Kaverina, I. (2003) Microtubules meet substrate adhesions to arrange cell polarity. *Current Opinion in Cell Biology*, **15**: 40-47

Smith, C. A. and R. S. Tuan. (1996) Functional involvement of Pax-1 in somite development: Somite dysmorphogenesis in chick embryos treated with Pax-1 paired-box antisense oligonucleotide. *Teratology*, **52**: 333–345

Sonnenberg, A. and Liem, R. K. (2007) Plakins in development and disease. *Experimental Cell Research*, **313**: 2189-2203

Steiner-Champliaud, M.F., Schneider, Y., Favre, B., Paulhe, F., Praetzel-Wunder, S., Faulkner, G., Konieczny, P., Raith, M., Wiche, G., Adebola, A., Liem, R. K., Langbein L., Sonnenberg, A., Fontao, L. and Borradori, L. (2010) BPAG1 isoform-b: complex distribution pattern in striated and heart muscle and association with plectin and alpha-actinin. *Experimental Cell Research*, **316**: 297-313

Stern, H. M., Brown, A. M. C. and Hauschka, S. D. (1995) Myogenesis in paraxial mesoderm: Preferential induction by dorsal neural tube and by cells expressing *Wnt-1. Development*, **121**: 3675–3686

Straube, A. and Merdes, A. (2007) EB3 regulates microtubule dynamics at the cell cortex and is required for myoblast elongation and fusion. *Current Biology*, **17**: 1318-1325

Subramanian, A., Prokop, A., Yamamoto, M., Sugimura, K., Uemura, T., Betschinger, J., Knoblich, J. A. and Volk, T. (2003) Shortstop recruits EB1/APC1 and promotes microtubule assembly at the muscle-tendon junction. *Current Biology*, **13**: 1086-1095

Sun, D., Leung, C. L. and Liem, R. K. (2001) Characterization of the microtubule binding domain of microtubule actin crosslinking factor (MACF): identification of a novel group of microtubule associated proteins. *Journal of Cell Science*, **114**: 161-172

Suozzi, K. C., Wu, X. and Fuchs, E. (2012) Spectraplakins: master orchestrators of cytoskeletal dynamics. *Journal of Cell Biology*, **197**: 465-475

Tajbakhsh, S., Borello, U., Vivarelli, E., Kelly, R., Papkoff, J., Duprez, D., Buckingham, M. and Cossu, G. (1998) Differential activation of Myf5 and MyoD by different Wnts in explants of mouse paraxial mesoderm and the later activation of myogenesis in the absence of Myf5. *Development*, **125**: 4155-4162

Takahashi, Y and Sato, Y. (2008) Somitogenesis as a model to study the formation of morphological boundaries and cell epithelialisation. *Develop. Growth Differ*, **50**: S149–S155

Tanda, N., Ohuchi, H., Yoshioka, H., Noji, S. and Nohno, T. (1995) A chicken Wnt gene, Wnt-11, is involved in dermal development. *Biochemical and Biophysical Research Communications*, **211**: 123-129

Tao, Q., Yokota, C., Puck, H., Kofron, M., Birsoy, B., Yan, D., Asashima, M., Wylie, C. C., Lin, X. and Heasman, J. (2005) Maternal wnt11 activates the canonical wnt signaling pathway required for axis formation in Xenopus embryos. *Cell*, **120**: 857-871

Tassin, A. M., Maro, B. and Bornens, M. (1985) Fate of microtubule-organizing centers during myogenesis in vitro. *Journal of Cell Biology*, **100**: 35-46

Venters, S. and Ordahl, C. (2002) Persistent myogenic capacity of the dermomyotome dorsomedial lip and restriction of myogenic competence. *Development*, **129**: 3873–3886

Venters, S. J. and Ordahl, C. P. (2005) Asymmetric cell divisions are concentrated in the dermomyotome dorsomedial lip during epaxial primary myotome morphogenesis. *Anatomy and Embryology (Berl)*, **209**: 449-460

Vladar, E. K., Antic, D. and Axelrod, J. D. (2009) Planar cell polarity signaling: the developing cell's compass. *Cold Spring Harb Perspect Biol*, **1**: a002964

Voiculescu, O., Bertocchini, F., Wolpert, L., Keller, R. E. and Stern, C. D. (2007) The amniote primitive streak is defined by epithelial cell intercalation before gastrulation. *Nature*, **449** (7165): 1049-52

von Maltzahn, J., Chang, N. C., Bentzinger, C. F. and Rudnicki, M. A. (2012) Wnt signaling in myogenesis. *Trends in Cell Biology*, **22**: 602-609

Wagner, J., Schmidt, C., Nikowits, W. Jr. and Christ, B. (2000) Compartmentalization of the somite and myogenesis in chick embryos are influenced by wnt expression. *Developmental Biology*, **228**: 86-94

Wagstaff, L. J., Bellett, G., Mogensen, M. M. and Münsterberg, A. (2008) Multicellular Rosette Formation During Cell Ingression in the Avian Primitive Streak. *Developmental Dynamics*, **237**: 91-96

Wallingford, J. B., Rowning, B. A., Vogeli, K. M., Rothbacher, U., Fraser, S. E. and Harland, R. M. (2000) Dishevelled controls cell polarity during Xenopus gastrulation. *Nature*, **405**: 81-85

Wallingford, J. B. and Harland, R. M. (2007) Vertebrate Gastrulation: The BMP Sticker Shock. *Current Biology*, **17** (6): 206-209

Walston, T., Tuskey, C., Edgar, L., Hawkins, N., Ellis, G., Bowerman, B., Wood, W. and Hardin, J. (2004) Multiple Wnt signaling pathways converge to orient the mitotic spindle in early C. elegans embryos. *Developmental Cell*, **7**: 831-841

Wang, H. W. and Nogales, E. (2005) Nucleotide-dependent bending of tubulin regulates microtubule assembly. *Nature*, **435**: 911-915

Watanabe, T., Noritake, J. and Kaibuchi, K. (2005) Regulation of microtubules in cell migration. *Trends in Cell Biology*, **15** (2): 76-83

Wei, Y. and Mikawa, T. (2000) Formation of the avian primitive streak from spatially restricted blastoderm: evidence for polarised cell division in the elongating streak. *Development*, **127**: 87-96

Wen, Y., Eng, C. H., Schmoranzer, J., Cabrera-Poch, N., Morris, E. J., Chen, M., Wallar, B. J., Alberts, A. S. and Gundersen, G. G. (2004) EB1 and APC bind to mDia to stabilize microtubules downstream of Rho and promote cell migration. *Nature Cell Biology*, **6**: 820-830

Williams, B. A. and Ordahl, C. P. (1997) Emergence of determined myotome precursor cells in the somite. *Development,* **124**: 4983-4997

Wilson-Rawls, J., Molkentin, J. D., Black, B. L. and Olson, E. N. (1999) Activated notch inhibits myogenic activity of the MADS-Box transcription factor myocyte enhancer factor 2C. *Mol Cell Biol*, **19**: 2853-2862

Wittmann, T. and Waterman-Storer, C. M. (2001) Cell motility: can Rho GTPases and microtubules point the way? *Journal of Cell Science*, **114**: 3795-3803

Witzel, S., Zimyanin, V., Carreira-Barbosa, F., Tada, M. and Heisenberg, C. P. (2006) Wnt11 controls cell contact persistence by local accumulation of Frizzled 7 at the plasma membrane. *Journal of Cell Biology*, **175**: 791-802

Wodarz, A. and Nusse, R. (1998) Mechanisms of Wnt signaling in development. *Annual Review of Cell and Developmental Biology*, **14**: 59-88

Wolpert, L., Jessel, T., Lawrence, P., Meyerowitz, E., Robertson, E. and Smith, J. (2007) Principles of Development Third Edition. Oxford University Press

Wu, D. and Pan, W. (2010) GSK3: a multifaceted kinase in Wnt signaling. *Trends Biochem Sci*, **35**: 161-168

Wu, X., Kodama, A. and Fuchs, E. (2008) ACF7 regulates cytoskeletal-focal adhesion dynamics and migration and has ATPase activity. *Cell*, **135**: 137-148

Wu, X., Shen, Q. T., Oristian, D.S., Lu, C. P., Zheng, Q., Wang, H. W. and Fuchs, E. (2011) Skin stem cells orchestrate directional migration by regulating microtubule-ACF7 connections through GSK3beta. *Cell*, **144**: 341-352

Yaffe, D. and Saxel, O. (1977) Serial passaging and differentiation of myogenic cells isolated from dystrophic mouse muscle. *Nature*, **270**: 725-727

Yang, X., Dormann, D., Münsterberg, A. E. and Weijer, C. J. (2002) Cell Movement Patterns During Gastrulation in the Chick Are Controlled by Positive and Negative Chemotaxis Mediated by FGF4 and FGF8. *Developmental Cell*, **3**: 425-437

Yang, Y., Dowling, J., Yu, Q. C., Kouklis, P., Cleveland, D. W. and Fuchs, E. (1996) An essential cytoskeletal linker protein connecting actin microfilaments to intermediate filaments. *Cell*, **86**: 655-665

Yost, C., Torres, M., Miller, J. R., Huang, E., Kimelman, D., and Moon, R. T. (1996) The axis-inducing activity, stability, and subcellular distribution of beta-catenin is regulated in Xenopus embryos by glycogen synthase kinase 3. *Genes Dev*, **10**: 1443-1454

Young, K. G., Pool, M. and Kothary, R. (2003) Bpag1 localization to actin filaments and to the nucleus is regulated by its N-terminus. *Journal of Cell Science*, **116**: 4543-4555

Yucel, G. and Oro, A. E. (2011) Cell migration: GSK3beta steers the cytoskeleton's tip. *Cell*, **144**: 319-321

Yusuf, F. and Brand-Saberi, B. (2006) The eventful somite: patterning, fate determination and cell division in the somite. *Anatomy and Embryology*, **211** (Suppl. 1): S21-S30

Zaoui, K., Honore, S., Isnardon, D., Braguer, D. and Badache, A. (2008) Memo-RhoA-mDia1 signaling controls microtubules, the actin network, and adhesion site formation in migrating cells. *Journal of Cell Biology*, **183**: 401-408

Zaoui, K., Benseddik, K., Daou, P., Salaun, D. and Badache, A. (2010) ErbB2 receptor controls microtubule capture by recruiting ACF7 to the plasma membrane of migrating cells. *Proceedings of the National Academy of Sciences of the United States of America*, **107**: 8517-18522

Zeng, X., Tamai, K., Doble, B., Li, S., Huang, H., Habas, R., Okamura, H., Woodgett, J. and He, X. (2005) A dual-kinase mechanism for Wnt co-receptor phosphorylation and activation. *Nature*, **438**: 873-877

Zhang, T., Zaal, K. J., Sheridan, J., Mehta, A., Gundersen, G. G. and Ralston, E. (2009) Microtubule plus-end binding protein EB1 is necessary for muscle cell differentiation, elongation and fusion. *Journal of Cell Science*, **122**: 1401-1409

Zhou, F. Q., Zhou, J., Dedhar, S., Wu, Y. H. and Snider, W. D. (2004) NGF-induced axon growth is mediated by localized inactivation of GSK-3beta and functions of the microtubule plus end binding protein APC. *Neuron*, **42**: 897-912

Abbreviations

+TIPS	Microtubule plus-end proteins
ABD	Actin-binding domain
ACF7	Actin crosslinking factor-7
APC	Adenomatous polyposis coli
ARPE-19	Human retinal pigment epithelial cells
ATG	Translation start site
ATP	Adenosine-5'-triphosphate
bHLH	Basic Helix-Loop-Helix
BLAST	Basic Local Alignment Search Tool
BMP4	Bone morphogenetic protein-4
BMPs	Bone morphogenetic proteins
BPAG-/-	BPAG1 knockout mice
BPAG1	Bullous pemphigoid antigen 1
CamKII	Calcium–calmodulin-dependent kinase II
Cdc42	Cell division control protein 42 homolog
CH	Calponin homology
CK1	Casein kinase I
cKO	Conditional knockout
CLASP2	Cytoplasmic linker associated protein-2
CLASPs	Cytoplasmic linker associated proteins
CLIP-170 - GFP	Cytoplasmic linker protein-170 - green fluorescent protein
CREB	cAMP response element-binding protein
DAPI	4',6-diamidino-2-phenylindole
DF-1s	Chicken embryo fibroblasts
Dlg1	Discs large 1
DLL1	NOTCH ligand Delta1
DML	Dorsomedial lip
DTT	Dithio threitol
Dvl	Dishevelled
EB	End-binding

EB1	End-binding 1
EB3	End-binding 3
EC	Early Chick
ECM	Extracellular matrix
EGF	Epidermal growth factor
EMT	Epithelial-to-mesenchymal transition
ErbB2	Tyrosine kinase receptor
EST	Expressed sequence tag
FITC	Fluorescein isothiocyanate
Fzd	Frizzled
GAR	Glycine/arginine-rich
GAR22	Gas2-related protein on chromosome 22
Gas2	Growth arrest-specific protein 2
GDP	Guanosine diphosphate
GFP	Green fluorescent protein
GPI	Glycophosphatidylinositol
GSK3β	Glycogen synthase kinase 3 β
GSR	Glycine-serine-arginine
GTP	Guanosine-5'-triphosphate
GTPases	Guanosine-5'-triphosphatases
HA	Human influenza hemagglutinin epitope
HES	Hairy/Enhancer-of-Split
HH	Hamburger-Hamilton
IQGAP1	IQ motif containing GTPase activating protein 1
JNK	c-Jun N-terminal kinase
Lef1	Lymphoid enhancer-binding factor 1
LFNG	Lunatic fringe
LRP	Lipoprotein receptor-related protein
MACF1	Microtubule and actin crosslinking factor-1
MAP1B	Microtubule-associated protein 1B
MAPs	Microtubule-associated proteins
MET	Mesenchymal-epithelial transition
MPCs	Myogenic precursor cells

MRCK	Myotonic-dystrophy kinase related Cdc42-binding kinase
MRFs	Myogenic regulatory factors
MTOC	Microtubule-organising centre
Myf5	Myogenic transcription factor-5
MyoD	Myogenic differentiation 1
Net1	Neuroepithelial-transforming-protein 1
NFAT	Nuclear factor of activated T cell
NICD	NOTCH intracellular domain
NT3	Neutrophin-3
PAK	p21-activated kinase
Pax1	Paired box protein 1
Pax3	Paired box protein 3
Pax7	Paired box protein 7
PBS	Phosphate buffered saline
PCP	Planar cell polarity
PI3K	Phosphatidylinositol 3-kinase
PKC	Protein kinase C
PKN	Protein kinase N
PLC	Phospholipase C
PRD	Plakin repeat domain
PVDF	Polyvinylidene difluoride
RNA	Ribonucleic acid
RNAi	RNA interference
RNase	Ribonuclease
ROCK	Rho-associated, coiled-coil containing protein kinase
RT-PCR	Reverse transcription-polymerase chain reaction
S:A mutant	Ser-Ala mutations
S:D mutant	Ser-Asp mutations
SDS-PAGE	Sodium dodecyl sulfate polyacrylamide gel electrophoresis
SEM	Scanning electron microscopy
Shh	Sonic hedgehog
siRNAs	Small interfering RNAs

Su(H)	Suppressor of hairless
TCF/LEF	T cell factor/lymphoid enhancer factor
TEM	Transmission electron microscopy
TGN	Trans-Golgi network
UTR	Untranslated region
WASP	Wiskott-Aldrich syndrome protein